

## Catalyst Transformation During Alkali-Catalyzed Carbon Gasification

F. Shadman, W.A. Punjak and D.A. Sams

Department of Chemical Engineering, University of Arizona  
Tucson, Arizona 85721

The kinetics and mechanism of carbon gasification reaction catalyzed by alkali metals have been the subject of numerous studies and comprehensive reviews are available (1-4). Although the mechanism of catalyst action is not completely understood, there is a general agreement that the reaction follows a redox mechanism (5-6). In this mechanism, the alkali catalyst cycles between an oxidized and a reduced form. During this cycle the catalyst transfers oxygen from the gaseous reactant to the carbon surface; the net effect is production of CO. Presently, the disagreement is on the nature and the stoichiometry of the catalytic intermediate compounds. The purpose of this study is to characterize the mechanism and the kinetics of the processes in which sodium and potassium carbonates are reduced from their initial forms to the catalytic intermediate forms.

### EXPERIMENTAL METHOD

Carbopack B (by Supelco) was used as the high purity carbon substrate. Catalyst in the initial form of sodium or potassium carbonate was applied by the incipient wetting technique. The catalyst/carbon ratio was controlled by varying the alkali concentration in the impregnation solution. Atomic emission spectroscopy was used to analyze the samples for alkali content. The catalyst type and concentration of the samples used in this study are given in Table 1.

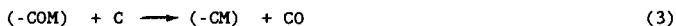
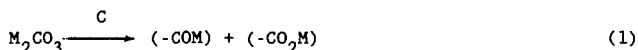
Two reactor systems were used in the course of this study. The first utilized a small differential reactor for quick response times while the second used an electronic microbalance for direct measurement of sample weight. Both systems included a movable furnace which allowed rapid heating and cooling or programmed temperature change in the reactor. The details of experimental set-up are given elsewhere (7,10).

For each run, 25-30 mg of the impregnated carbon was loaded into the reactor. The reactor was then purged with Ultra high purity nitrogen to remove the oxygen before heating the sample. The experiments were conducted under Temperature and Concentration Programmed Reaction (TCPR) conditions. Three schedules of programmed conditions were used. In Schedule 1 (Fig. 1), the samples were rapidly heated to 800°C under nitrogen. After complete evolution of H<sub>2</sub>O, CO<sub>2</sub> and CO, the samples were cooled rapidly and removed for analysis. Schedule 2 (Fig. 2) was similar except the samples were

quenched before complete catalyst reduction to determine the relationship between CO evolution and catalyst loss. In Schedule 3, (Fig. 3) the partial reduction under nitrogen was followed by gasification under a mixture of 15% CO<sub>2</sub> in nitrogen. After a short gasification stage to measure the gasification rate, the samples were quenched and removed for analysis.

### RESULTS AND DISCUSSION

In an earlier study (11), a mechanism was suggested for the interaction between carbon and potassium carbonate under inert conditions above 700°C. This mechanism, which is expected to hold for both sodium and potassium carbonates, can be written in the following general form:



This mechanism allows for the sequential reduction of the catalyst followed by catalyst vaporization and loss.

In the early stage of the sample heat up, a small CO<sub>2</sub> peak is observed. This peak is due to the decomposition of bicarbonate to carbonate (10,11). During the rest of the reduction stage, carbon monoxide is the only significant gaseous product. Therefore, the time profile of CO is a direct measure of the overall reduction kinetics. The CO profile shown in Figure 1 is a typical profile for initial catalyst loadings above saturation. The CO concentration exhibits a plateau with almost constant CO gasification rate. As the initial loading is decreased, the width of the CO plateau decreases while the rate of CO production does not change significantly. For very low concentrations the profile does not exhibit a plateau. These results indicate that at catalyst loadings greater than what is required for surface saturation, catalyst is the excess reactant and carbon surface is the limiting reactant. Under these conditions, the reduction rate is determined by the carbon substrate area which is independent of catalyst loading. The very small increase in CO across the plateau is due to the increase in carbon surface area caused by conversion. At initial concentrations lower than saturation (initial metal to carbon atomic ratio of about 0.01 for potassium and 0.04 for sodium) the rate of reduction varies with both loading and time and no plateau is observed.

The rise and fall of the CO peak are primarily due to the effect of reaction kinetics and not simply an artifact of the reactor residence time response. Without these effects the rise and fall would have been much sharper. This is because dispersion in the reactor is relatively negligible. The rise is due to the increase in

the concentrations of (-CO<sub>2</sub>M) and (-COM) supplied by reaction 1. The fall is due to the depletion of the carbonate.

The dependence of the average catalyst reduction rate on loading is shown in Figure 4. Total reduction time is a linear function of the initial catalyst loading. This indicates that the average rate is independent of loading as long as the carbon substrate is saturated. The rate will vary with loading for unsaturated samples as indicated by the curvature of the lines at low catalyst loadings. As expected, the shape of the curve indicates that the turnover number (measure of rate per catalyst atom) for an unsaturated surface is higher than that for a saturated surface.

The reduction mechanism suggests that the catalyst is reduced prior to loss by vaporization. To measure the relative rates of catalyst reduction and vaporization, a series of runs were conducted where the samples were removed after various levels of catalyst reduction and analyzed for catalyst content (Schedule 2). The results are shown in Figure 5 and indicate that the catalyst vaporizes rapidly upon complete reduction. This can occur only if reaction 4 is substantially faster than reaction 3.

An important observation is that the rate of catalyst loss is dramatically decreased after all the catalyst is reduced. In other words, the residual catalyst left on the surface at the end of the reduction process is relatively stable. This means that reaction 4 is somehow enhanced by the presence of carbonate. A possible explanation is that the strong attraction of carbonate to carbon sites causes the decomposition of (-CM) and the release of carbon sites which interact with carbonate.

#### CONCLUSION

The reduction of potassium and sodium carbonates is a prerequisite for the formation of surface catalytic sites, and further reduction of these surface sites is an integral part of the mechanism suggested for catalytic gasification. In addition, the alkali catalyst is lost from a site only after it has been completely reduced.

For a sufficiently high loading, a sodium or potassium impregnated carbon sample subjected to heat under an inert atmosphere will generate a CO concentration/time profile with a distinct plateau region. In this region, catalyst is the excess reactant and carbon surface area is the limiting reactant. For low loading samples, catalyst is the limiting reactant and no plateau is observed. The reduction rate is independent of loading for high loading samples while for low loading samples the rate is a function of both loading and time.

There is a saturation limit for the alkali catalyst on carbon substrates. This limit appears to be the same for both sodium and potassium on molar basis. In general, the surface saturation limit is independent of the initial loading but depends on the total surface area of the substrate.

#### REFERENCES

1. Wen, W.Y., Catal. Rev.-Sci. Eng., 22(1), 1 (1980).
2. McKee, D.W., Chem. Phys. Carbon, 16, 1 (1981).
3. Wood, B.J. and K.M. Sancier, Catal. Rev.-Sci. Eng., 26(2), 233 (1984).
4. Pullen, J.R., IEA Coal Research, No. ITCIS/TR26 (1984).
5. McKee, D.W., Fuel, 62(2), 170 (1982).
6. Moulijn, J.A., M.B. Cerfontain and F. Kapteijn, Fuel, 63(8), 1043 (1984).
7. Sams, D.A. and F. Shadman, accepted for publication in AIChE J.
8. Sams, D.A., T. Talverdian and F. Shadman, In Press, Fuel (1985).
9. Talverdian, T., "Catalyst Loss During Potassium-Catalyzed CO<sub>2</sub> Gasification of Coal Char and Carbon," M.S. Thesis, University of Arizona (1984).
10. Sams, D.A. "The Kinetics and Mechanism of the Potassium Catalyzed Carbon/Carbon Dioxide Gasification Reaction", Ph.D. Dissertation, University of Arizona (1985).
11. Shadman, F. and Sams, D.A., Proceedings of the 17th Biennial Conference of the American Carbon Society, Lexington, Ky., 182 (1985).

**Table 1. Catalyst Specifications in the Studied Samples**

Sample	Catalyst	(M/C) <sub>o</sub> atomic ratio
A	K	0.00089
B	K	0.0027
C	K	0.0054
D	K	0.013
E	K	0.021
F	K	0.025
G	K	0.027
H	Na	0.011
I	Na	0.029
J	Na	0.049
K	Na	0.067
L	Na	0.091
M	Na	0.131

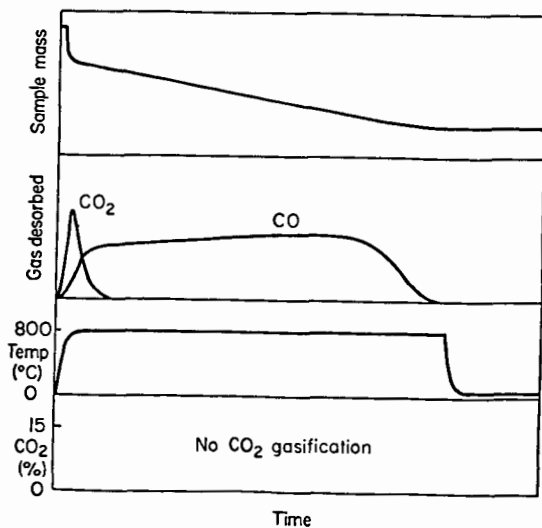


Figure 1. Temperature-programmed reaction; Schedule 1

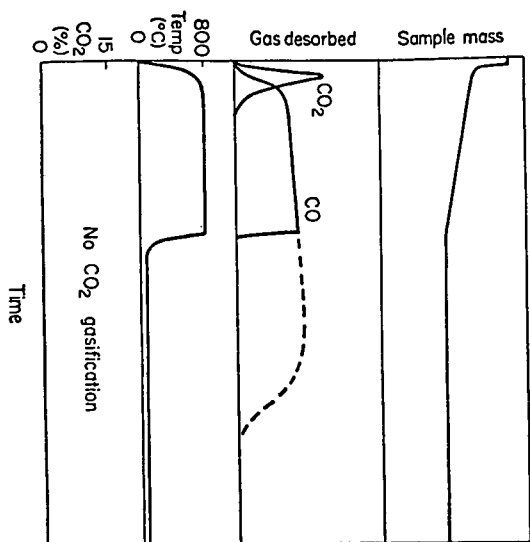


Figure 2. Temperature-programmed reaction; Schedule 2

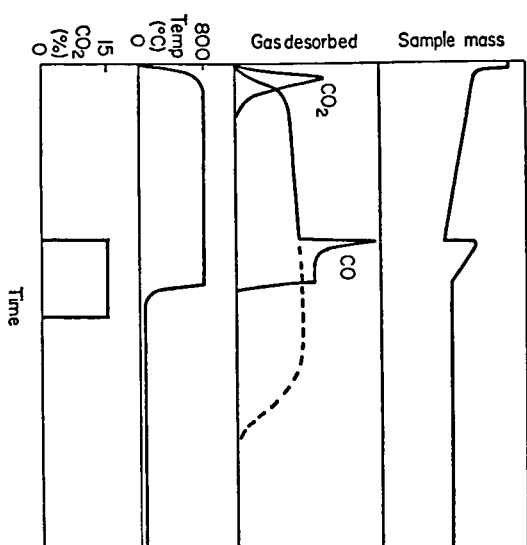


Figure 3. Temperature- and concentration-programmed reaction; Schedule 3

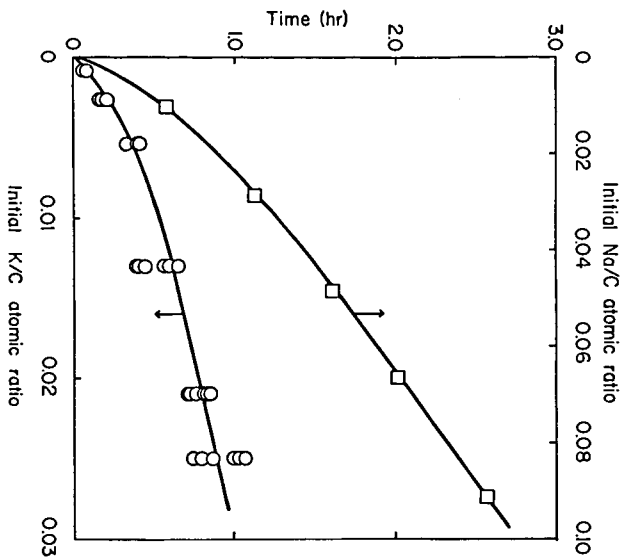


Figure 4. Dependence of total reduction time on the initial catalyst loading

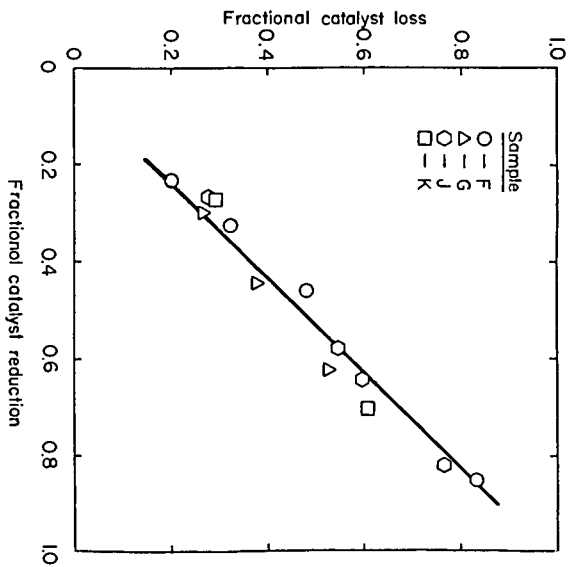


Figure 5. Catalyst loss during reduction

## ROLE OF OXYGEN IN ALKALI-CATALYZED HYDROGEN GASIFICATION OF CARBON BLACK

Michael H. Treptau, Hossein Zoheidi, and Dennis J. Miller

Department of Chemical Engineering  
Michigan State University  
East Lansing, MI 48824-1226

### INTRODUCTION

The hydrogen gasification of carbon in the presence of alkali metal salts has been reported in only a few studies [1-3], and little information about reaction kinetics or catalytic enhancement is available. The uncatalyzed reaction, in contrast, has received considerable attention [4,5]. Of particular interest are the results of Cao and Back [6] and Blackwood [7], who reported the effects of oxygen on the methane production rate.

Hydrogen gasification is under investigation in our laboratory because it is a direct route to methane production and because it offers a unique environment in which to study gasification catalyst behavior. Hydrogen gasification involves an elemental feed gas ( $H_2$ ) and a single product ( $CH_4$ ), thus facilitating accounting of carbon and oxygen from both reactant and catalyst during gasification. The work presented in this paper focuses on the importance of oxygen in hydrogen gasification, and discusses results of experiments involving both alkali-metal catalyzed and uncatalyzed reactions. This study is a continuation of earlier work [8].

### EXPERIMENTS

The carbon used in this study is a graphitic carbon lampblack (Fisher Scientific) with an initial BET surface area of 20 square meters per gram and an impurity content of less than 0.1 per cent. The catalysts ( $K_2CO_3$ ,  $Na_2CO_3$ ,  $KCl$ ) were deposited on the carbon by wet impregnation in metal to carbon molar ratios of approximately 0.01 and 0.02. Uncatalyzed carbon samples were also put through the same impregnation procedure but without addition of catalyst. Actual M/C ratios, measured by neutron activation analysis, are  $K/C = 0.0093$  and  $0.0192$  for  $K_2CO_3$ ,  $Na/C = 0.0111$  and  $0.0221$  for  $Na_2CO_3$ , and  $K/C = 0.019$  for  $KCl$ . Typical sample sizes gasified were 60-70 milligrams.

The gasification apparatus consists of a fixed bed differential reactor equipped with a gas collection system and gas chromatograph for rate measurement and product gas analysis. The pressure vessel is a Haynes Alloy tube (0.875" ID and 2.0" OD) designed for simultaneous operation at 1000°C and 1000 psi. Rate is measured as rate of methane evolution via timed collection of product gas; evolution rates as low as 0.005 ml/min can be accurately measured. Further details are given elsewhere [8].

All gasification experiments were carried out in pure hydrogen (Airco, 99.999%) at 500 psi pressure and a flow rate of 3-5 liters(STP)/minute/gram initial carbon. In all reactions the apparatus was evacuated three times and then purged in helium during initial heating. Hydrogen was then added to the reactor at 500°C in most experiments. In some experiments uncatalyzed samples were degassed by heating to 1000°C in vacuum for twelve hours before gasification, and in others hydrogen was added at room temperature.

## RESULTS

All gasification experiments were conducted in a large excess of hydrogen, so that the methane formation reaction was far from equilibrium. In addition, repeated experiments in which sample size and flow rate were changed and in which sample temperature was measured allow us to conclude that the results represent intrinsic and reproducible kinetic rate measurements for the hydrogen gasification.

Catalyzed Gasification: The experimental data are represented as rate of methane evolution versus time during gasification. The start of reaction ( $t=0$ ) is taken as the time where hydrogen is added to the reaction vessel ( $500^{\circ}\text{C}$ ); steady state temperature is reached after about 55 minutes. In the Figures, the symbols represent individual collection points; the curve represents the best fit of the rate data. Methane evolution rate is normalized to initial carbon weight; integration of the rate curve gives a carbon conversion close to that obtained by weighing the sample residue.

Methane evolution rate for gasification in the presence of  $\text{Na}_2\text{CO}_3$  and  $\text{K}_2\text{CO}_3$  catalysts at  $865^{\circ}\text{C}$  are given in Figure 1 for  $M/C = 0.02$  and in Figure 2 for  $M/C = 0.01$ . The rate curve for sodium is scaled to the same  $M/C$  ratio as potassium. The results show that both catalysts enhance the rate of hydrogen gasification, but show different catalytic effects as carbon is consumed. For  $\text{Na}_2\text{CO}_3$ , rate is a maximum near the time where steady state temperature is first reached, whereas for  $\text{K}_2\text{CO}_3$  the rate increases as gasification proceeds. The results for gasification in the presence of  $\text{KCl}$  are also given in Figure 1, and show that  $\text{KCl}$  has little catalytic effect in hydrogen gasification.

Activation energy of the hydrogen gasification reaction was measured over the temperature range of  $730$ – $900^{\circ}\text{C}$  for the uncatalyzed reaction and in the presence of the carbonate catalysts. The Arrhenius plots are given in Figure 3 at 20% carbon conversion for all three samples; also shown (by dotted line) is the plot at 30% conversion for the  $\text{Na}_2\text{CO}_3$  sample. The calculated activation energy at 20% conversion is  $220$  kJ/mole for  $\text{K}_2\text{CO}_3$ ,  $251$  kJ/mole for  $\text{Na}_2\text{CO}_3$ , and  $264$  kJ/mole for the uncatalyzed reaction. The lower value for the potassium catalyst results from scatter in the data, as potassium catalyst gave the highest reaction rate and thus the fewest number of collection points. Therefore, the activation energy is the same within experimental uncertainty for both catalyzed and uncatalyzed reactions and approximately equal to  $250$  kJ/mole.

The different gasification rate curves for sodium and potassium catalyzed reactions led to investigation of the interaction between catalyst and carbon and evolution of oxygen species during heatup. In these experiments, the reactor was purged as usual, but the sample was heated in hydrogen and gas evolution was monitored during heatup. The results of these experiments are given in Table 1. The primary gas evolved from  $\text{K}_2\text{CO}_3$  is  $\text{CO}_2$ , which appears in the temperature range of  $300$ – $500^{\circ}\text{C}$ , while  $\text{Na}_2\text{CO}_3$  releases primarily  $\text{CO}$  at  $400$ – $700^{\circ}\text{C}$ . The uncatalyzed reaction releases very small quantities of each gas at similar temperatures, probably from weakly bound oxygen species on the carbon surface.

**TABLE 1**  
Gas Evolution during Sample Heatup  
(M/C = 0.02)

Catalyst	CO (mg)	CO <sub>2</sub> (mg)	Total Oxygen (mg)	Fraction of Oxygen in Catalyst Evolved	
				as CO	as CO <sub>2</sub>
K <sub>2</sub> CO <sub>3</sub>	0.50	1.05	1.04	0.12	0.31
Na <sub>2</sub> CO <sub>3</sub>	1.05	0.29	0.81	0.22	0.05
none	0.031	0.102	0.093	-	-

**Uncatalyzed Gasification:** The effects of indigenous oxygen, present on the surface or in the bulk of the unimpregnated carbon, was investigated by conducting several experiments in which the carbon was either degassed or partially reacted in oxygen. Carbon was degassed by heating to 1000°C in vacuum to remove adsorbed oxygen. Oxygen was replenished on the carbon surface by partial combustion in air at 400°C. The partial combustion was controlled by admitting a finite amount of oxygen into the pressure vessel and then allowing the reaction to go to completion.

Results of the experiments are given in Figure 4 as methane formation rate versus carbon conversion. The solid circles represent rate for an untreated sample. The open squares represent a sample initially degassed, gasified in hydrogen (to 20% conversion), partially combusted in oxygen (to 35% conversion), and then further gasified in hydrogen. The open triangles represent a sample initially gasified in hydrogen (to 25% conversion), partially combusted in oxygen (to 35% conversion), and then further gasified in hydrogen. The results show that degassing reduces gasification rate, and that partial combustion in oxygen recovers some reactivity toward hydrogen. It was necessary to partially combust the carbon to recover reactivity; an experiment in which the carbon was exposed to oxygen at room temperature showed no subsequent increase in reactivity toward hydrogen, thus indicating little reaction between oxygen and carbon.

### DISCUSSION

Figures 1 and 2 illustrate that both sodium and potassium carbonate are effective hydrogen gasification catalysts. The curves also show that the gasification rate changes significantly as carbon is consumed, and in a different manner for each catalyst.

Two quantities pertaining to gasification of this carbon, measured in an earlier work [8], must be mentioned. First, specific BET surface area of the carbon black increases dramatically during gasification [8], increasing approximately linearly with conversion from 20 m<sup>2</sup>/g initially to 400 m<sup>2</sup>/g at sixty per cent conversion for both catalyzed and uncatalyzed reactions. Absolute carbon surface area therefore increases about six-fold up to 60% conversion. Specific reaction rate based on this area is nearly constant for the K<sub>2</sub>CO<sub>3</sub>-catalyzed samples over the course of gasification, but decreases strongly for other samples. This indicates that, at least for the uncatalyzed case, rate is not related to total surface area. Secondly, significant catalyst is lost from the sample during gasification [8]; the amount of catalyst after gasification, determined by neutron activation analysis, decreases linearly with conversion to approximately one-third of

the initial value at 80% for both  $\text{Na}_2\text{CO}_3$  and  $\text{K}_2\text{CO}_3$ . Total surface area development and catalyst loss do not explain the increase in rate with conversion, however, and other factors must therefore account for the observed behavior.

The Arrhenius plot in Figure 3 shows that apparent activation energy is nearly the same both for catalyzed and uncatalyzed reactions and at different conversions. This is in accordance with results of other investigators [9-10] for steam and carbon dioxide gasification, and suggests that the role of the catalyst is to increase the number of active sites without changing the reaction mechanism. This indicates that the active sites in both catalyzed and uncatalyzed gasification must perform a similar function, and that different shapes of the rate curves in Figures 1 and 2 for sodium and potassium catalysts must be attributed not to different reaction mechanisms but to differences in active site population as gasification progresses. The value of apparent activation energy (250 kJ/mole) is somewhat higher than values reported (150-210 kJ/mole) [4,5,11] for uncatalyzed methane formation. The only study for which a higher activation energy (300 kJ/mole) was found was for the reaction with graphite at 1200-1600°C [12]. This is further evidence that the rate measurements represents intrinsic reaction kinetics, and suggests that values of activation energy measured for porous carbons and chars may include effects of diffusion resistances and mineral matter.

Results from degassing and partial combustion of uncatalyzed carbon, given in Figure 4, show that the presence of oxygen on the carbon surface strongly enhances gasification rate. This is in agreement with the results of Cao and Back [6], who report an order of magnitude increase in methane formation rate when 0.1% oxygen is added to the hydrogen feed stream, and with the results of Blackwood [7], who observed that methane formation rate was proportional to oxygen content of coconut char. If oxygen is the key entity which enhances gasification rate, then the observed decrease in rate with time for uncatalyzed and untreated carbon (solid circles in Figure 4) is consistent with the concept that surface oxygen is slowly stripped from the carbon during reaction at 865°C. This concept is supported by the slower or nearly nonexistent decrease in rate with time for the uncatalyzed reaction at lower temperatures, in which oxygen is not removed from the surface.

Degassing the carbon (open squares in Figure 4) decreases the rate to a low level (0.8 ml  $\text{CH}_4$ /min/gram C) which is essentially invariant with time. The finite rate after degassing results either from the intrinsic carbon-hydrogen reactivity or from the presence of low levels of oxygen impurities in the carbon or reactant gas. When the degassed sample is combusted in oxygen at 400°C, gasification rate increases by approximately 2.0 ml  $\text{CH}_4$ /min/gram C. Similarly, when a sample not initially degassed (triangles in Figure 4) is combusted in oxygen at 400°C the rate also increases by approximately 2.0 ml  $\text{CH}_4$ /min/gram C, suggesting that partial combustion results in formation of a similar number of new active sites in both cases. Further, these results indicate that new active sites are formed in addition to those already existing on the surface. The total methane evolution rate is therefore the sum of the rates from the original oxygen-bearing sites which are still active and from the sites created by partial combustion.

The different rate curves for sodium and potassium carbonate catalysts and the evolution of different gases during heatup shows that the catalyst-carbon interactions are substantially different for the two cases. For  $\text{K}_2\text{CO}_3$  (M/C=0.02), the evolution of one-third of the oxygen in the catalyst as  $\text{CO}_2$  is consistent with results reported by Mims and Pabst [13] and Wood and Sancier [14] for formation of a surface oxide. It is not known at this time

if a K-O-C type complex is formed in the presence of hydrogen; however, based on the fact that absolute rate increases and specific rate is maintained, it can be concluded that the potassium catalyst disperses in a stable state on the carbon surface and forms new active sites as gasification progresses. These observations are consistent with those reported for a surface oxide complex; however no conclusions can be made.

The low initial catalytic activity for K/C=0.01 samples and the observed pyrophoric nature of potassium-containing sample residues from low temperature gasification make it impossible to rule out intercalation of potassium as an intermediate step in gasification. This phenomena has been dismissed for carbon oxidation reactions but has not been investigated for the reducing hydrogen gasification environment, and it is possible that both intercalation and surface oxide formation take place. Intercalation is reported to be a sink for potassium [15], thus explaining the low initial activity for K/C=0.01 samples. Sodium does not intercalate; this may provide an explanation of observed gasification behavior.

For the Na<sub>2</sub>CO<sub>3</sub> catalyst, evolution of primarily CO at higher temperatures during heatup suggests that the carbothermic reaction is taking place. It has been reported that sodium metal interacts with surface oxygen [16] to form an oxide complex similar to that for potassium; it is possible that such a complex is responsible for the catalytic activity.

Two observations suggest that the interaction of the sodium catalyst with carbon is not as strong as that of potassium. First, after gasification in hydrogen the carbon residues contained visible particles of sodium carbonate, indicating that significant agglomeration of catalyst occurred. Also, the total amount of oxygen evolved during heatup for the M/C=0.02 samples (Table 1) was less for sodium than for potassium. These observations indicate that the overall interaction of sodium carbonate with carbon is not as strong as the interaction of potassium carbonate with carbon, and it is likely that sodium forms few new active sites as gasification proceeds. The observed rate is therefore seen to decrease with conversion.

The mechanism by which the oxygen-bearing species (whether oxygen in the uncatalyzed sample or an M-O- complex for the catalyzed reactions) promote hydrogen gasification has not been studied. However, there is some evidence which allows the role of these species to be postulated. Yang and Duan [17] have recently reported using etch pit analysis that the arm-chair {1121} face of graphite is more reactive than the zig-zag {1011} face, and that hydrogen inhibits gasification in CO<sub>2</sub> and H<sub>2</sub>O by preferentially adsorbing on and thus stabilizing the zig-zag face. The presence of hydrogen results in the formation of hexagonal (zig-zag) etch pits of low reactivity. Along with this, chemisorbed hydrogen is known to strongly bind to carbon and reduce oxygen adsorption capacity [18]. In contrast, gasification in CO<sub>2</sub> alone results in round pits with arm-chair edges. For hydrogen gasification, Zielke and Gorin [11] postulated that reaction is sterically more suited to the arm-chair face. Thus it is likely that the function of the oxygen-bearing surface species is to maintain and propagate arm-chair reaction sites on the carbon during gasification. Removal of oxygen species, either by desorption or reduction, results in consumption of arm-chair sites, leaving only residual and unreactive zig-zag faces to which hydrogen strongly binds. Combustion in oxygen results in formation of new arm-chair faces, resulting in enhancement of hydrogen gasification rate. Similarly, the addition of catalyst results in the presence of a larger quantity and possibly more stable oxygen-containing species which propagate the arm-chair faces, thus catalyzing the reaction.

This idea is also consistent with results reported by Baker *et al.* [19] and Tomita and Tamai [20] for barium and transition metal catalyzed hydrogen gasification, in which reaction occurs via channeling of catalyst particles in the <1120> crystallographic direction. The residual zig-zag faces left by the channel show no reactivity. These catalysts therefore propagate the arm chair face at the head of the channel, resulting in continued gasification.

#### CONCLUSIONS

The similar apparent activation energy and surface area development for uncatalyzed and catalyzed hydrogen gasification reactions suggests that catalysts increase the number of available reaction sites without changing the reaction mechanism. Surface oxygen enhances the rate of gasification; this along with evolution of CO<sub>2</sub> from potassium carbonate during heatup makes possible the idea that a surface oxygen complex is the catalytic agent. Based on evidence in the literature, the role of surface oxygen is postulated to be propagation of the arm-chair configuration of edge sites during gasification. These arm-chair sites are believed to be the sites at which hydrogen gasification occurs.

#### ACKNOWLEDGMENT

This material is based upon work supported by the National Science Foundation under Grant No. CPE-83-07963.

#### REFERENCES

1. Gardner, N., E. Samuels, and K. Wilks, Coal Gasification, ACS Advances in Chemistry Series, **131**, 209 (1974).
2. Walker, P.L. Jr., S. Matsumoto, T. Hanzawa, T. Muira, and I.M.K. Ismail, Proc. Int. Symp. on Catalyzed Carbon and Coal Gasification, Amsterdam, **11** (1982).
3. Wigmans, T., M. Elfrins, A. Hoogland, and J.A. Moulijn, Proc. Int. Conf. on Coal Science, Dusseldorf, 301 (1980).
4. Cao, J.R., and M.H. Back, Carbon **20**, 505 (1982).
5. Tomita, A., D.P. Mahajan, and P.L. Walker Jr., Fuel **56**, 137 (1980).
6. Cao, J.R., and M.H. Back, Carbon **23**, 141 (1985).
7. Blackwood, J.D., Australian J. Chem. **12**, 14 (1959).
8. Zoheidi, H., and D.J. Miller, Carbon (in review) (1986).
9. Adjorlolo, A.A., and Y.K. Rao, Carbon **22**, 173 (1984).
10. Otto, K., and M. Shelef, Chem. Eng. Commun. **5**, 223 (1980).
11. Zielke, C.W., and E. Gorin, Ind. and Eng. Chem. **47**, 820 (1955).
12. Gulbransen, E.A., K.F. Andrew, and F.A. Brassart, J. Electrochem. Soc. **112**, 49 (1965).
13. Mims, C.A., and J.K. Pabst, Fuel **62**, 176 (1983).
14. Wood, B.J., and K.M. Sancier, Catal. Rev.-Sci. Eng. **26**(2), 233 (1984).
15. Wigmans, T., R. Elfring, and J.A. Moulijn, Carbon **21**, 1 (1983).
16. Yuh, S.J., and E.E. Wolf, Fuel **63**, 1604 (1984).
17. Yang, R.T., and R.Z. Duan, Carbon **23**, 325 (1985).
18. Bansal, R.C., F.J. Vastola, and P.L. Walker, Jr., Carbon **12**, 355 (1974).
19. Baker, R.T.K., C.R.F. Lund, and J.J. Chludzinski, Jr., J. Catal. **87**, 255 (1984).
20. Tomita, A., and Y. Tamai, J. Phys. Chem. **78**, 2254 (1974).

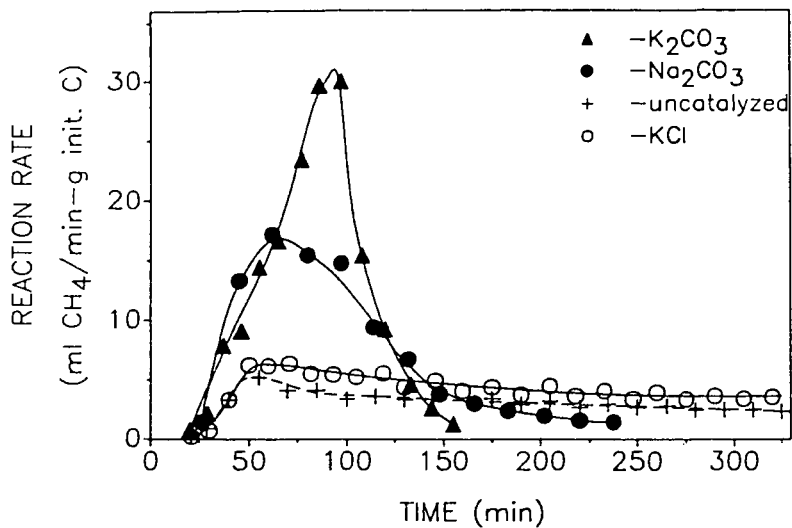


FIGURE 1. Methane evolution rate at 865°C for M/C=0.02

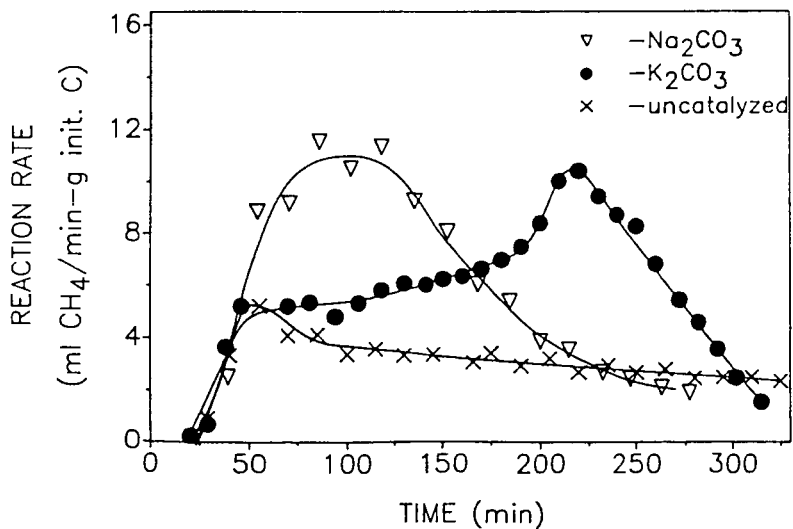


FIGURE 2. Methane evolution rate at 865°C FOR M/C=0.01

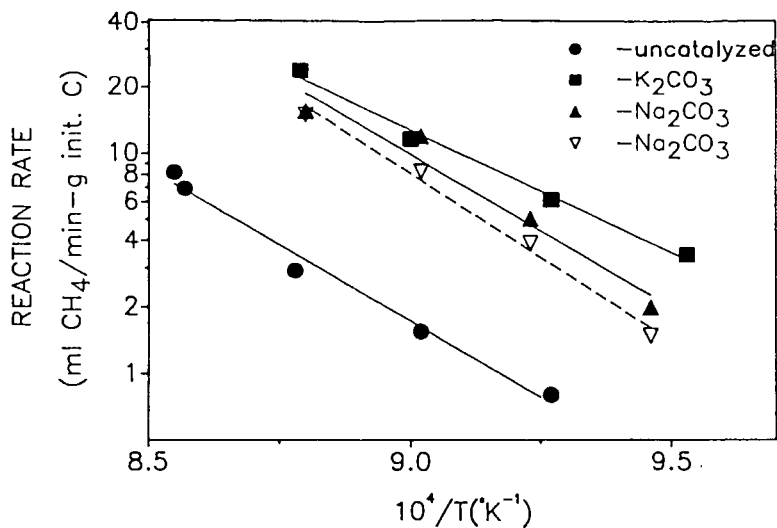


FIGURE 3. Arrhenius plot for  $M/C=0.02$

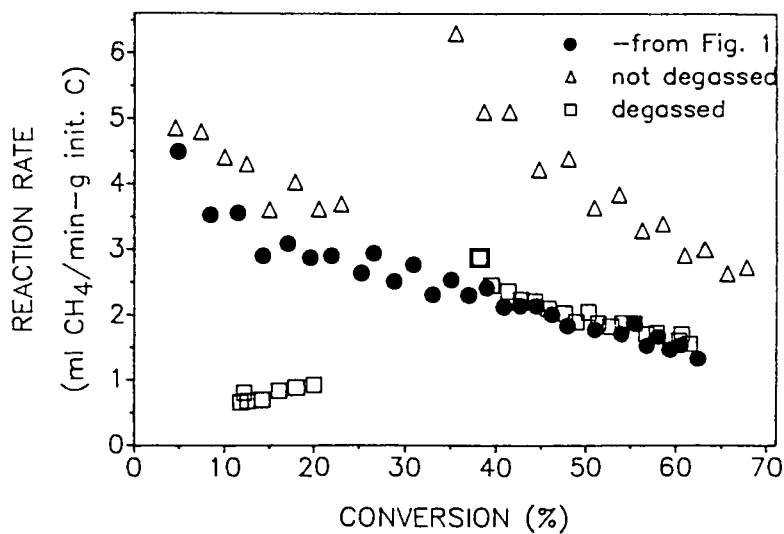


FIGURE 4. Oxygen effects on uncatylzed rates.

STEAM GASIFICATION OF CARBONACEOUS SOLIDS CATALYZED BY A  
MIXTURE OF POTASSIUM AND NICKEL OXIDES BELOW 1000 K

J. Carrazza, G. A. Somorjai and H. Heinemann

Materials and Molecular Research Division  
Lawrence Berkeley Laboratory  
University of California  
Berkeley, CA 94720

Introduction

The gasification of carbon with water vapor is an important reaction in the industrial production of  $H_2$ ,  $CH_4$ ,  $CO$  and  $CO_2$ . The use of catalysts is necessary if the process is carried out at temperatures below 1400 K. Two recent reviews discuss the properties of the various catalysts used for this purpose.(1,2) Alkaline and alkaline-earth hydroxides and carbonates are the catalysts most commonly studied. These compounds only show catalytic activity at temperatures above 1000 K. Previous work in our laboratory shows that below this temperature KOH reacts stoichiometrically with graphite and water vapor to produce  $H_2$  and a stable surface compound.(3) Transition metals, in particular nickel and iron, are able to catalyze this process at temperatures as low as 750 K, but they deactivate much faster than the alkaline and alkaline-earth salts. Several authors have reported that nickel and iron are only active as catalysts for this process if the reaction conditions favors their presence in the metallic state.(4,5)

We have recently reported that several mixtures of a transition metal oxide with potassium hydroxide are excellent catalysts for the gasification of graphite with steam.(6) These catalysts are active at temperatures much lower than the alkaline and alkaline-earth salts and they deactivate more slowly than nickel and iron. In this previous publication it was shown that there is a synergistic effect between the transition metal and potassium.

This communication summarizes recent results in the study of this type of catalyst. We have focused on the use of mixtures of potassium hydroxide and nickel oxide, since they showed the highest activity of all the systems previously studied.(6) A kinetic study of the gasification of several chars and the dependence of the ratio of potassium to nickel on the rate of graphite gasification are presented. Also the interaction between nickel and potassium is studied using X-ray Photoelectron Spectroscopy (XPS).

Experimental

The gasification rates of graphite and five different chars have been obtained. The chars pretreatment, elemental composition and ASTM rank are summarized in Table 1. Nickel and potassium were loaded on the carbon substrate by incipient wetness using solutions of  $Ni(NO_3)_2$  and KOH. A detailed explanation of the sample treatment after catalyst loading is given in a previous publication.(6)

A detailed explanation of the equipment used in these studies is given elsewhere.(6,7) The kinetic studies were done in a fixed bed flow reactor with an online gas chromatograph used for product analysis. The total gas production as a function of time was determined using a gas burette after the steam was condensed. The XPS study was done in an Ultra High Vacuum (UHV) chamber coupled to a high pressure cell. This apparatus allowed us to treat the sample under reaction conditions and to further transfer it to UHV for surface characterization without exposure to air.

All the kinetic results were obtained in isothermal experiments. The steam flow through the sample was equivalent to 1 ml of liquid water per minute. The reactor diameter was 0.6 cm. The reaction temperature was measured using a chromel-alumel thermocouple in contact with the external wall of the reactor. At the beginning of each experiment, a stabilization period of 15 min was allowed before data was collected. The principal reaction products were H<sub>2</sub> and CO<sub>2</sub>. The gasification rates were determined measuring the H<sub>2</sub> production because its solubility in water is much smaller than that of CO<sub>2</sub>. The carbon conversions were determined by dividing the number of H<sub>2</sub> moles produced by two times the initial number of carbon moles.

The XPS experiments were carried out using a Mg-anode source (hv = 1253.6 eV). The data was collected using a detector pass energy equal to 40 eV. The position of the peaks was calibrated with respect to the position of the C1s peak of graphite (binding energy = 284.6 eV).

## Results

The rate of graphite gasification as a function of time has been studied at 893 K for several mixtures of nickel and potassium oxides and for the components deposited alone. Some of the results are shown in Figure 1. The activity corresponding to nickel deposited alone is given by Curve A. A very fast initial activity is observed, but the sample deactivates almost completely after two hours, giving a total carbon conversion of 20%. When potassium is deposited alone from a KOH solution, no steady state gasification rate is observed after 15 min of initiating the experiment. Curve B shows the rate when nickel and potassium oxides are codeposited on graphite with a Ni/C molar ratio equal to  $1.0 \times 10^{-2}$  and a Ni/K molar ratio equal to 0.1. Initially, the steady state rate is two orders of magnitude lower than that of nickel deposited alone (Curve A), but after 6.0 hours the Ni-K mixture has kept its initial activity while Ni alone has deactivated completely. The carbon conversion for this catalyst after 6.0 hours is 2.5%, ten times lower than that of nickel alone. But when the experiment represented by Curve B was followed 400 hours, a total carbon conversion of 20% was obtained and the catalyst was still active. When a mixture of nickel and potassium oxides is deposited on graphite with a Ni/K molar ratio equal to 10.0 and a Ni/C molar ratio equal to  $1.0 \times 10^{-2}$ , an initial rate similar to that of nickel deposited alone is obtained (Curve C), but instead of deactivating completely after two hours, the rate levels out at the same rate obtained with the 1:10 Ni:K mixture (Curve B). These results indicate that for the 10:1 Ni:K mixture only a fraction of the total nickel loading interacts with potassium. The remaining fraction behaves like Ni metal and it is completely inactive after one hour. The reaction rate decreases faster than in Curve A because there is less free nickel on the surface.

The rate of gasification of several chars with steam was studied as a function of time in the presence of a 1:1 mixture of nickel and potassium oxides. A description of the five chars studied is given in Table 1. For all of them, the steady state rate after 1.0 hour is at least one order of magnitude higher than that of graphite (see Figure 2a). This is reflected in a much higher carbon conversion after 6.0 hours (see Figure 2b), even though by then the char steam gasification rates have decreased to values similar to those of graphite.

A comparison of the gasification rates for a 1:1 mixture of potassium and nickel oxides with that of the components deposited alone is given in Figures 3a and 3b for two of the chars studied (Illinois No. 6 High Temp. Treat. and

Montana). In the case of Illinois No. 6 char, it is clear that the mixture is more active than the sum of the rates of the components deposited alone. (Compare Curves A and D in Figure 3a.) In contrast to the results obtained with graphite, the mixture in this case is more than two times as active as nickel deposited alone. For Montana subbituminous char the rate of gasification of the mixture is similar to that of nickel alone and higher than that of potassium (see Figure 3b).

A surface science study of the interaction of potassium, nickel and carbon in the presence of water is currently being done and some preliminary results are included in this communication. XPS of the  $Ni_{2p_{3/2}}$  signal of two systems, a 1:1 Ni:K mixture codeposited on graphite and nickel deposited alone have been obtained after exposing them to 24 torrs of water vapor at 950 K. The kinetic results show that at this temperature both systems are catalytically active. Figure 4 Curve A shows the spectrum corresponding to nickel deposited alone. There is a peak at 854.2 eV with a small satellite peak at 862.7 eV. This is characteristic of nickel in the metallic state and agrees with results obtained by us for nickel foil. The shoulder at 857.5 eV is due to small amounts of NiO in the sample. When nickel and potassium are codeposited on graphite (Curve B in Figure 4) the binding energy of the  $Ni_{2p_{3/2}}$  XPS peak is at 856.4 eV. This indicates that nickel is present in its +2 oxidation state. The much larger satellite peak at 864.6 eV also shows that nickel forms an oxide at this temperature in the presence of potassium. The lower binding energy of the  $Ni_{2p_{3/2}}$  peak in the nickel-potassium mixture compared to NiO shows that there is an electronic interaction between nickel and potassium.

### Discussion

The kinetic results presented in this paper indicate that mixtures of potassium and nickel oxides are good catalysts for the gasification of carbonaceous solids with steam. The high reaction rates and carbon conversions obtained with the several chars studied (Figures 2 and 3) and the graphite gasification activity after 400 hours support this conclusion.

In a previous publication we concluded that there is a cooperative effect between potassium and nickel in this catalyst.(6) The results in this paper present the clearest evidence obtained so far for this effect. In Figure 3a the gasification rate of Illinois N-6 char in the presence of the mixed catalyst is higher than that of the mathematical sum of the rates of the components deposited alone. The XPS results in Figure 4 show that nickel deposited alone is active as a gasification catalyst when it is present in the metallic state, while in the nickel-potassium mixture, the nickel is catalytically active being in the +2 oxidation state. Also, the shift to lower binding energies for the  $Ni_{2p_{3/2}}$  peak in the potassium-nickel catalyst when compared to the position of the NiO peak is evidence for chemical interaction between nickel and potassium. We propose that this synergistic effect is due to the formation of a mixed oxide ( $K_xNi_yO$ ) that is not readily reduced by carbon under our reaction conditions (< 1000K). There is evidence in the literature for the presence of several nickel-potassium mixed oxides,(8) but we do not have enough information to decide which one of them is present in our system.

The results presented in Figure 1 show that there is no interaction between the nickel metal catalyst and this potassium-nickel mixed oxide. When the ratio of nickel to potassium is high enough to allow the coexistence of these two catalysts on the graphite surface, the catalytic behavior observed can be explained by just adding the rates of the two catalysts; i.e. a very

high initial rate due to nickel metal that decays to a lower value and then remains constant for a long period of time due to the catalytic activity of the nickel-potassium mixed oxide.

Mixtures of transition metals and alkaline metals as catalysts for steam gasification of various carbon sources have been reported previously. Wigmams and Moulijn(9) reported that there was no interaction between nickel and  $K_2CO_3$  for the steam gasification of chars at 1023 K. Similar results were obtained in our laboratory when the gasification of graphite was studied above 1000 K. Also, XPS data obtained in our laboratory show that at 1000 K the nickel is present in the metallic state, even in the presence of potassium. We suggest that these results are due to the decomposition to this mixed oxide and reduction of the nickel by carbon. In contrast with the results reported by Moulijn and Wigmams, a cooperative effect between a transition metal and an alkaline metal has been reported by other authors. Adler and Hüttinger(10) found that mixtures of  $FeSO_4$  and  $K_2SO_4$  deposited on PVC coke were better catalysts than the salts deposited alone. Also, Suzuki et. al.(11) reported that  $Na(HFe(CO)_4)$  is a good catalyst for the gasification of various coals with steam. They suggest that this high activity is due to the interaction between iron and sodium.

Further work is currently being done to obtain more direct evidence of the existence of these mixed oxides and to characterize and understand their catalytic behavior toward carbon gasification.

#### Acknowledgment

The authors want to thank Dr. B. J. Wood of SRI International for providing the char samples used in this work and their elemental analysis.

This work was supported by the Assistant Secretary for Fossil Energy, Office of Management Planning and Technical Coordination, Technical Coordination Division of the U.S. Department of Energy under Contract Number DE-AC03-76SF00098, through the Morgantown Energy Technology Center, Morgantown, W.VA. 26505.

J. Carrazza acknowledges CEPET of Venezuela for a research fellowship.

#### References

1. B.J. Wood and K.M. Sancier, Catal. Rev.-Sci. Eng. 26, 233 (1984).
2. W.Y. Wen, Catal. Rev.-Sci. Eng. 22, 1 (1980).
3. F. Delannay, W.T. Tysoe, H. Heinemann and G.A. Somorjai, Carbon 22, 401 (1984).
4. D.W. McKee, Carbon 12, 453 (1974).
5. P.L. Walker, Jr., S. Matsuura, T. Hanzana, T. Muira and I.M.K. Ismail, Fuel 62, 140 (1983).
6. J. Carrazza, W.T. Tysoe, H. Heinemann and G.A. Somorjai, J. Catal. 96, 234 (1985).
7. A.L. Cabrera, H. Heinemann and G.A. Somorjai, J. Catal. 75, 7 (1982).
8. M.G. Baker and A.P. Dawson, J. Less. Common Met. 45, 323 (1976).
9. T. Wigmams and J.A. Moulijn, Stud. Surf. Sci. Catal. 7, 501 (1981).
10. J. Adler and K.J. Hüttinger, Fuel 63, 1393 (1984).
11. T. Suzuki, M. Mishima and Y. Watanabe, Fuel 64, 661 (1985).
12. O.P. Mahajan, R. Yarzab and P.L. Walker, Jr., Fuel 57, 643 (1978).

TABLE 1  
 Characteristics of Coal Char and Graphite Samples Used in this Study

Name	ASTM Rank <sup>d</sup>	Pre-treatment	Analysis (wt%) <sup>b</sup>					
			C	H	M	O	S <sup>c</sup> Ash <sup>d</sup>	
Western Kentucky Washed (MS)	HW.B.Bit.	Unspecified	72.3	3.2	1.4	7.9	3.2	12
North Dakota Husky (NOHL)	Lightite	Partial Steam Gasification T = 1200K	71.2	1.1	0.37	13-17	2.0	8-12 <sup>e</sup>
Montana (MS)	Subbituminous	Partial Steam gasification: T = 1200K	66.0	1.1	0.20	-	0.92	-
Illinois M-6 High Temp. (I & HT)	HW.C. Bit.	Heated Under He T = 1300K	-	-	-	-	-	-
Illinois M-6 Low Temp. (I & LT)	HW.C. Bit.	Pregasifier Heater T = 800K	72.0	3.3	1.5	10.9	2.6	9.1
Graphite UCP-2		None	100	0	0	0	0	0

<sup>a</sup> HW. = High volatility B and C indicate bituminous classes.  
<sup>b</sup> Dry mineral matter containing basis. Oxygen by difference.  
<sup>c</sup> Total sulfur.  
<sup>d</sup> By low temperature technique (oxygen plasma).  
<sup>e</sup> Not measured. Range of values reported in reference 12.

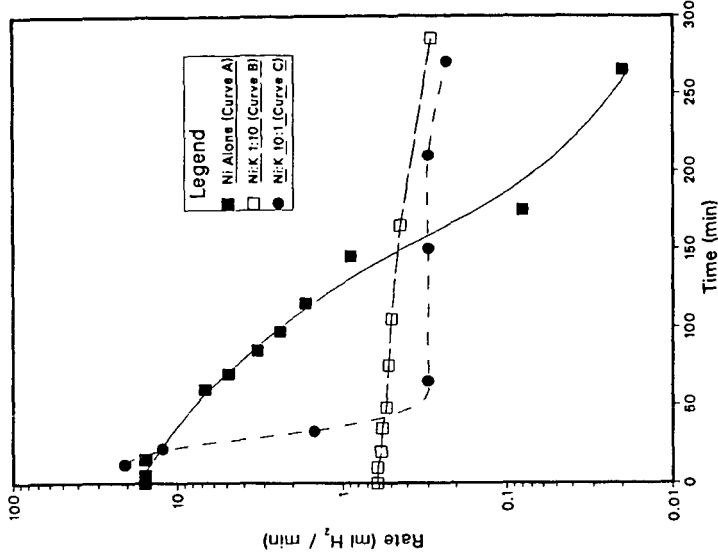


Figure 1: Steam gasification rates of graphite at 893 K catalyzed by three different compounds: nickel metal (Curve A) and two mixtures of nickel and potassium oxides, Ni:K 1:10 (Curve B) and Ni:K 10:1 (Curve C). In all cases the Ni/C molar ratio is equal to 1.0 x 10<sup>-2</sup>.

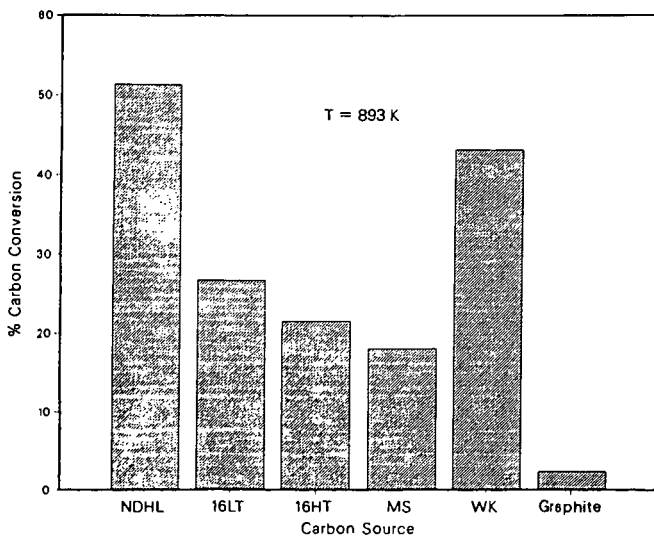
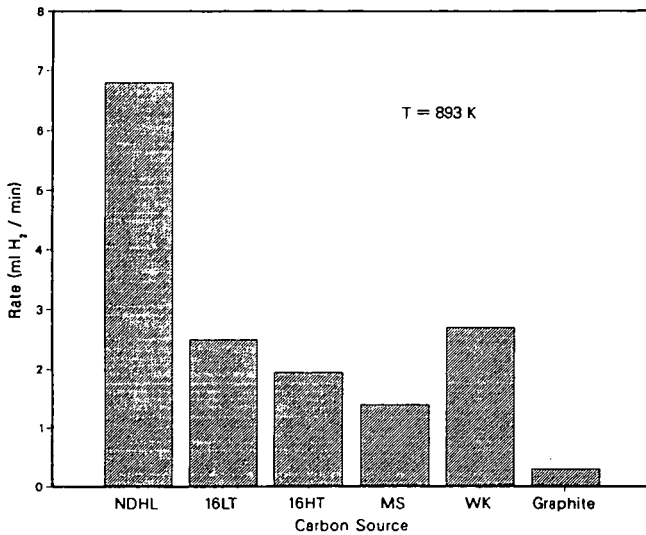


Figure 2a (Top). Steady state steam gasification rates of several carbonaceous solids after 1.0 hours when a mixture of nickel and potassium oxides is used as a catalyst.  
 Figure 2b (Bottom). Percentage of carbon conversion obtained after 6.0 hours when the same catalyst is used.

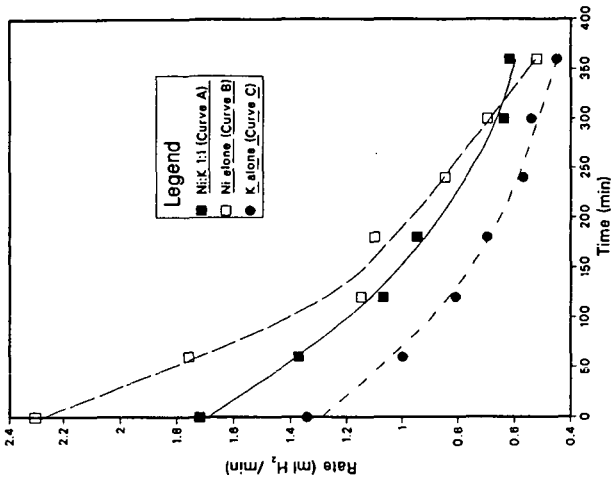


Figure 3b

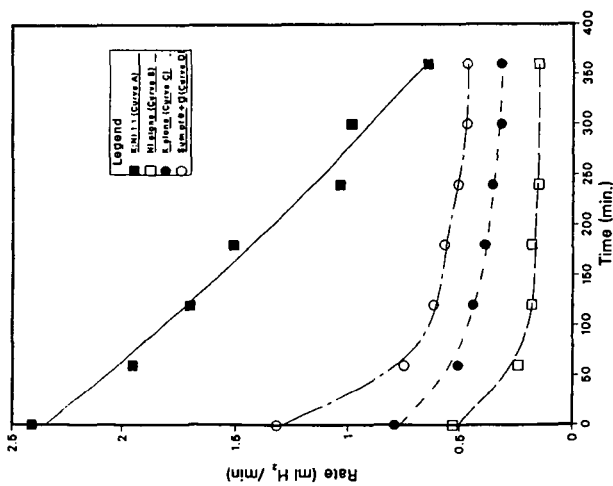


Figure 3a

Figure 3: Steam gasification rates at 893 K for two chars, Illinois #1 and Montana (right), catalyzed by three different compounds, a 1:1 mixture of nickel and potassium (Curve A), nickel alone (Curve B) and potassium alone (Curve C). In figure 3a, Curve D is the mathematical sum of curves B and C.

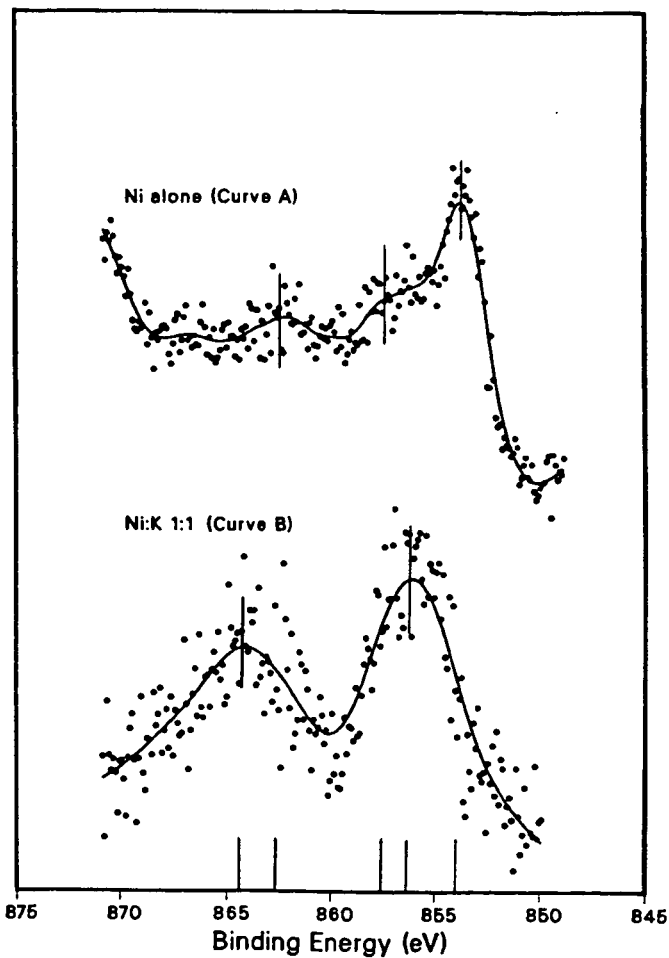


Figure 4. Ni  $2p_{3/2}$  XPS of nickel (Curve A) and a 1:1 Ni:K mixture (Curve B) deposited on graphite. The spectra was taken after exposing the samples to 24 torr of water at 923 K for 15 min.

## CATALYZED STEAM GASIFICATION OF LOW-RANK COALS TO PRODUCE HYDROGEN

R.E. Sears, R.C. Timpe, S.J. Galegher, and W.G. Willson

University of North Dakota Energy Research Center  
Box 8213, University Station  
Grand Forks, North Dakota 58202

### Abstract

Advance coal gasification technologies using low-rank coal is a promising alternative for meeting future demand for hydrogen. Steam gasification tests conducted at temperatures between 700° and 800°C and atmospheric pressure resulted in product gas compositions matching those predicted by thermodynamic equilibrium calculations, 63-65 mol% hydrogen and less than 1 mol% methane. Steam gasification tests with four low-rank coals and a single bituminous coal were performed in a laboratory-scale thermogravimetric analyzer (TGA) at temperatures of 700°, 750°, and 800°C to evaluate process kinetics with and without catalyst addition. Catalysts screened included  $K_2CO_3$ ,  $Na_2CO_3$ , trona, nahcolite, sunflower hull ash, and recycled lignite ash. North Dakota and Texas lignite chars were slightly more reactive than a Wyoming subbituminous coal char and eight to ten times more reactive than an Illinois bituminous coal char. Pure and mineral (trona and nahcolite) alkali carbonates and recycled ash from  $K_2CO_3$ -catalyzed steam gasification tests substantially improved low-rank coal steam gasification rates. The reactivities obtained using trona and nahcolite to catalyze the steam gasification were the highest, at nearly 3.5 times those without catalysts.

### Introduction

Hydrogen is a key component in petroleum refining, petrochemical processing, the production of coal-derived synfuels, and can also be used directly as a fuel. Over the next 45 years, the demand for hydrogen has been projected to increase by a factor of 15 to 20 (1). Most of the hydrogen currently used in chemical applications is produced through steam reforming of natural gas; and in refining applications partial oxidation of petroleum is also used. Advanced coal gasification technologies appear to be the most probable alternative for meeting the future demand for large quantities of hydrogen. Low-rank coals (lignites and subbituminous coals) are candidate feedstocks for such applications because of their low mining cost and higher reactivity relative to higher rank coals.

The two most important considerations in the design of a process for producing hydrogen from coal are to maintain operating conditions that thermodynamically favor the production of hydrogen and carbon dioxide over carbon monoxide and methane, and to obtain reaction rates that result in reasonable gasifier throughput. Optimization of the hydrogen content of the product gas requires steam gasification at relatively mild temperatures in the range of 700° to 800°C and at atmospheric pressure. In tests at the University of North Dakota Energy Research Center (UNDERC), a dry synthesis gas containing 63 mol% hydrogen was produced by steam gasification of low-rank coal (2), which is predicted by equilibrium thermodynamics. These mild conditions do not, however, promote high reaction rates. As a result, achieving the maximum coal reactivity by the use of catalysts is perhaps the most critical factor in producing hydrogen from coal.

The physical and chemical nature of low-rank coals (LRCs) offer several advantages for a gasification process producing hydrogen. One of these is their enhanced reactivity compared to coals of higher rank. This increase in reactivity is caused by higher concentrations of active sites, higher porosity, and a more uniform dispersion of alkali impurities that act as inherent catalysts (3,4,5).

The high volatile matter content of lignites could also support their use in steam gasification to produce hydrogen. If introduced into the hot zone of a gasifier, devolatilization products may be cracked to form additional hydrogen (6). Under suitable reaction conditions raw product gas from such a system would then contain essentially only hydrogen, carbon dioxide, carbon monoxide, and only small quantities of methane and sulfur gases. In addition to producing hydrogen and simplifying downstream gas clean-up, cracking of tars and oils in the gasifier would also reduce contaminant concentrations in the process condensate.

Even with the higher reactivities of LRCs, it will be necessary to enhance reaction kinetics through the use of catalysts to obtain economic reactor throughput. There is a wealth of data relating to the use of a variety of catalysts to enhance the steam gasification kinetics (7 - 16). Alkali metals are generally accepted as the premier steam gasification catalyst (12,13,16) and thus their interactions with ash constituents and subsequent recovery are important factors in the process economics. Catalyst recovery problems associated with the formation of insoluble potassium aluminosilicates were identified during recovery of the  $K_2CO_3$  catalyst in the Exxon Catalytic Coal Gasification (CCG) process (6). For some high sodium LRCs, a problem of sodium dilution of the recovered potassium catalyst could be significant. However, if sodium carbonates are also effective catalysts, the problem of alkali recovery will be mitigated, especially with high sodium LRCs.

The overall objective of the program at UNDERC is to establish the feasibility of using low-rank coal gasification to produce hydrogen. This paper summarizes the findings of a thermogravimetric analysis (TGA) study of steam-char gasification kinetics. This work focused on low-rank coals, with limited testing using a bituminous coal for comparison purposes, and the addition of various catalysts to enhance low-rank coal reactivity.

### Experimental

The reaction between low-rank coal chars and steam was studied using a DuPont 951 Thermogravimetric Analyzer (TGA) interfaced with a DuPont 1090 Thermal Analyzer. The TGA reaction chamber was an open quartz tube, secured to the balance by means of a threaded nut as shown at point (A) in Figure 1. The opposite end of the quartz tube (point (B) in Figure 1) was connected by rubber tubing to a ventilation hood. The commercially available TGA system was modified for char/steam experiments by adding the steam sidearm shown as point (C) in Figure 1. This port was sealed with a high-temperature gas chromatography septum. The steam inlet line (1/8-inch stainless steel) was passed through this septum and into the reaction chamber (point (D) in Figure 1). Steam was prepared using a "Hot Shot" MB-3L electric steam boiler. The length of steam line from the exit of the boiler to the reaction chamber sidearm was heated continuously at 200°C using electrical heat tape. The reaction chamber was heated in a program-controlled tube furnace.

Approximately 20 mg, weighed to the nearest 0.01 mg, of as-received coal ground to particle sizes of -100 x +140 mesh, was evenly distributed on a tared 11-mm diameter platinum pan supported at the end of the TGA's quartz balance beam. Coal samples were devolatilized in argon prior to the introduction of steam into the reaction chamber. Argon flow was maintained at approximately 160 cc/min while the coal sample was heated from room temperature to the target reaction temperature (700° to 800°C) at a rate of 100°C/min. The average time for devolatilization of these samples was about 15 minutes.

Char samples produced by the devolatilization procedure were weighed in the TGA reaction chamber without cooling. Argon flow was reduced from 160 to 60 cc/min, and steam to the reactor was then started at rates of 1-5 mg/min. Steam flow rates were determined prior to experiments by collecting steam from the gas outlet (point (B) in Figure 1) in a cold, tared vessel for approximately 15 minutes.

Weight, time, and temperature were recorded by the DuPont 1090 Thermal Analyzer as the char-steam reaction proceeded. Experiments were terminated when the sample's weight loss approached zero, or in the case of very slowly reacting materials after 150 minutes of reaction time. The 1090 Thermal Analyzer was then used to plot sample weight loss versus time and to print sample weight, temperature, and reaction time data. Product gases from the system were not analyzed.

Both aqueous impregnation and dry catalyst mixing were evaluated in the TGA steam gasification test. Preliminary TGA tests showed that reactivity was not dependent on catalyst addition technique; therefore, only dry-mix systems were used in the remainder of the TGA test program.

## Results

The matrix of char-steam gasification tests conducted by laboratory TGA included experiments for evaluation of coals, catalysts, temperature, and catalyst loading. Indian Head and Velva lignites from North Dakota, Martin Lake lignite from Texas, Wyodak subbituminous coal from Wyoming and River King bituminous coal from Illinois were evaluated. Proximate and ultimate analyses of these coals are given in Table 1. The coal analyses in Table 1 show an uncharacteristically low moisture content for Indian Head lignite. The low moisture content of this sample, 12.6 wt%, resulted from storage in a large nitrogen purged bunker in which a definite moisture gradient was observed from top to bottom, but did not effect the reactivity of the char.

Table 1. Coal Proximate and Ultimate Analysis

	Indian Head		Velva	Martin Lake	Wyodak	River King
	A <sup>a</sup>	B <sup>b</sup>				
<b>Test Coal Analyses:</b>						
Moisture, %	12.6	29.5	33.7	25.1	27.5	11.5
Ash, wt%, mf	17.7	9.0	10.4	22.1	9.6	12.1
Volatile Matter, wt%, mf	38.4	41.2	42.8	39.5	42.3	42.5
Fixed Carbon, wt%, mf	43.9	49.8	46.8	38.4	48.1	45.3
Heating Value, Btu/lb, as-rec'd	8,383	7,721	6,755	7,258	8,043	11,000
<b>Ultimate Analysis of Raw Coals, wt%, mf:</b>						
Ash	17.7	9.0	10.4	22.1	9.6	12.2
Carbon	58.9	65.0	62.4	56.7	65.7	68.3
Hydrogen	3.3	4.2	3.8	3.8	4.3	5.1
Nitrogen	1.6	1.9	1.4	1.2	1.2	1.3
Sulfur	1.0	0.8	0.5	1.9	0.5	4.0
Oxygen (by diff)	17.5	19.1	21.5	14.3	18.7	9.1

<sup>a</sup>Low-moisture Indian Head coal used for majority of TGA work.

<sup>b</sup>Indian Head sample used to verify initial TGA results.

Various alkali sources were tested as catalysts to promote the steam-carbon reaction. These were  $K_2CO_3$ ,  $Na_2CO_3$ , trona, nahcolite, sunflower hull ash (a naturally high potassium containing ash), and recycled lignite gasification ash. These substances were selected as prospective catalysts based on their high alkali content. Catalysis with inexpensive or "disposable" catalysts would substantially improve the economics of a hydrogen-from-coal process. Likewise, trona and nahcolite, naturally occurring alkali carbonate materials, are inexpensive relative to pure carbonates ( 0.04/lb for trona compared to 0.34/lb for  $K_2CO_3$  and 0.20/lb for  $Na_2CO_3$ ). This cost differential suggests their use as disposable catalysts.

### Reactivity of Coals for Steam Gasification

Tests were performed to establish the uncatalyzed reactivities of the five test coal chars and plotted in Figure 2. It shows the higher reactivity of low-rank coals compared to that of River King bituminous coal. The higher reactivity of low-rank coal chars, documented by many research groups (3,4,5), is believed to be a result of the higher mineral content, higher concentrations of active sites and increased porosity of the low-rank coals. Figure 2 also illustrates the linearity of conversion over the 0 to 50 % carbon conversion range.

Over the initial linear portion of the curves in Figure 2, the carbon conversion rates for the three lignites were nearly identical, with Indian Head being only slightly less reactive than the Velva and Martin Lake lignites. However, a definite hierarchy of reactivity developed as the available carbon supply was depleted. During reaction of the final 40% of the carbon, Martin Lake lignite showed the most rapid conversion, followed by Velva and Indian Head.

Steam gasification kinetic data was collected over the range of 700° to 800°C for assessing temperature effects. The increase in reactivity of each LRC with increasing temperature is shown in Figure 3. Increasing the gasification temperature from 700° to 800°C was found to increase reactivities from 2.5 times for Martin Lake lignite to 3.8 times for Wyodak subbituminous coal. Equilibrium gas composition modeling and actual product gases from a 1-lb fixed-bed system showed that the hydrogen content of the gas is virtually unaffected by this temperature increase (17). Apparent energies of activation were also calculated from this data and have been reported previously (18).

### Steam Gasification of Catalyzed Coals

Figure 4 shows the rates of carbon conversion at 750°C for each test coal with a 10 wt%  $K_2CO_3$  loading. Comparison of the data in Figure 2 to that in Figure 4 shows that  $K_2CO_3$  addition significantly enhanced the reactivity of each coal. As was the case for the uncatalyzed coals, the reactivity of the catalyzed low-rank coals was far superior to that of the  $K_2CO_3$ -catalyzed bituminous coal. However, the reactivity ranking of the four low-rank coals was not the same as that observed without catalyst addition. In Figure 2 Martin Lake lignite was shown to have the most rapid uncatalyzed conversion rate; however, in Figure 4, Martin Lake was shown to have the poorest reactivity of the four similarly catalyzed low-rank coals. Conversely, Wyodak subbituminous coal was the least reactive uncatalyzed low-rank coal, but showed excellent carbon conversion rates in tests using  $K_2CO_3$ .

The effect of temperature on the reactivity of each of the four  $K_2CO_3$ -catalyzed low-rank coals is illustrated in the bar graph of Figure 5. The trend in reactivity of the  $K_2CO_3$ -catalyzed coals with a temperature increase from 700° to 800°C was very similar to that shown for the uncatalyzed coals in Figure 3, with reactivity increasing by a factor of two over the temperature range. For the uncatalyzed coals, the average reactivity increased by a factor of three over this temperature range. It has previously been reported that the addition of  $K_2CO_3$  decreased the apparent energies of activation by as much as 60% compared to the uncatalyzed coals (18).

Several TGA steam gasification tests were performed to evaluate the effect of  $K_2CO_3$  concentration on lignite reactivity. Velva lignite was used for these tests as it resulted in the highest reactivity of the four LRCs tested. Tests were conducted at 750°C using catalyst loadings from 2 to 20 wt%. Data collected from these experiments were used both to evaluate the effect of catalyst loading for each of the two carbonates, and to compare the two carbonates catalytic effect over a range of loadings. Table 2 presents the average reactivities at 50% carbon conversion for the range of loadings evaluated with both  $K_2CO_3$  and  $Na_2CO_3$ , which indicates a lesser dependence of reaction kinetics on catalyst loading using  $Na_2CO_3$ . Neither catalyst produced a significant rate increase at loadings over 10 wt%; however, the reactivity increase with increasing catalyst loading upto 10 wt% was more pronounced for  $K_2CO_3$  catalysis. Over the 2 to 10 wt% loading range, reactivity values for  $K_2CO_3$ -catalyzed Velva lignite increased from 3.3 to 5.5 (g/hr)/g, while the corresponding increase for the  $Na_2CO_3$ -catalyzed lignite was from 4.8 to 5.5 (g/hr)/g.

Table 2. Effect of Variable Catalyst Loadings on Velva Lignite Char Reactivity in Steam at 750°C

Catalyst Loading wt% of As-received Coal	$\bar{k}_{0.5}$ , (g/hr)/g	
	$K_2CO_3$	$Na_2CO_3$
0	2.0	2.0
2	3.3	4.8
5	4.1	4.9
10	5.5	5.5
15	5.7	5.9
20	5.7	6.1

#### Comparison of Catalyst Effectiveness

Data plotted in Figure 6, compares carbon conversion rates for uncatalyzed Velva lignite and for Velva catalyzed with each of the six additives found to give positive catalytic effects. The nearly identical reactivities observed for  $K_2CO_3$  and  $Na_2CO_3$  catalysis are illustrated, as the two conversion curves are superimposable throughout the gasification phase. Figure 6 also illustrates the catalytic effects of sunflower hull ash and the mineral additives. Twenty percent sunflower hull ash (23 wt% potassium) was less effective than 10% loadings of the carbonates; however, reactivity was much improved over the uncatalyzed coal, with complete conversion occurring in less than 20 minutes. The reactivity for the 20% sunflower hull ash/Velva lignite system at 750°C was 4.3 (g/hr)/g as compared to only 2.0 (g/hr)/g without additives.

Perhaps the most significant results illustrated in Figure 6 were the rapid carbon conversions obtained using trona and nahcolite as gasification catalysts. Both trona and nahcolite produced more rapid conversion of Velva lignite than did addition of the pure carbonates. Approximately 90% carbon conversion was achieved in 8 minutes using either 10 wt% trona (29% sodium) or nahcolite (15% sodium), whereas when using the same wt% pure  $K_2CO_3$  (47% potassium) or  $Na_2CO_3$  (37% sodium) about 10 minutes was required to achieve 90% conversion. For trona catalysis a reactivity of 6.9 (g/hr)/g was obtained compared to 5.5 (g/hr)/g using an identical loading of either  $K_2CO_3$  or  $Na_2CO_3$  at the same gasification conditions. At these conditions, nahcolite catalysis resulted in a reactivity slightly lower than that obtained using trona (6.2 (g/hr)/g).

The effectiveness of these naturally occurring mineral catalysts is important to the development of a commercial hydrogen-producing steam coal gasification process. Based on the relative costs of the feedstock, use of these materials would be more favorable to process economics than would pure alkali carbonates. An additional consideration is that cost and availability of these materials may be such that catalyst recovery would be unnecessary.

### Conclusions

Uncatalyzed lignites and a subbituminous coal were found to be eight to ten times more reactive with steam at 700°-800°C than an Illinois bituminous coal. This relationship, within this narrow temperature range, is important as this is the range that thermodynamically favors the production of hydrogen from steam gasification at atmospheric pressure. The reactivity of the uncatalyzed coals increased 3 to 4 times with an increase in steam gasification temperature from 700° to 800°C.

For the catalyzed coals during steam gasification:

- o Reactivity increased approximately 2 times over the 700° - 800°C temperature range for low-rank coals catalyzed with potassium carbonate.
- o Sodium carbonate was found to be as effective a catalyst as potassium carbonate for the steam gasification of low-rank coal chars on a mass loading basis.
- o Alkali carbonate loadings equal to 10 wt% of the as-received coal mass resulted in low-rank coal reactivities 2.5 to 3.5 times higher than those measured for the uncatalyzed low-rank coals.
- o Naturally occurring mineral sources of sodium carbonates/bicarbonates, trona and nahcolite, are as effective in catalyzing low-rank coal steam gasification as the pure carbonates.
- o Use of these naturally-occurring carbonates sources should be a primary focus of continued research. The low cost of trona or nahcolite relative to the pure carbonates suggests that a potential for their use as disposable catalysts exists which would enhance operability and process economics in a hydrogen-from-coal gasification process.

### Acknowledgments

The authors would like to acknowledge Robert C. Ellman and John G. Hendrikson who were instrumental in development and initial supervision of the research. This research was sponsored through the Grand Forks Project Office (GFPO) of the United States Department of Energy. A special thanks for their enthusiastic support is extended to Leland E. Paulson, Technical Project Officer, Fred Bauer of the GFPO, and to Madhav Ghatge, Manager AR & TD Gasification - Morgantown for funding.

## References

1. Pohani, B.P. J. Japan Petrol. Inst., 27, 1, 1984.
2. Low-Rank Coal Research, University of North Dakota Energy Research Center, Quarterly Technical Progress Report, July-September, 1984, DOE/FE/60181-1682.
3. Johnson, J.L. "Kinetics of Coal Gasification." Wiley and Sons, New York, 1979, 324 pp.
4. Linares-Solano, O.P. Mahajan, and P.L. Walker. Fuel, 58, 327, 1979.
5. Walker, P.L., S. Matsumoto, T. Hanzawa, T. Muira, and I.M.K. Ismail. Fuel, 62, 140, 1983.
6. Euker, C.A. and R.D. Wesselhoft. Energy Progress, 1, 12, 1981.
7. Taylor, H.S. and H.J. Neville, J. Am. Chem. Soc., 43, 2055, 1921.
8. Dent, F.J. et al., Trans. Instn. Gas Engrs., 88, 150, 1938.
9. Weller, S. and Pelipetz, M.C., Ind. Energy Chem., 43, 243, 1951.
10. Walker, P.L. et al., Chem. and Phy. of Carbon, 4, 287, 1968.
11. Haynes, W.P. et al., ACS Div. Fuel Chem. Proc., 18, No.2, 1, 1973.
12. Willson, W.G. et al., Adv. in Chem.-Coal Gasif., 154, 203, 1974.
13. Veraa, M.J. and A.T. Bell, Fuel, 57, 194, 1978.
14. Serageldin, M.A. and W.P. Pan, Thermochimica Acta, 76, 145, 1984.
15. Radovic, L.R. et al., Fuel, 63, 1028, 1984.
16. Tomita, A. et al., Fuel, 62, 150, 1983.
17. Low-Rank Coal Research. University of North Dakota Energy Research Center, Quarterly Technical Progress Report, April-June 1984, DOE/FE/60181-1642.
18. Timpe, R.C. et al., ACS Div. Fuel Chem., 30, No.4, 481, 1985.

## THERMOGRAVIMETRIC ANALYZER

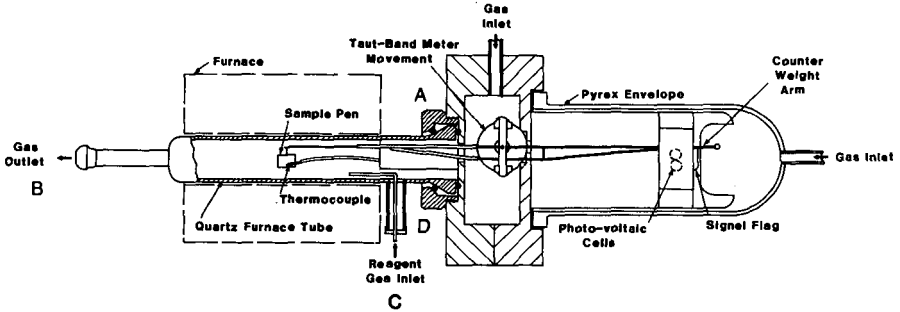


Figure 1. Thermogravimetric analyzer.

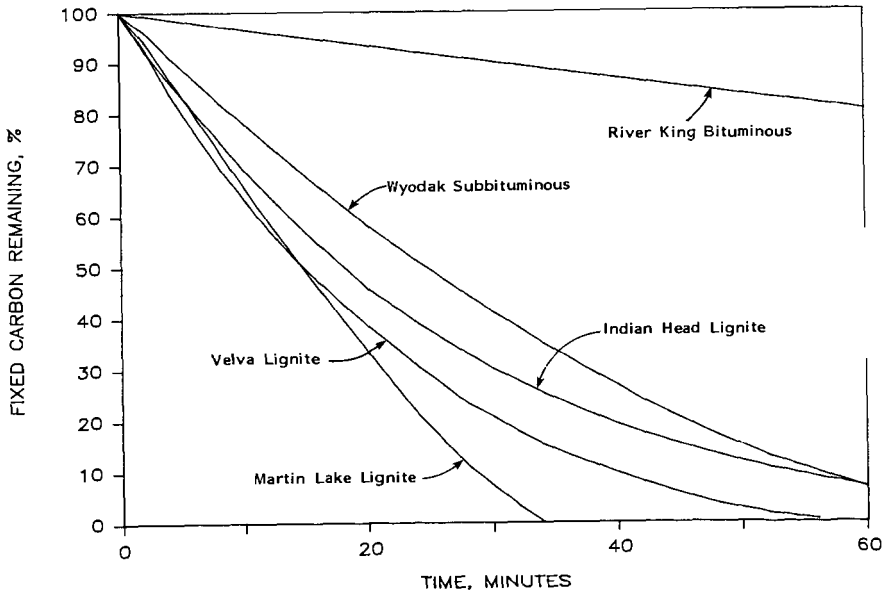


Figure 2. Rate of carbon conversion at 750°C - variation with coal rank.

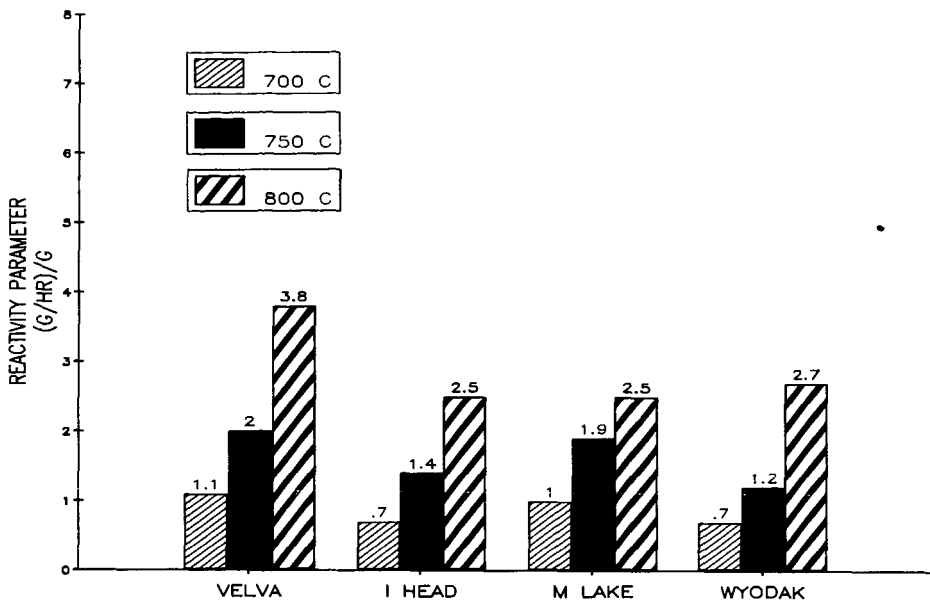


Figure 3. Reactivity of uncatalyzed low-rank coal chars as a function of steam gasification temperature.

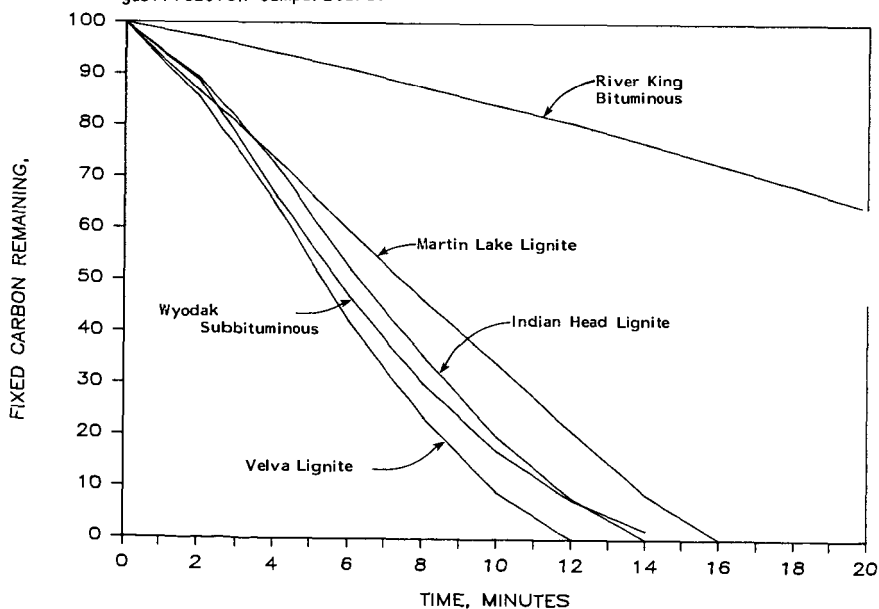


Figure 4. Carbon conversion of  $K_2CO_3$ -catalyzed coal chars at 750°C.

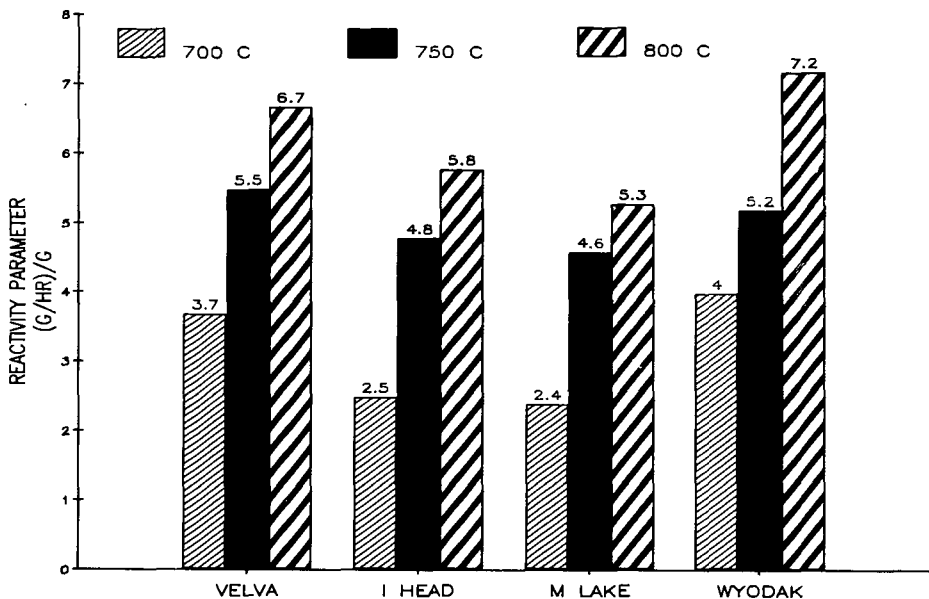


Figure 5. Effect of steam gasification temperature on the reactivity of  $K_2CO_3$ -catalyzed low-rank coal chars.

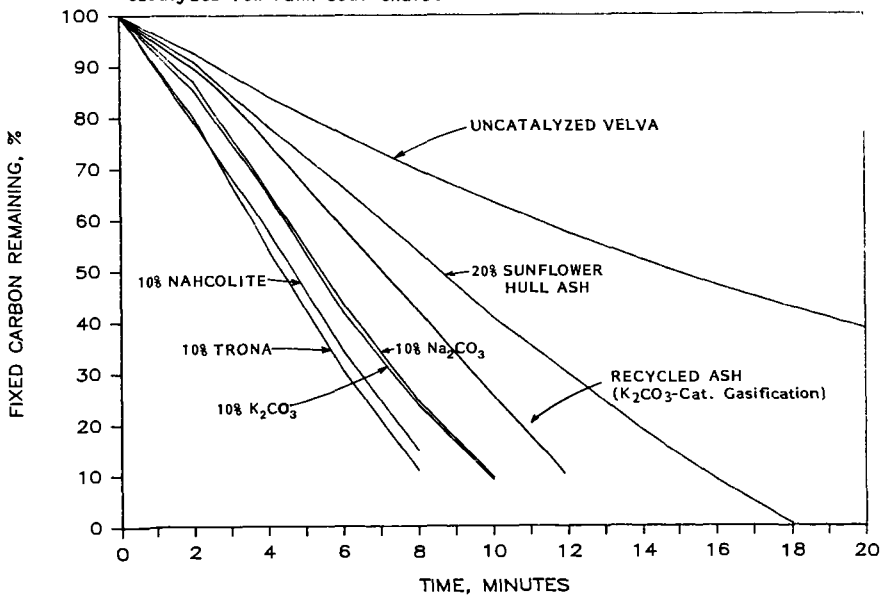


Figure 6. Rate of carbon conversion at 750°C for Velva lignite char catalyzed with various alkali sources.

## COAL GASIFICATION WITH INTERNAL RECIRCULATION CATALYSTS

by

A. H. Hill, G. L. Anderson  
Institute of Gas Technology  
3424 S. State Street  
Chicago, IL 60616

and

M. R. Ghatge, W. Liou  
U.S. Department of Energy  
Morgantown Energy Technology Center  
P.O. Box 880  
Morgantown, WV 26507

One of the primary economic penalties of many catalytic coal gasification processes is recovery of the added catalysts from the spent char. For example, the EXXON catalytic coal gasification process as presently conceived, requires several stages of digestion with calcium hydroxide to recover potassium from the converted char and then the digestion only recovers between 65 and 85% of the potassium.<sup>1</sup>

Recently, IGT has been exploring a process concept that might avoid this complex and costly situation. In the IGT process concept, a coal gasification process with an inherent thermal gradient (e.g., Lurgi, staged fluidized-bed processes, etc.) and a catalyst that is semivolatile under gasification conditions are used. The semivolatile catalyst is sufficiently volatile at the highest temperature encountered in the lower section of the gasifier, that it is completely vaporized from the char before the char is discharged. The catalyst, however, is nonvolatile at the lowest temperature encountered in the upper section of the gasifier so that it precipitates on the cold, feed coal. The catalyst, therefore, is automatically recycled from the product char to the fresh coal and the need for catalyst recovery is eliminated.

Three different materials have been undergoing testing by IGT as semivolatile catalysts. These materials were selected based on an examination of their vapor pressures and the following process assumptions. It was assumed that a catalyst loading of approximately 5 wt % is sufficient for catalyzing the gasification reactions, that the temperatures in the gasifier vary from 600° to 1600°F, that the gasifier operates at 1000 psig with a product gas/coal feed ratio of 15 SCF/lb, and that a rate of loss of catalyst in the product gas of less than 1% of the circulation rate of the catalyst in the gasifier is acceptable. With these assumptions, the requisite vapor pressure of the "semivolatile" catalyst in the hottest section and the coldest section of the gasifier was calculated to be greater than 1.0 atmosphere at 1600°F (870°C) but less than 10 mm Hg at 600°F (315°C).

The materials identified to have the proper physical properties are shown in Table 1. Arsenic in its elemental form is relatively stable under reducing conditions. Some arsine, AsH<sub>3</sub>, formation is expected; but at high total arsenic partial pressures and moderate temperatures, more than 99% of the gas phase arsenic is expected to be present as As<sub>2</sub> and As<sub>4</sub>. Although less is known about the behavior of cadmium, studies have shown that fines generated in coal gasification are highly enriched in cadmium, indicating "semivolatile"

Table 1. MATERIALS WITH VAPOR PRESSURES IN THE DESIRED RANGE FOR A "SEMIVOLATILE" CATALYTIC COAL GASIFICATION PROCESS

Element	Temperature (°F) for a Vapor Pressure of:	
	10 mm HG	1 atm
Arsenic	819	1130
Cadmium	903	1403
Cesium Hydroxide	1160	1790

behavior in the gasifier. Cesium hydroxide, on the other hand, is known to enhance the reactivity of carbon towards steam.<sup>2</sup> Studies have also presented evidence for the volatility of cesium hydroxide under gasification conditions.<sup>3</sup>

This paper summarizes the results of 1) laboratory-scale batch reactor screening tests conducted to evaluate the performance of arsenic, cadmium and cesium hydroxide as catalysts for coal gasification and 2) continuous bench-scale tests with cesium hydroxide, the most effective catalyst tested in the initial screening tests, to determine the volatility of cesium hydroxide, i.e., its release from the char before discharge, under continuous gasification conditions.

#### EXPERIMENTAL

**Laboratory-Scale Screening Tests.** During the catalyst screening portion of the project, 49 char gasification tests were conducted in the laboratory-scale batch reactor catalyst testing unit pictured in Figure 1. The reactor is constructed of Rene 41 steel and is 12-inches high with a 0.05-inch I.D., a 2-inch O.D., and a 28-cm<sup>3</sup> capacity. The high temperature valve (Figure 1) has an extended stuffing box which allows the body of the valve to be located in the furnace with the reactor. This is necessary to avoid condensation of both the steam and semivolatile catalyst during the test. Tests were conducted with devolatilized North Dakota lignite and Illinois No. 6 bituminous coal chars. The chars were prepared in a separate 1-inch-diameter fluidized-bed reactor with nitrogen as the fluidizing gas. Analyses of the chars used in the study are presented in Table 2.

The batch reactor char gasification tests were conducted under the following conditions:

Temperature:	1200°, 1300°, 1400°F
Initial Pressure:	~160 psig
Gasifying Medium:	Steam, Hydrogen
Char Particle Size:	~200 Mesh
Char Residence Time:	3, 6 h
Catalyst Loading:	10 Wt %
Char Sample Weight:	~200 mg

The experimental procedure was as follows. With arsenic or cadmium, the char and the appropriate amount of powdered metal were thoroughly mixed in a high-speed pulverizing shaker. About 220 milligrams of the mixture was then weighed out and placed in a small quartz test tube. A sufficient amount of water (~240µl) was then added to the mixture with a volumetric syringe such that the resultant water-to-carbon molar ratio was 1. In tests with cesium hydroxide, a 50 wt % solution of cesium hydroxide in water was added to the char in the test tube. Additional water was then added to give the required water/carbon molar ratio of 1.

Table 2. ANALYSIS OF THE CHARS USED IN THE LABORATORY-SCALE BATCH REACTOR GASIFICATION TESTS

<u>Elemental Analysis*</u>	North Dakota	Illinois No. 6
	<u>Lignite</u>	<u>Bituminous</u>
	-----wt % dry-----	
Carbon	75.88	80.90
Hydrogen	0.65	0.58
Nitrogen	0.86	1.21
Ash	20.86	14.16
Total	98.25	96.85

\* Carbon, hydrogen and nitrogen determined by ERBA analyzer (Automated Elemental Analyzer) which was used to analyze residues of all batch reactor tests.

The test tube containing the char/catalyst/water mixture was placed into the reactor, the reactor was reconnected to the system, and the system and reactor were then evacuated. To prevent losing the added water during evacuation, the reactor was placed in a dry-ice bath to freeze the water in the test tube. After evacuating the reactor, the dry-ice bath was removed, and the reactor was allowed to come to ambient temperature. The reactor was then placed into the furnace and was charged with sufficient hydrogen (~160 psig) such that the resultant hydrogen-to-carbon molar ratio is 1. After the reactor was charged with hydrogen, the high-temperature valve was closed, the remainder of the system was evacuated, and the furnace was allowed to heat up to the desired operating temperature. When the desired time had elapsed, the furnace was turned off and opened, allowing the reactor to cool to ambient temperature.

The reactor valve was then opened and the total system pressure was measured. This allowed the total moles of non-condensable gas in the system at the end of the test to be calculated. A sample of the product gas was then taken for analysis, and reactor was depressurized and opened. The test tube containing the mixture was removed from the reactor, and the residue was submitted for chemical analysis.

Bench-Scale Tests. Cesium hydroxide catalyzed and uncatalyzed char gasification tests were conducted in a 2-inch I.D. bench-scale unit (BSU). Nine tests were conducted in the BSU with North Dakota lignite and Illinois No. 6 bituminous chars. The chars used in the BSU gasification tests were prepared in an IGT 4-inch I.D. fluidized-bed reactor. Analyses of the chars used in the gasification tests are given in Table 3. The cesium hydroxide catalyst (Alfa Products®) was obtained as a hydrated solid containing about 85 wt % cesium hydroxide. It was deposited on the char by evaporation from solution under vacuum at 105°C.

The BSU is shown in Figure 2. It consists of a reactor (2-inch I.D., 39.125-inches long) and associated equipment for feeding and measuring the flow rates of char, steam, reference/purge gas (argon); for collecting and/or measuring the flow rates of residue char, liquid product, and product gas; and for collecting representative samples of the product gas.

In this unit char is fed to the top of the reactor by a calibrated screw feeder from a pressurized feed hopper, while the residue char is discharged from the bottom of the reactor into a pressurized residue receiver by a discharge screw. A piston-type metering pump is used to pump water from a reservoir into a steam generator that provides steam for the reactor.

Table 3. ANALYSES OF CHARs USED IN THE BSU GASIFICATION TESTS

Char Type	North Dakota Lignite	Illinois No. 6 Bituminous
Proximate Analysis, wt %		
Moisture	6.06	0.00
Volatile Matter	14.38	2.34
Fixed Carbon	64.69	81.59
Ash	14.87	16.07
	<u>100.00</u>	<u>100.00</u>
Ultimate Analysis, wt %		
Ash	15.83	16.07
Carbon	71.25	77.63
Hydrogen	1.87	0.91
Sulfur	1.54	2.58
Nitrogen	0.79	1.11
Oxygen	8.72	1.70
	<u>100.00</u>	<u>100.00</u>

The reactor steam enters the bottom of the reactor above the discharge screw through a dip tube. Metered and preheated argon is added as an internal reference and carrier gas and enters the bottom of the reactor between discharge screw and the exit of the steam dip tube.

Effluent gases from the top of the reactor pass through two water-cooled condensers in series. The condensed liquids are drained into separate vessels and weighed. An "aliquot" sample of the product gas is taken for componential analysis by feeding a portion of it into a water-sealed gas holder during selected periods of each test. "Spot" gas samples are also taken throughout the test period for componential analysis.

In a typical run, the reactor was initially filled with char and/or a char/catalyst mixture. After charging the reactor the system was flushed with argon. The temperatures of the reactor, steam pre-heater, super-heater and line heaters were then brought to operating temperatures in 1 to 2 hours and (except for Test 9) were maintained at these values for the duration of the test.

Gasification data were collected beginning immediately after the reactor furnace heaters were turned on and continued to be collected for 3 hours after the introduction of the steam to the reactor (fixed-bed operating period). Steam was fed after the lower zones of the reactor reached 1400°F.

Gasification data were also collected for an additional 5 hours after the 3-hour fixed-bed operating period under moving-bed conditions. Steady-state conditions were attained during the last two hours of the moving-bed operating period of Tests 2 and 3. "Steady-state" is defined as a condition wherein the reactor pressure is stable, the temperature profile in the bed, char feed rate and bed height are essentially constant.

In this study product gas compositions were determined by gas chromatography. Feed and residue char compositions and the carbon content of the condensate samples were determined by standard ASTM methods. The cesium content of the catalyzed feed and residue chars, steam condensate and the water used to rinse the reactor and product gas exit lines were determined by atomic absorption spectroscopy.

After each test was completed, the weight of the char fed was determined by weighing the char initially charged to the feed hopper and the char remaining in the feed hopper at the end of the test. The residue char was

also weighed after the test. Feed and residue char rates were calculated by dividing these weights by the measured char feeding time.

Results and Discussion. Figures 3 and 4 compare the measured effects of arsenic, cadmium and cesium hydroxide on the rate of gasification of lignite and bituminous char in the laboratory-scale batch reactor char gasification tests. The relative rate of gasification of the uncatalyzed and catalyzed chars are expressed in Figures 3 and 4 as reactivity ratios, i.e., the ratio of carbon conversions ( $X_c$ ) obtained in the catalyzed tests and the average of all the carbon conversions ( $X_c$ ) in the uncatalyzed tests at each temperature. A reactivity ratio value of one (shown by the horizontal line in each figure) indicates no effect of the catalyst on the char reactivity by the catalyst.

Although a great deal of scatter remains in the data shown in Figures 3 and 4, it is apparent that cesium hydroxide is more effective than arsenic or cadmium for char gasification. Increasing the reaction temperature strongly increases the catalytic effect of cesium hydroxide on the bituminous char reactivity, but has little effect on the lignite char reactivity.

A summary of the BSU gasification tests is given in Table 4. A number of operational problems prevented all but Tests 2 and 3 from being conducted under continuous moving-bed conditions. In Tests 4 and 5 (in which the catalyst was placed in reactor Zones 2 and 3 only), the formation of a clinker-like mass blocked the downward movement of the bed and, therefore, prevented residue discharge. In Tests 6, 7 and 9, moving-bed conditions could not be attained because the catalyzed char adhered to the reactor walls and prevented residue discharge.

The dry gas production rates for the tests with uncatalyzed and catalyzed bituminous char during the reactor heat-up and the fixed-bed operating periods are shown in Figure 5. The addition of catalyst to the bituminous char increased the gas production rate by as much as 72%.

The tests with catalyzed lignite char also showed consistently higher gas production rates than the tests without catalyst. In Tests 4 and 5, the catalyst was placed in the hottest zone of the reactor. The gasification rate with this distribution of catalyst quickly increased to very high values but then decreased rapidly as gasification proceeded, to the rates obtained with the uncatalyzed char. Distributing the catalyst evenly throughout the reactor, as was done in Tests 6 and 7, resulted in gasification rates that were initially slightly higher than in the tests with the uncatalyzed chars but the rate of gasification tended to decrease less rapidly with time. Although the lignite char showed higher overall gasification reactivity, the catalyst is 33% more effective in catalyzing the gasification of the less reactive bituminous as compared to the lignite char.

The dry gas constituent production rates during the reactor heat-up and fixed-bed operating periods for the uncatalyzed and catalyzed bituminous char are shown in Figure 6. Hydrogen and carbon dioxide account for most of the increases in the catalyzed dry gas production rates in both the bituminous and lignite char gasification tests. In the two lignite gasification tests, where the catalyst was concentrated in the two hottest zones of the reactor (Tests 4 and 5), a small increase in the production rate of carbon monoxide and methane relative to the hydrogen was observed.

Figures 7 and 8 compare the cumulative carbon gasified as a function of time for both char types during the fixed-bed operating period. A significant increase in the total amount of carbon gasified is shown in the catalyzed char tests. The extent of the increase is highly dependent on where the catalyzed char was initially placed in the reactor before heating.

The disposition of the cesium catalyst in the various solid and liquid product streams from the bench-scale reactor has been investigated. The results have thus far indicated minimal movement of the cesium from its initial position under the applied test conditions. This suggests that either higher temperatures or lower pressures might be required to effect cesium volatilization from the char.

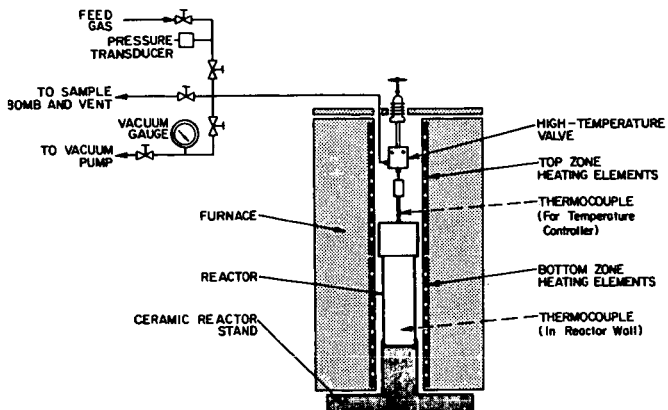
Plans are to conduct larger-scale BSU tests, wherein the operating problems encountered in the 2-inch BSU might be avoided, to answer this question.

#### ACKNOWLEDGEMENT

This work has been supported by the U.S. Department of Energy (Morgantown Energy Technology Center) under Contract Number DE-AC21-84MC21203

#### REFERENCES

1. Gallagher, J. E., Jr. and Euker, C. A., Jr., "Catalytic Coal Gasification for SNG Manufacture," International Journal of Energy Research 4, 137-147 (1980).
2. Cabera, A. L., Heinemann, H. and Somorjai, G. A., "Methane Production From the Catalyzed Reaction of Graphite and Water Vapor at Low Temperatures (500-600 K)," J. of Catalysis 75, 7-22 (1982).
3. Kosky, P. G. et al., "Coal Gasification Catalysis Mechanisms," Final Report to DOE for the period September 29, 1980-November 29, 1982. DOE/MC/14591-1397 (DE83011051), by General Electric Company, September 1982.



AB412117

Figure 1. LABORATORY-SCALE BATCH REACTOR CATALYST TESTING UNIT

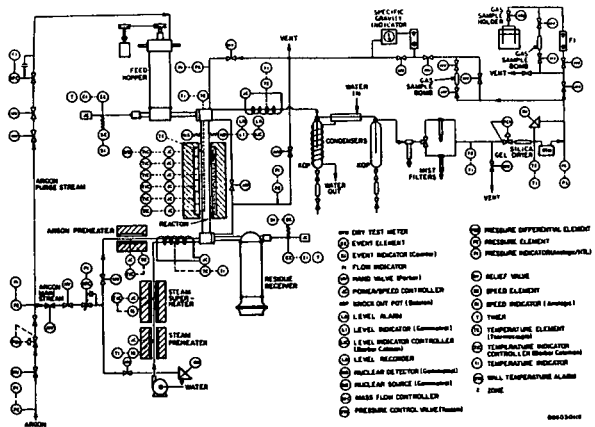


Figure 2. BENCH-SCALE REACTOR UNIT

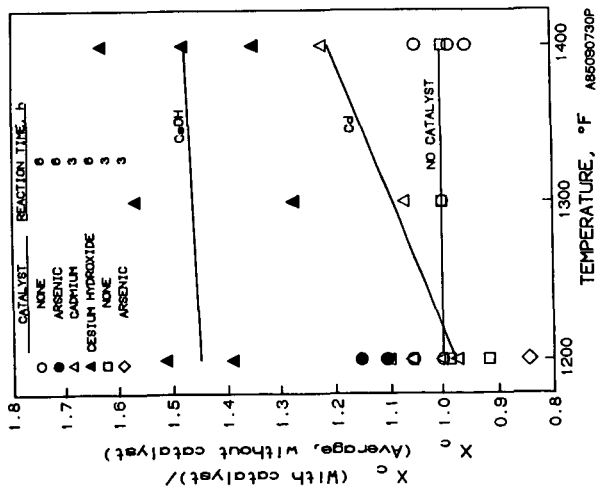


Figure 3. COMPARISON OF THE EFFECT OF ARSENIC, CADMIUM AND CESIUM HYDROXIDE ON THE REACTIVITY OF LIGNITE CHAR

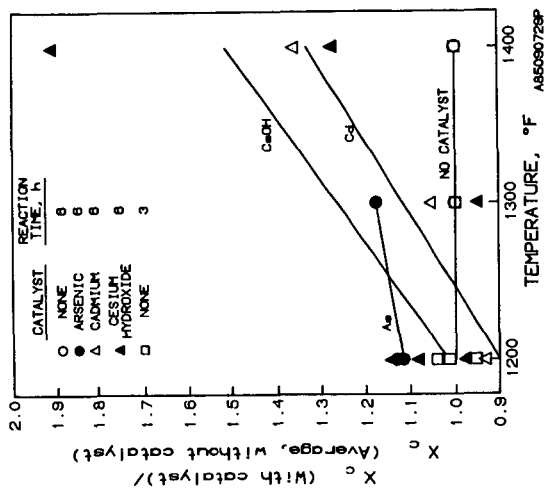


Figure 4. COMPARISON OF THE EFFECT OF ARSENIC, CADMIUM AND CESIUM HYDROXIDE ON THE REACTIVITY OF BITUMINOUS CHAR

Table 4. SUMMARY OF THE NORTH DAKOTA LIGNITE AND ILLINOIS NO. 6 BITUMINOUS CHAR BSU GASIFICATION TESTS

Test No.	Operating Period, min											
	1	2	3	4	5	6	7	8	9	10		
Char Particle Size (U.S. Sieve)	None											
Catalyst	None											
Operating Period, min	1800-1815											
Fixed-Bed Operation	1815-1845											
Moving-Bed Operation	1845-1900											
Steam-Bed Operation	1900-1915											
Operating Period, min	1915-1930											
Reactor Pressure, psia	1930-1945											
Average Reactor Temperature, °F	1945-1960											
Zone 7 (top)	1960-1975											
1	2	3	4	5	6	7	8	9	10			
292	210	0	0	225	0	0	222	234	225	235	291	322 <sup>1</sup>
0	0	300	0	0	300	0	0	0	0	0	0	0
0	0	0	120	0	0	120	0	0	0	0	0	0
152	152	152	152	152	152	152	152	152	152	153	149	149
1000	--	--	--	--	--	--	--	--	--	--	--	--
825	777	892	892	675	518	518	741	761	665	676	578	709
--	--	--	--	--	--	--	--	1049	893	911	1037	1019
--	--	--	--	--	--	--	--	1166	1001	1024	1128	1106
1299	1330	1375	1191	1161	1237	1237	1243	1128	1136	1225	1193	1337
1452	1398	1406	1406	1297	1297	1297	1345	1330	1265	1267	1337	1303
1452	1488	1488	1488	1488	1488	1488	1488	1488	1488	1488	1488	1488
1372	1117	1174	1174	1338	1390	1390	1343	1369	1384	1410	1381	1372

Initial Reactor Char Charge, g<sup>b</sup>

Below Steam Injection Point, uncatalyzed } 1244 8 88 888 } 1277 } 277 } 487 532 535 535 260

Above Steam Injection Point, uncatalyzed } 0 0 0 0 0 0 0 191 255 775 508 0 610

Ceasium Hydroxide, g } 0 0 0 0 0 0 0 85 87 88 170 0 88

Char Feed Rate, g/min<sup>a</sup> } 201 216 217 217 217 217 217 217 217 217 217 217 217

Char Feed Rate, g/min<sup>b</sup> } 0 0 8.23 7.87 0 7.84 7.87 0 7.84 7.87 0 7.84 7.87

Char Residue, g<sup>c</sup>/min<sup>a</sup> } 907 0 1705<sup>d</sup> 383 0 221<sup>d</sup> 593 939 938 906 1055<sup>e</sup> 846<sup>c</sup> 935<sup>c,1</sup>

Char Residue Discharge Rate, g/min<sup>c</sup> } 0 0 5.68<sup>d</sup> 3.19 0 7.39<sup>d</sup> 4.94 0 0 0 0 0 0

Carbon in Condensate, g } 4.4 0 12.6<sup>e</sup> 0 1.9 10.3<sup>e</sup> 3.4 3.0 3.6 3.5 3.4 0 0

Steam Feed Rate, g/min } 6.70 6.38 6.91 6.91 6.60 6.85 6.85 6.63 5.88 6.84 5.92 8.34 8.41

Argon Reference Gas Rate, SLPM } 4.96 4.96 4.96 4.96 4.96 4.96 4.96 4.96 4.96 4.96 4.96 4.96 4.96

Argon Feed Hopper Charge Rate, SLPM } 0.25 0.25 0.25 0.25 0.25 0.25 0.25 0.25 0.25 0.25 0.25 0.25 0.25

Average Gas Composition, %

H<sub>2</sub> } 63.3 64.2 53.5 32.2 66.1 57.0 26.2 63.6 65.2 59.1 60.6 62.0

CO<sub>2</sub> } 27.6 26.6 23.9 22.5 27.3 25.7 25.0 23.9 26.8 26.2 30.4 33.0

CO } 5.7 4.5 14.3 16.5 4.3 9.7 10.7 8.3 8.6 4.6 9.0 5.7 2.5

CH<sub>4</sub> } 3.2 4.5 8.1 8.6 2.3 7.6 8.1 4.0 3.8 3.3 5.6 3.3 2.5

C<sub>2</sub>H<sub>6</sub> } 0.2 0.2 0.2 0.2 0.2 0.2 0.2 0.2 0.2 0.2 0.2 0.2 0.2

C<sub>3</sub>H<sub>8</sub> } 0.02 0.02 0.03 0.03 0.001 0.001 0.001 0.004 0.007 0.003 0.004 0.001 0.001

C<sub>4</sub>H<sub>10</sub> } 0.001 0.001 0.001 0.001 0.001 0.001 0.001 0.001 0.001 0.001 0.001 0.001 0.001

C<sub>5</sub>H<sub>12</sub> } 0.001 0.001 0.001 0.001 0.001 0.001 0.001 0.001 0.001 0.001 0.001 0.001 0.001

C<sub>6</sub>H<sub>14</sub> } 0.001 0.001 0.001 0.001 0.001 0.001 0.001 0.001 0.001 0.001 0.001 0.001 0.001

Total } 100.0 100.0 100.0 100.0 100.0 100.0 100.0 100.0 100.0 100.0 100.0 100.0 100.0

<sup>1</sup>Rise from when steam was first fed to reactor until beginning of moving-bed operating period or end of test.

<sup>2</sup>Rate on an as-received basis.

<sup>3</sup>Rate on a moisture-free basis.

<sup>4</sup>Also includes fixed-bed operating period.

<sup>5</sup>Also includes reactor heat-up and fixed bed operating periods.

<sup>6</sup>Includes gas produced during reactor heat-up for fixed-bed operating periods only.

<sup>7</sup>Reactor volume filled with gravel

<sup>8</sup>Produced after fixed-bed operating period, when the temperatures of all reactor zones were raised to 1400°F.

<sup>9</sup>Includes 44 minutes when all reactor zones were at 1400°F.

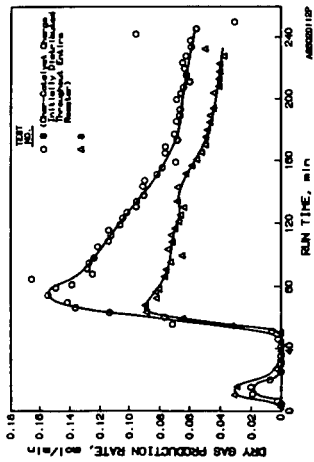


Figure 5. GASIFICATION RATES FOR UNCATALYZED AND CATALYZED BITUMINOUS CHAR

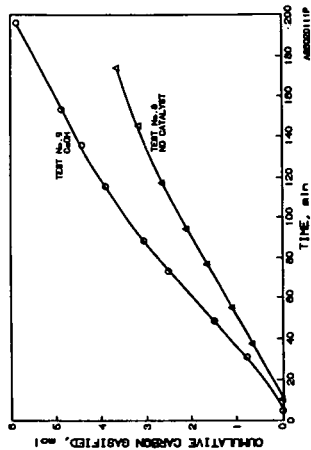


Figure 7. EFFECT OF CATALYST ON THE CUMULATIVE CARBON GASIFIED FOR THE BITUMINOUS CHAR

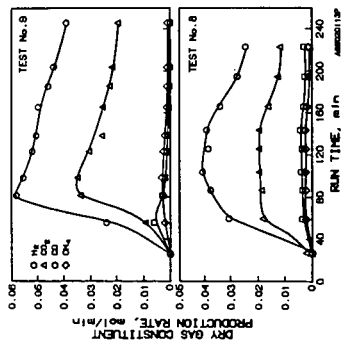


Figure 6. DRY GAS PRODUCTION RATES OF  $H_2$ ,  $CO_2$ ,  $CO$  AND  $CH_4$  FOR THE UNCATALYZED AND CATALYZED BITUMINOUS CHAR

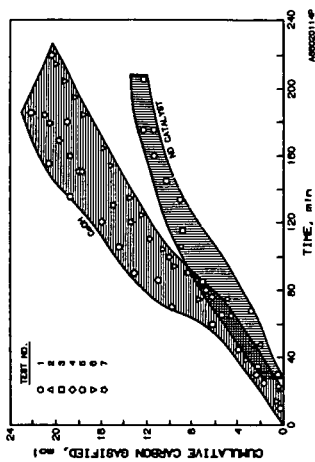


Figure 8. EFFECT OF CATALYST ON THE CUMULATIVE CARBON GASIFIED FOR THE LIGNITE CHAR

## OXYGEN CHEMISORPTION AS A TOOL FOR CHARACTERIZING "YOUNG" CHARs

E. M. Suuberg, J. M. Calo, and M. Wojtowicz  
Division of Engineering  
Brown University  
Providence, Rhode Island 02912

The introduction of the concept of active surface area (ASA) as measured by oxygen adsorption [N. R. Laine, F. J. Vastola, and P. L. Walker, Jr., J. Phys. Chem., **67**, 2030 (1963)] has led in recent years to various attempts to correlate char reactivity towards oxygen-containing gasification agents (e.g., CO<sub>2</sub>). As may be seen from the literature, this approach has met with some, although not universal, success. Theories have been advanced which suggest that only a portion of active sites may participate in actual gasification reactions.

Hampering a fundamental understanding of what the role of active sites might be is lack of information on their nature. A wide variety of conditions has been suggested for measurement of ASA, generally involving temperatures in the range from 100°C to 350°C and oxygen pressures from fractions of a torr to atmospheric. Only in a few cases have these conditions been critically evaluated. In this paper, a series of experiments is reported upon, which seek to establish the importance of these conditions on determining the ASA of "young" chars (i.e., not heat treated for extended times).

### 1.0 Introduction

Gasification of carbonaceous solids has historically been and remains an area of significant scientific and technological interest (1-7). It has been well established that the reactivity of char to gasification generally depends upon three principal factors: (a) the concentration of "active sites" in the char; (b) mass transfer within the char; and (c) the type and concentration of catalytic impurities in the char. This paper is concerned with the nature of the active sites, and attempts to elucidate further what is normally being measured as active sites. It has been shown, or at least implied, by the results of various workers that active surface area (ASA) is a better predictor of char reactivity than is total surface area (TSA) (8-10). The most frequently employed technique for determining active sites in chars is oxygen chemisorption (8-16).

The gradual pyrolytic evolution of hydrocarbons (possibly including heteroatoms) to highly carbonaceous solids is accompanied by dramatic changes in the gasification reactivity of such materials. Here we are concerned with the gasification behavior of chars that have already undergone active pyrolysis in which most hydrocarbon gases and tars are evolved. The issues involved in transient high rate hydrogasification or steam reactivity during pyrolysis (e.g., 1, 17, 18) are not addressed here.

Active sites in relatively pure carbons are normally thought to be associated with various types of imperfections in the carbon structure. Work with graphite has suggested the important role of carbon crystallite edges or dislocations. The majority

of mechanistic theories of carbon gasification are based on the "pure-carbon-surface-imperfections" model. This is appropriate for chars that have been heat-treated at high temperatures for extended periods of time and thus have relatively low residual oxygen and hydrogen contents (i.e., "old" chars). Some caution must be exercised in applying results obtained from pure carbons to "young" chars. This point will be considered further below.

Carbon gasification theories are based largely upon chemisorption-desorption mechanisms (some also allow for surface diffusion of intermediates). There is some evidence to suggest that the same type of oxygen-carbon complexes are involved in oxygen, steam, and carbon dioxide gasification (2,19). A correlation has also been demonstrated between active sites involved in hydrogen gasification and those involved in carbon dioxide gasification, although there is no direct proof that the sites involved are indeed the same in both cases (1). There is, however, a legitimate concern that the concept of "active sites" may be too broad, and that active sites may in fact be quite different in "young" chars than in "old" chars. It is the issue of what exactly is being measured by oxygen chemisorption which will be addressed in this paper.

There exists a distinction between "active" sites that are reactive and those that are nonreactive at a given temperature. The reactive "active" sites are responsible for the release of surface carbon oxides, while the nonreactive "active" sites will chemisorb oxygen but will not release surface oxides at the temperature under consideration. Raising the temperature of the carbon converts some nonreactive to reactive "active" sites (5,8). This mechanism, combined with the expected Arrhenius-type enhancement of chemical reaction rates, results in increasing gasification rate with temperature.

The preceding effect, however, is not always observed, and thus other factors must also play a role. For example, it has been observed that the rate of carbon combustion normally increases with increasing temperature, up to about 1500K. In the 1500-2000K temperature range, however, it has often been noted that the rate of combustion actually decreases with increasing temperature (5, 20-23). One explanation for this behavior is known as "thermal annealing" (3,5, 24-26). This same effect has also been postulated as being responsible for a decrease in reactivity towards other gases as well (1, 27, 28). There is a trend towards lower reactivity with increased time and temperature of char heat treatment (1, 29-35). This behavior reflects a progressive and continuous ordering of the remaining carbon and is actually an extension of the pyrolysis process.

It would, therefore, seem logical to associate the temperature dependence of the annealing process in chars with the activation energies of the latter phases of pyrolysis; i.e., 100 to 200 kcal/mol typical for high temperature H<sub>2</sub> release (36) and graphitization (37), respectively. In fact, this range is consistent with the results of a few studies on pure, relatively graphitic carbons (21, 26). The values of annealing reaction activation energies derived from experiments with younger chars have been generally lower, however.

In the present study, we examine the chemisorption behavior of relatively young chars only, so in comparing this study to those on graphites or chars produced by prolonged heating at high temperature, caution must be exercised. In this study, the effects of temperature and oxygen pressure on chemisorption behavior are considered.

### Experimental

Two different kinds of chars were examined in the course of this study. One was prepared from pyrolysis of a previously demineralized North Dakota lignite, the composition of which is shown in Table I. Demineralization was accomplished by washing the sample with HCl, followed by HF and again followed by HCl, according to the technique of Bishop and Ward (38). The residual mineral matter content of the lignite was determined to be approximately 0.8%. The other char which was examined was derived from a phenol-formaldehyde resin, carefully synthesized so as to avoid any cation contamination.

Table I

	<u>C</u>	<u>H</u>	<u>N</u>	<u>S</u>	<u>Ash</u>	<u>O</u>
North Dakota Lignite <sup>+</sup>	65.6	3.6	1.1	0.8	11.0	17.9
Phenolic Resin	73.9	5.5	0	0	0	20.6
Phenolic Resin Char*	87.2	1.6	0	0	0	11.2

All analyses on a weight percent, dry basis. Oxygen by difference.

<sup>+</sup>The analysis is for the as-received lignite, prior to demineralization.

\*Pyrolysis as indicated in the text.

Both samples were pyrolyzed at similar conditions. Pyrolysis was performed under inert gas (helium). The resin samples were heated at a rate of 4 to 5°C/min to a maximum temperature of 950°C, held for about 2 hours at temperature, and then cooled to room temperature at a rate of 2 to 25°C/min. Samples were never permitted to contact oxygen while at high temperatures, except during the actual chemisorption experiments. The weight loss during pyrolysis was approximately 40%. The total surface area of chars produced this way was roughly 300m<sup>2</sup>/g. The lignite sample was heated at a rate of about 3°C/min to 1000°C, held at this temperature for 2 hours, and then cooled to room temperature at a rate comparable to the heating rate. The weight loss of the lignite during pyrolysis was 42.3%.

Prior to chemisorption, samples were always outgassed for about 2 hours at 950°C, under helium.

Generally, chemisorption was performed in a TGA type device. About 50-100 mg of powdered sample was placed in a quartz bucket, the system tared, and mass change followed as a function of time, at the desired oxygen partial pressure and temperature. Experiments were performed to assess the effects of oxygen pressure and temperature on oxygen chemisorption behavior.

#### Effect of Temperature on Oxygen Chemisorption Behavior

There exists a voluminous literature on low temperature oxidation of coals and a significant number of studies on low temperature oxidation of chars. Generally, the analysis of oxygen uptake in these systems has been analyzed in terms of the Elovich equation, expressed as

$$dq/dt = a \exp(-bq)$$

where  $q$  is the amount of oxygen chemisorbed per gram of char, and  $a$  and  $b$  are constants. Recent work on 550°C cellulose char has shown the data on oxygen uptake at temperatures between 74 and 207°C to be reasonably fit by this equation, and implies a linear increase in chemisorption activation energy from 13 to 25 kcal/mol with increasing extent of uptake (39). These data were interpreted, together with ESR data, to suggest that far more oxygen is chemisorbed than there are free radical sites initially available. A chain reaction via peroxy radicals was ruled out on the basis of the high activation energies. A Diels Alder reaction was postulated, but not vigorously supported. This is representative of the uncertainty concerning oxygen uptake mechanisms on chars. The mere fact that the Elovich equation fits data does little to establish mechanism; as has been pointed out, the Elovich equation may be consistent with several different types of sorption isotherms (5). Its validity in interpreting results from porous samples has been questioned as well (40).

It is against this background of uncertainty in mechanism that the data on the effect of temperature on chemisorption are analyzed. Generally, a fresh young char surface, when first exposed to oxygen, rapidly picks up oxygen and then continues to pick up oxygen at an ever decreasing rate for many hours subsequently (consistent with the form of the Elovich equation).

The effect of temperature on the amount of oxygen chemisorbed by a char has been studied to a limited extent previously. An Australian brown coal char pyrolyzed for more than 10 hours at 1000°C showed a trend of increasing oxygen capacity with increasing temperature of chemisorption between 25 and 200°C (41). Experiments with a higher rank coal char prepared at similar temperatures showed that oxygen capacity increased with temperature only up to about 100°C (16), while a 550°C cellulose char showed increasing oxygen uptake with increasing temperature up to at least 207°C (39). An activated graphon (highly graphitized carbon black) showed increasing chemisorption capacity with increasing temperature up to at least 550°C (13). The actual temperature dependence of saturation amounts of uptake was seen to be quite complex (12).

As a result of the uncertainty concerning the effect of temperature on chemisorption behavior, several tests were performed with the chars of interest in this study. In both series of experiments, chars with initially clean surfaces were subjected to "staircase" temperature profiles under an atmosphere of dry air. Figure 1 shows the results of these tests. In the case of the resin char, there is evidence for increased capacity with increasing temperature up to 300°C, at which temperature the mass begins to decrease due to decomposition of the surface oxides. In the case of the lignite char, the effect of temperature is much less pronounced and mass loss becomes evident at 250°C.

Thus, it must be concluded that the effect of temperature on chemisorption may vary widely from char to char, and there is a legitimate question as to what exactly is being measured at any arbitrary condition. Depending upon the situation, the maximum uptake may be an artifact due to competing processes of continued chemisorption and desorption of complexes. In the case of the resin char, the apparent activation energy for the high temperature decomposition process is 29 kcal/mol.

#### Effect of Oxygen Pressure on Chemisorption Behavior

The effect of oxygen pressure on chemisorption behavior has also been

studied to only a limited extent previously. It was found for 1000°C Australian brown coal char that both reversibly sorbed and chemisorbed oxygen increased in amount with increasing pressure of oxygen (from 161 torr to 760 torr) (41). On the other hand, a sample of higher rank coal char which had been pyrolyzed at 1000°C showed no variation in oxygen chemisorption capacity for pressures ranging from about 7.6 torr to 760 torr (16). In another study, a graphon sample displayed oxygen chemisorption capacity which was markedly pressure dependent in the pressure range 0.5 torr to 700 torr (13). The increase in oxygen chemisorption with oxygen pressure was also observed at high temperatures (615°C, 42).

In seeking to better characterize oxygen chemisorption as a diagnostic technique, a series of experiments was conducted in the present study at various partial pressures of oxygen. The results of these tests are shown in Figure 2. It is apparent that the partial pressure of oxygen has a marked influence on the rate of uptake of oxygen, and apparently, on the ultimate oxygen capacity of the sample.

#### Conclusions

The obvious conclusion that can be drawn from this work is that oxygen chemisorption can hardly be termed a site-specific analytical technique, at least when applied to typical young chars. The fact that apparent oxygen capacities are sensitive to temperature and pressure does not necessarily imply that oxygen chemisorption is not useful as a correlative tool; it has been shown that active site concentrations, as measured by chemisorption of oxygen, do correlate reasonably well with char reactivity in several cases (e.g., 8,9). Still, the solid evidence for the relationship between chemisorbed oxygen complexes and gasification have come mainly from a series of very careful studies on very "old" chars, oxidized at moderate temperatures (8,11-15).

This raises the question as to what value oxygen chemisorption techniques are in characterizing young chars. Clearly, as a characterization technique, chemisorption is difficult enough so as to make actual gasification reactivity tests look more attractive, if this is the information which is actually desired. At present, when applied to young chars, the oxygen chemisorption technique must derive its value from being a tool for studying the actual mechanism of gasification of these materials.

#### Acknowledgment

We gratefully acknowledge the support of the U. S. Department of Energy through grant DE-FG22-83PC60800.

#### References

- (1) Johnson, J. L., Kinetics of Coal Gasification, Chapter I, Wiley, 1979.
- (2) Laurendeau, N. M., Prog. Energy Combust. Sci., **4**, 221 (1978).
- (3) Von Fredersdorff, C. G., and Elliott, M. A., in Chemistry of Coal Utilization, Supplementary Volume, (H. H. Lowry, Ed.), Chapter 20, Wiley, 1963.
- (4) Walker, P. L., Jr., Rusinko, F., Jr., and Austin, L. G., in Advances in Catalysis, **XI**, 133 (1959).
- (5) Essenhigh, R. H., in Chemistry of Coal Utilization Second Supplementary Volume, (M. Elliott, Ed.), Chapter 19, Wiley, 1981.

- (6) Field, M. A., Gill, D. W., Morgan, B. B., and Hawksley, P. G. W., Combustion of Pulverized Coal, BCURA, Leatherhead, England (1967).
- (7) Mulcahy, M. F. R., and Smith, I. W., Rev. Pure Appl. Chem., **19**, 81 (1969).
- (8) Laine, N. R., Vastola, F. J., and Walker, P. L., Jr., J. Phys. Chem., **67**, 2030 (1963).
- (9) Radovic, L. R., Walker, P. L., Jr., and Jenkins, R. G., Fuel, **62**, 849 (1983).
- (10) Tong, S. B., Pareja, P., and Back, M. H., Carbon, **20**, 191 (1982).
- (11) Vastola, F. J., Hart, P. J., and Walker, P. L., Jr., Carbon, **2**, 65 (1964).
- (12) Hart, P. J., Vastola, F. J., and Walker, P. L., Jr., Carbon, **5**, 363 (1967).
- (13) Lussow, R. O., Vastola, F. J., and Walker, P. L., Jr., Carbon, **5**, 591 (1967).
- (14) Bansal, P. C., Vastola, F. J., and Walker, P. L., Jr., J. Coll. and Int. Sci., **32**, 187 (1970).
- (15) Phillips, R., Vastola, F. J., and Walker, P. L., Jr., Carbon, **8**, 197 (1970).
- (16) Canston, P.I, and McEnaney, B., Fuel, **64**, 1447 (1985).
- (17) Suuberg, E. M., Peters, W. A., and Howard, J. B., Fuel, **59**, 405 (1980).
- (18) Graff, R., and LaCava, A., U.S.D.O.E. Report FE-2340-9, 1978.
- (19) Ergun, S., and Mentser, M., in Chemistry and Physics of Carbon, **1**, (P. L. Walker, Jr., Ed.), Chap. 4, Dekker, 1965.
- (20) Eucken, A., Z. Angew. Chem., **43**, 986 (1930).
- (21) Strickland-Constable, R. T., Trans. Faraday Soc., **40**, 333 (1944), also Nagle, J., and Strickland-Constable, R. T., Proc. 5th Conf. on Carbon, Vol. p. 154, Pergamon (1962).
- (22) Meyer, L., Z. Phys. Chem., **17(B)**, 385 (1932).
- (23) Duval, X., J. Chim. Phys., **47**, 339 (1950) and **58**, 3 (1961).
- (24) Duval, X., Ann. Chim. (Paris), **10**, 903 (1955).
- (25) Spokes, G. N., and Benson, S. W., Fundamentals of Gas-Surface Reactions, p. 318, Academic Press, (1969).
- (26) Blyholder, G., Binford, J. S., Jr., and Eyring, H., J. Phys. Chem., **62**, 263 (1958).
- (27) Moseley, F., and Patterson, D., J. Inst. of Fuel, **38**, 378 (1965), also **40**, 523 (1967).
- (28) Zahradnik, R. L., and Glenn, R. A., Fuel, **50**, 77 (1971).
- (29) Walker, P. L., Jr., in Scientific Problems of Coal Utilization, (B. R. Cooper, Ed.), p. 237, U.S.D.O.E., 1978.
- (30) Jenkins, R. G., Nandi, S. P., and Walker, P. L., Jr., Fuel, **52**, 288 (1973).
- (31) Hippo, E., and Walker, P. L., Jr., Fuel, **54**, 245 (1975).
- (32) Blackwood, J. D., and McTaggart, F. K., Aust. J. Chem., **12**, 533 (1959).
- (33) Blackwood, J. D., Cullis, B. D., and McCarthy, D. J., Aust. J. Chem., **20**, 1561 (1967).
- (34) Gray, J. A., Donatelli, D. J., and Yavorsky, P. M., ACS Div. Fuel Chem. Prep., **20** (4), 103 (1975).
- (35) Blake, J. H., Bopp, G. R., Jones, J. F., Miller, M. G., and Tanbo, W., Fuel, **46**, 115 (1967).
- (36) Chermin, H. A. G., and Van Krevelen, D. W., Fuel, **36**, 85 (1957).
- (37) Fischbach, D. B., in Chemistry and Physics of Carbon, **7**, (P. L. Walker, Jr., Ed.), p. 1, 1971.
- (38) Bishop, M., and Ward, D. L., Fuel, **37**, 191 (1958).
- (39) Bradbury, A., and Shafizadeh, F., Carbon, **18**, 109 (1980).
- (40) Harris, J., and Evans, D., Fuel, **54**, 276 (1975).
- (41) Allardice, D., Carbon, **4**, 255 (1966).
- (42) Phillips, R., Vastola, F., and Walker, P., Carbon, **7**, 479 (1969).

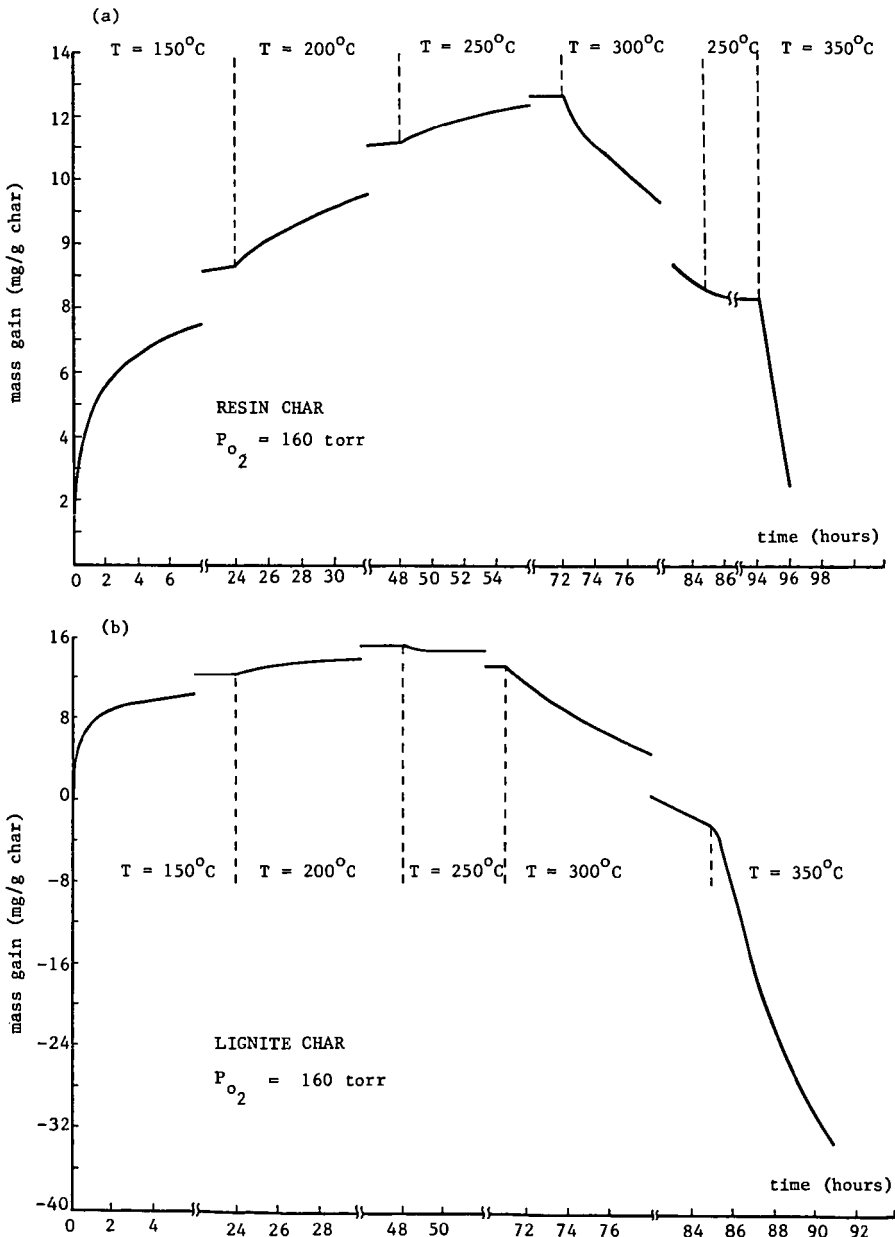


Figure 1. Effect of Temperature Changes on Oxygen Chemisorption Behavior  
 (a) Resin Char   (b) Lignite Char

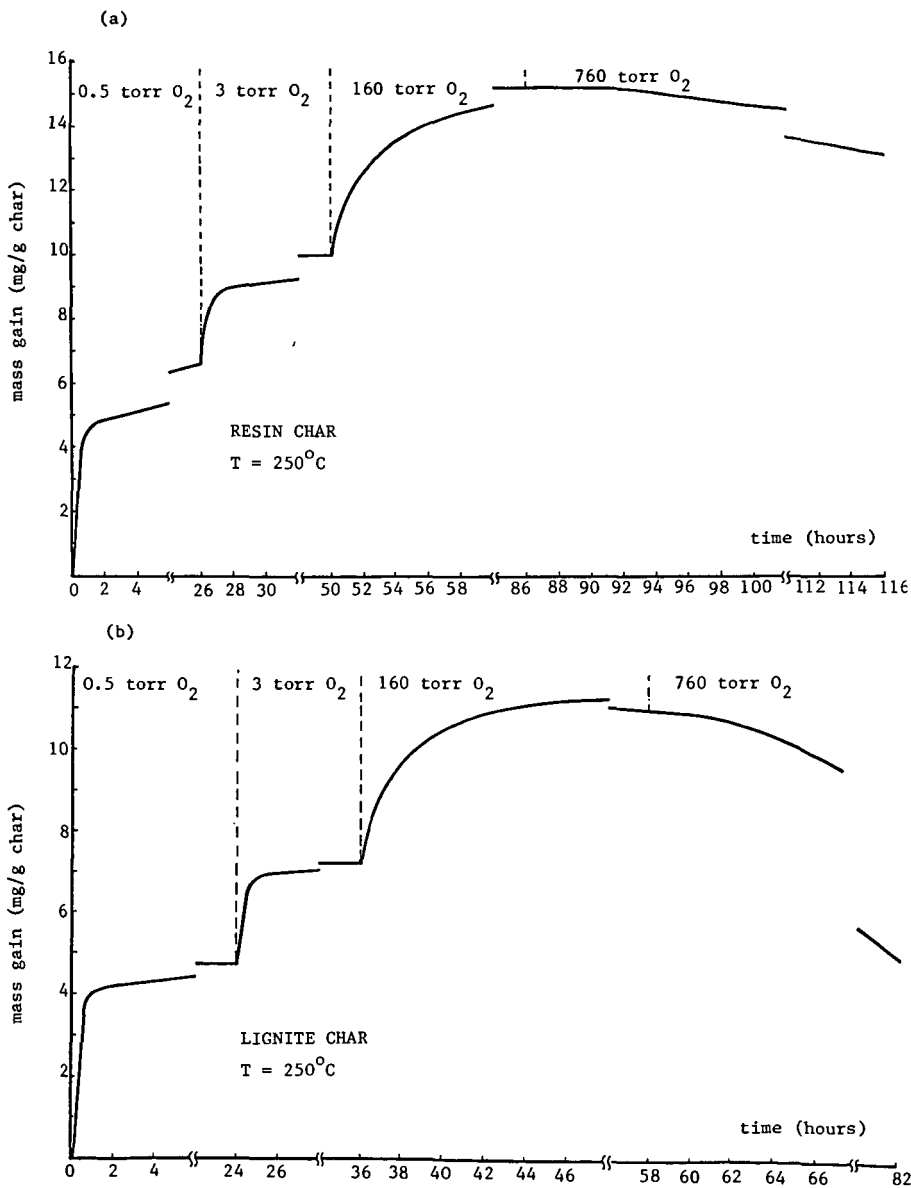


Figure 2. Effect of Oxygen Partial Pressure Changes on Oxygen Chemisorption Behavior

(a) Resin Char (b) Lignite Char

## IN-MINE VARIATION AND ITS EFFECTS ON COAL GASIFICATION

Scott F. Ross and David R. Kleesattel

University of North Dakota Energy Research Center  
Box 8213, University Station  
Grand Forks, North Dakota 58202

### Abstract

As reported earlier (1), four different lithologic layers have been identified in the Freedom Mine (Mercer County, North Dakota) which supplies the lignite for the Great Plains Gasification Associates plant in Beulah, North Dakota. The layers were identified on the basis of readily observable megascopic characteristics including luster, fracture characteristics and the presence of clay and silt zones. Lignite sampled from each of the four layers has been pyrolyzed in a bench scale reactor system designed to simulate the production of gas liquor condensate from the pyrolysis zone of an actual gasifier. The yields of water-soluble organic effluents from each of the layers were found to differ significantly, particularly the yields of phenol, cresol and catechol.

### Introduction

The treatment and removal of water-soluble organic effluents from wastewater is an important issue facing coal gasification technology. The extent of treatment is governed by the reuse or environmentally acceptable disposal of the wastewater. Downstream effluent treatment is also dependent on the nature and quantity of tars pyrolysis and devolatilization reactions in the upper portion of the gasifier. It is desirable to develop a laboratory test to simulate the production of water-soluble organic effluents from a gasifier, thereby eliminating expensive pilot-plant tests. Such a test could eventually be a method of assessing the gasification potential of various coals, and the resulting data base would be helpful in designing effluent treatment systems for gasification plants.

In working towards the development of such a test, the technique was found to be sensitive to changes in coal quality which occur within the same mine. With the discovery of distinct lithologic layering within a mine which supplies coal to an actual commercial gasifier, an investigation into the effects of in-mine variation on coal gasification was initiated.

### Experimental

A laboratory scale tubular reactor was constructed which allows for the pyrolysis of up to five grams of coal in a variety of gas atmospheres. A Lindbergh split-type furnace with a maximum temperature of 1100 C and a programmable heating rate of 5°C/min. to 45°C/min. allowed for reproducible heating of the samples. A liquid nitrogen cooled trap was used for the collection of water-soluble organic effluents. After completion of the experiment the trap was allowed to warm to above 0°C and the water-soluble organics analyzed by gas chromatography (2).

The coal samples used in this study were collected at the Freedom Mine (Mercer County, North Dakota). The samples were ground to -60 mesh and pyrolyzed in a nitrogen atmosphere using a heating rate of 45°C/min. and a final temperature of 850°C.

TOSCO Material Balance Assays were provided by J & A Associates, Inc., Golden, Colorado. The procedure has been described elsewhere (3).

Standard quantitative maceral analyses (4) were performed on representative samples from each of the four lithologic layers. Lignite samples were prepared for micropetrographic analysis as described in ASTM procedures (5).

### Results and Discussion

During a mine study in May 1984, major lithologic units occurring as layers in the Beulah-Zap bed of the Sentinel Butte Formation (Paleocene) were observed. The seam was subdivided into four lithologic units on the basis of overall megascopic characteristics (Figure 1). The criteria for these subdivisions were:

1. appearance of the broken surfaces of the units on a large scale as they appear in the high wall;
2. luster of the coal;
3. fracture characteristics, hardness and surface appearance of the coal on a small scale (1-10 cm);
4. presence of lithologically distinct units including thin layers of fragmental coal, clay, and silt layers and concretionary zones.

There is evidence to suggest that the units are not entirely local in extent but persist widely in the Beulah-Zap bed (6).

Lignite was sampled from each of the four layers in a vertical sequence with the samples being collected within a few meters of each other. The samples were pyrolyzed as described above and the water-soluble organic effluents were analyzed. The yields of the water-soluble organics from each of these four samples and their corresponding proximate and ultimate analyses are given in Table 1. Based on the pyrolysis yield data, the top three layers appear to be quite similar. However, layer four shows considerable differences in the yields of methanol, phenol, cresols and catechol. In fact, layer four appears to be an entirely different coal. Layer four is separated from the other three layers by a locally thin, inorganic-rich zone or clay layer, suggesting that a marked difference in the depositional environment could have occurred. The proximate and ultimate analyses for the four layers are quite similar, however, and provide no explanation as to why the fourth layer should behave so differently upon pyrolysis than the other three layers. In particular, a comparison of maf ultimate data for layers 2 and 4 shows great similarity, yet pyrolysis yields of water-soluble organics are radically different. This suggests that a plant operator could not rely on routine coal analysis as the predictor of wastewater characteristics.

The data from the TOSCO Material Balance Assays are given in Table 2. The most obvious difference is the tar yields for the four layers. There is a 44% decrease in tar yield between layer 1 and layer 2. The yields of water, CO and C<sub>1</sub> also differ significantly between the four layers. However, unlike with the water-soluble organic effluent data, the fourth layer doesn't stand out as being different from the other three layers.

Petrographic analyses for the four layers are presented in Table 3. Unlike the proximate and ultimate analyses, which suggest little difference between the four layers, the petrographic analyses indicate that there might be considerable organic structural differences between the layers. There exists a good correlation between catechol yields upon pyrolysis and the amount of corphuminite found in each layer. A linear estimation of the data results in a correlation coefficient of 0.92.

Table 1. Pyrolysis Yields for Four Lithologic Layers in the Freedom Mine<sup>a</sup>

Coal	(Top) Layer 1	Layer 2	Layer 3	(Bottom) Layer 4
<b>Compound:</b>				
Methanol	990	1010	940	1590
Acetone	1350	1320	1490	1420
Acetonitrile	240	250	260	190
2-Butanone	360	340	420	350
Propionitrile	70	130	280	190
Phenol	2110	1720	1800	3820
o-Cresol	610	520	580	980
p-Cresol	680	570	600	1190
m-Cresol	710	630	720	1420
Catechol	990	1010	1200	3150
<b>Proximate Analysis</b> (as rec'd; % by wt):				
Moisture	23.51	23.11	27.93	30.62
Volatile matter	29.32	33.93	34.22	36.74
Fixed carbon	31.61	36.56	32.91	27.93
Ash 15.55	6.40	4.94	4.72	
<b>Ultimate Analysis</b> (maf; % by wt):				
Hydrogen	4.66	5.09	4.75	5.13
Carbon	68.20	69.14	70.37	69.32
Nitrogen	1.08	1.11	1.12	1.07
Sulfur	2.75	0.66	0.68	0.84
Oxygen	23.30	23.99	23.09	23.65

<sup>a</sup>Compound yields are reported in micrograms/g maf coal.

Table 2. TOSCO Material Balance Assay

Fischer Assay Yields	Normalized Values (Moisture Free)			
	Layer 1	Layer 2	Layer 3	Layer 4
Tar (lb/ton)	119.3	67.1	103.7	89.1
(gal/ton)	14.6	8.2	12.7	10.9
Gas (lb/ton)	311.9	333.5	329.0	306.6
(scf/ton)	3311.0	3597.7	3627.6	3402.9
Water (lb/ton)	129.9	192.3	158.7	191.2
(gal/ton)	15.6	23.1	19.0	22.9
Char (lb/ton)	1438.9	1407.1	1408.5	1413.1
H <sub>2</sub> (lb/ton)	1.22	1.11	1.33	1.14
CO (lb/ton)	30.76	37.51	36.85	40.89
CO <sub>2</sub> (lb/ton)	243.23	256.50	251.62	224.00
Cl (lb/ton)	17.44	19.78	22.32	20.63

Table 3. Petrographic Analyses of Freedom Mine, Four Lithologic Layers

Maceral Analysis (% Volume)	<u>Layer 1</u>	<u>Layer 2</u>	<u>Layer 3</u>	<u>Layer 4</u>
<b>Humanite Group</b>				
Ulminite	35.5	38.9	38.2	42.8
Humodetrinite	25.2	23.1	21.9	18.0
Gelinite	0.5	0.4	1.4	1.3
Corpohuminite	1.0	2.6	2.0	6.2
<b>Liptinite Group</b>				
Sporinite	0.9	2.4	1.4	3.3
Cutinite	0.7	0.5	0.5	0.5
Resinite	2.7	1.9	0.9	1.7
Suberinite	0.0	0.5	0.4	1.5
Alginite	1.2	0.4	0.9	1.2
Liptodetrinite	5.0	5.9	3.8	5.3
Fluorinite	0.0	0.4	0.0	0.0
Bituminite	0.0	0.0	0.0	2.0
<b>Inertinite Group</b>				
Fusinite	4.5	4.6	8.5	2.7
Semifusinite	6.8	8.1	7.2	5.3
Macrinite	0.7	0.5	0.2	0.0
Sclerotinite	0.3	0.5	0.4	0.3
Inertodetrinite	8.9	7.6	8.5	4.2
Micrinite	1.3	0.7	1.8	1.3

### Conclusions

The composition of gas liquor condensate can vary greatly due to variations within an individual seam. The samples used in this study were collected within a few meters of each other but indicate significant vertical variation exists in a particular mine. The ultimate analyses of these layers are virtually identical, but the actual chemistry, as evidenced by the pyrolysis results and the TOSCO Material Balance Assays, is very different from layer to layer. These differences could result in substantial changes in wastewater composition and operability of a tar/water separator in an actual gasification plant when coal from different layers is gasified.

Petrographic analysis reflects, to an extent, the structural chemistry of the coal because the macerals generally derive from different kinds of plant constituents, and these original plant constituents in turn have different structures. Therefore, petrography should be a useful predictor of some pyrolyzate yields.

Reasonably steady operation of wastewater treatment plants and tar/water separators depend on having reasonably steady wastewater composition and tar production, or at least the ability to predict these in advance. In order to achieve this it is important to characterize the pyrolysis behavior of the coal layers to provide for blending or preferential mining and selective utilization.

### Acknowledgment

This work was supported by the U.S. Department of Energy, Contract No. DE-FC21-83FE60181.

The authors would like to acknowledge John W. Diehl for doing the gas chromatographic analyses and Harold H. Schobert for his helpful comments.

### Literature Cited

1. UNDERC Quarterly Technical Progress Report for the Period July-September 1984, Section 15, DOE/FE/60181-1682, November 1984.
2. Olson, E.S. and J.W. Diehl, 186th ACS National Meeting, Washington, D.C., Abstract of Papers, Anyl 63, (1983).
3. Goodfellow, Lawrence and M. T. Atwood, presented at the 7th Oil Shale Symposium, April 18-19, 1974.
4. Stach, E., Taylor, G.H., Mackowsky, M.T., Chandra, D., Teichmuller, M., and Teichmuller, R., 1982, 3rd edition, Coal Petrology, Gerbruder-Borntraegger, Berlin-Stuttgart, 535 p.
5. Annual Book of ASTM Standards, 1980, Gaseous Fuels: Coal and Coke, Part 26, D 2797-72 (1980), Preparing Coal Samples for Microscopical Analysis by Reflected Light, pp. 363-371.
6. Kleesattel, D.R., M.A. Thesis, University of North Dakota, 1985.

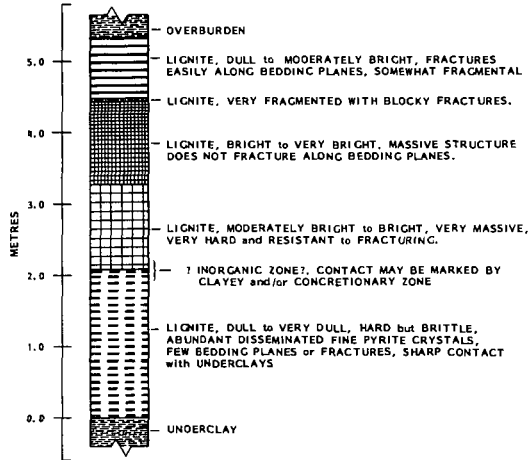


Figure 1. Lithologic units of the Beulah-Zap lignite bed as described at the Freedom Mine.

**VARIATIONS IN CHAR REACTIVITY WITH COAL TYPE AND PYROLYSIS CONDITIONS**

Peter R. Solomon, Michael A. Serio and Steven G. Heninger

Advanced Fuel Research, Inc. 87 Church Street, East Hartford, CT 06108

Understanding char reactivity is important since the consumption of char is the slowest and, therefore, the controlling process in combustion or gasification. Reviews of char reactivity (1,2) demonstrate that there is a wide variation in observed reactivities. Work described by Smoot (3) highlights the very large variations (one and half orders of magnitude) in char reactivity with method of formation. Similarly, Ashu et al. (4) found an enhanced reactivity of char caused by rapid heating of the precursor coal. More recently, in a vertical tunnel furnace, Essenhigh and Farzar (5) measured very rapid burnout times for small coal particles. They ascribed this to the firing condition which gave rates of heating in the  $10^6$  K/s regime, compared with the more usual value of  $10^4$  K/s in slower burning flames. Nsakala has reported a wide variation in reactivity associated with rank (6).

The gasification or combustion reactions of char are generally described as falling into three rate controlling regimes where the reaction rate is limited by: 1) intrinsic reactivity of the char itself, 2) diffusion of reactants within the char pores, and 3) diffusion of reactants between the char's surface and the ambient atmosphere. In this work the focus is on the intrinsic reactivity where the controlling factors are the surface area, active site density, and catalytic effect of minerals. The objective of the study described here was to determine how these factors vary with coal rank, char formation conditions and mineral matter content.

This paper reports on an empirical study of the reactivity of a set of chars from a variety of different coals prepared by pyrolysis at heating rates between 0.5 and 20,000°C/sec to temperatures between 400 and 1600°C. Reactivities were measured with a TGA, using the widely used method of monitoring the weight loss at constant temperature in the presence of  $O_2$  or  $CO_2$ . A new technique was developed in which the weight loss was measured while the sample was heated at a constant heating rate in the presence of the reactive gas. This method has the advantage that the same conditions can be used for chars of widely varying reactivity. Reactivities measured by the two methods correlated well with each other. The paper will present correlations of the reactivities with the char formation conditions and the char properties (including surface area, hydrogen concentration and mineral concentration).

**EXPERIMENTAL**

**Char Preparation** - Chars for this study were prepared from the 200 x 325 mesh sieved fractions of coals and lignites listed in Table I. The chars were prepared by pyrolysis in an inert atmosphere in one of four reactors: 1) an atmospheric pressure entrained flow reactor (EFR) (7,8) with coal particle temperatures between 650 and 1600°C at heating rates of  $\sim 10,000^\circ\text{C}/\text{sec}$ ; 2) a heated tube reactor (9) with coal particle temperatures between 650°C and 950°C at heating rates of  $\sim 20,000^\circ\text{C}/\text{sec}$ ; 3) a thermogravimetric analyzer (TGA) with coal particle temperatures of 450°C to 900°C at heating rates of  $0.5^\circ\text{C}/\text{sec}$ ; and 4) a heated grid reactor (HGR) with coal temperatures of 400°C to 900°C at heating rates of  $\sim 1000^\circ\text{C}/\text{sec}$ . (10).

**Reactivity Measurements** - Initial char reactivity measurements were made using the isothermal measurement developed at Pennsylvania State University (11). In this method, the char is heated in a TGA in nitrogen to the desired temperature, usually 400-500°C. The temperature level is chosen to make sure no oxygen diffusion limitations are present, i.e., by varying the flow rate, bed depth and particle size. After the weight of the sample has stabilized at the selected temperature level, the nitrogen flow is switched to air and the weight loss is monitored. The time for 50%

burnoff,  $\tau_{0.5}$ , is used as the reactivity index. Another group at Penn State has used the maximum rate of weight loss as a reactivity index, which is determined in a similar isothermal experiment (12).

In our char characterization work, we had difficulty applying the isothermal techniques to chars formed over a wide range of conditions. A temperature level selected for one char was inappropriate for another. The temperature was either too high for the rate to be chemically controlled or too low for the  $\tau_{0.5}$  to be reached in a reasonable time period.

In order to overcome this difficulty, a non-isothermal technique was developed. A Perkin-Elmer TGA 2 was used for this method. The sample size is about 1.5 mg. The sample is heated in air at a rate of 30 K/min until a temperature of 900°C is reached. The TGA records the sample weight continuously and, at the end of the experiment, the weight and derivative are plotted. Some representative curves for the North Dakota (Zap) lignite, the Montana Rosebud subbituminous coal and the Pittsburgh Seam bituminous coal are shown in Fig. 1. The Zap and Pittsburgh were chars prepared in the (EFR), in which it was calculated that the particles were heated at about 7000 K/s to 700°C before being quenched. The Montana Rosebud char was prepared in the heated tube reactor (HTR) under similar conditions. The samples were oxidized with an air flow of 40 cc/min and a nitrogen purge flow of 40 cc/min. The Zap lignite indicates burnout of several components of the char of different reactivity, while the Rosebud and Pittsburgh coals show more homogeneous burnout at higher temperatures.

The characteristics of the weight loss curve can be understood as follows: 1) At low temperature, there is an initial weight loss as moisture is removed. 2) As the temperature is raised, the reactivity of the char increases until the fractional weight loss rate is sufficiently large to be observed. The sample size and oxygen flows are chosen so that the initial 10% of weight loss occurs under intrinsic reactivity control. 3) As the temperature continues to increase, the reactivity increases until eventually all the oxygen reaching the sample bed is consumed and the weight loss is controlled by the oxygen supply to the sample bed alone. Then the fractional weight loss rate becomes constant for all samples. 4) When the char has components of different reactivity, the weight loss can switch between being oxygen supply limited and being intrinsic reactivity limited as each component is consumed.

Figure 2 compared the weight loss curves for the same char sample but with different sample sizes. The curves are identical for the initial weight loss which is controlled by the intrinsic reactivity. As expected, the fractional rate of weight loss  $(1/m_0)(dm/dt)$  decreases with increasing sample size in the oxygen supply limited regime.

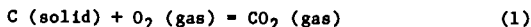
## RESULTS

**Comparison of Isothermal and Constant Heating Rate Reactivity Tests** - The temperature ( $T_{cr}$ ) at which the derivative of the fractional weight loss with respect to time reaches a value of 0.1 wt. fraction/min was chosen as an index of reactivity to be compared with the  $\tau_{0.5}$  values measured by the isothermal technique. The actual critical slope used is arbitrary. A value is chosen which is large enough to be unambiguously determined, but small enough so that reaction occurs in the chemically controlled regime. Values of  $\ln \tau_{0.5}$  were plotted against  $1/T_{cr}$  and a good correlation was observed.

It was subsequently decided that a comparison to  $\tau_{0.1}$  (time for 10% burnoff) would be more relevant since the initial reactivity indicated by  $T_{cr}$  would be measured, rather than an integral reactivity over a large extent of conversion which is affected by reactivity variations due to changes in the pore structure or sample

inhomogeneity. A plot of  $\ln \gamma_{0.1}$  vs  $1/T_{cr}$  is shown in Fig. 3. This plot includes data for chars from all three coals in all four reactors. The experimental conditions covered the following ranges: heating rate = 0.5 to 20,000 K/sec; temperature = 400 to 1600°C; residence time = .020 s to 30 min; pressure = 0 to 200 psig.

It can be shown that a plot of  $\ln \gamma_{0.1}$  vs  $1/T_{cr}$  will be linear with a slope equal to  $E/R$ , where  $E$  is the global activation energy for the intrinsic oxidation rate and  $R$  is the gas constant. For the reaction



the global rate of disappearance of carbon can be represented as follows:

$$dm/dt = -k_s C_s^n W \beta S \quad (2)$$

where  $dm/dt$  is the mass loss of carbon per particle in unit time (g/min),  $k_s$  is the intrinsic reaction rate constant based on unit surface (cm/min),  $C_s^n$  is the concentration of oxygen at the surface in moles/cm<sup>3</sup> raised to some power  $n$ ,  $W$  is the molecular weight of carbon in g/mole,  $\beta$  is the ratio of active area per unit accessible surface area (cm<sup>2</sup>/cm<sup>2</sup>) and  $S$  is the accessible surface area in cm<sup>2</sup> per particle. Since the reaction occurs under chemical reaction control, the concentration of oxygen at the surface will be equal to the bulk concentration, which allows one to drop the subscript.

In the isothermal experiment, the burn-off rate is nearly constant up to 10% weight loss:

$$dm/dt \approx \Delta m / \Delta t \approx -0.1 m / \gamma_{0.1} \quad (3)$$

Substituting Eq. 2 for  $dm/dt$ :

$$-k_s C^n W \beta S = 0.1 m / \gamma_{0.1} \quad (4)$$

$$\gamma_{0.1} = \left[ 0.1 m / k_s(T_0) C^n W \right] \cdot \left[ 1 / \beta S \right] \quad (5)$$

$$= K_1 \left[ 1 / \beta S \right] \quad (6)$$

The quantities in the first set of brackets in Eq. 5 are nearly constant for a given isothermal (temperature =  $T_0$ ) experiment at low conversions and independent of coal type, while the second set of brackets contain quantities which vary with coal type and char formation conditions.

For the non-isothermal experiment, the relative rate of mass loss is constant at some critical temperature,  $T_{cr}$ :

$$\left[ 1/m \right] \cdot \left[ dm/dt \right] = -0.11 = \left[ 1/m \right] \cdot \left[ -k_s(T_{cr}) C^n W \beta S \right] \quad (7)$$

$$k_s(T_{cr}) = \left[ 0.11 m / C^n W \right] \cdot \left[ 1 / \beta S \right] \quad (8)$$

$$= K_2 \left[ 1 / \beta S \right] \quad (9)$$

The result obtained is that  $k_s$  is proportional to an experimental constant and inversely proportional to char properties.

For data collected on the same char sample, ( $\beta S$ ) can be eliminated between Eqs. 6 and 9:

$$\gamma_{0.1} = \left[ K_1 / K_2 \right] k_s(T_{cr}) = \left[ 0.9 / k_s(T_0) \right] k_s(T_{cr}) \quad (10)$$

or

$$\tau_{0.1} = 0.9 \exp \left[ -E/R \left( 1/T_{CR} - 1/T_0 \right) \right] \quad (11)$$

assuming that  $k_g$  can be expressed as an Arrhenius expression  $k_g(T) = k_0 \exp(-E/RT)$ .

Consequently, a plot of  $\ln \tau_{0.1}$  vs  $1/T_{CR}$  will have a slope equal to  $-E/R$  of the intrinsic global oxidation rate. In the absence of catalytic effects, the value of  $E$  should be the same for chars from all coals and chars from the same coal prepared under a wide variety of conditions. The nearly linear data in Fig. 3 appears to support this conclusion. A problem may arise if  $T_{CR}$  and  $T_0$  are significantly different. The mechanism of the oxidation reaction probably changes with temperature, as indicated by the wide range of activation energies and reaction orders reported for the char oxidation reaction in the literature (13). The best fit value of about 35 kcal/mole determined from Fig. 3 is intermediate in reported values and close to the value of 31 kcal/mole determined by Radovic and Walker for a wide range of chars in TGA experiments (14).

In our case, the Zap lignite chars appear to fall on a line of lower slope. This is probably due to catalytic effects. When a lignite char was acid-washed, it was less reactive in the non-isothermal test. The companion isothermal test has not yet been done, so we have not yet determined where the acid-washed char falls on the plot of Fig. 3.

**Variations in Reactivity** - The reactivities were determined for a number of chars which had been prepared under carefully controlled conditions to study their pyrolysis behavior (7-11,15). Examples to illustrate the observed trends are presented in Fig. 4. Figure 4a illustrates the results for the Zap lignite. The three curves are for: 1) 150 msec with maximum temperature of 700°C (with reactivity measured in air); 2) 460 msec with maximum temperature of 1600°C (in air); 3) same as 2 but reactivity in CO<sub>2</sub>. The curves illustrate the observation that the reactivity goes down with increased exposure to high temperature (or "extent of pyrolysis") and that for the same chars, CO<sub>2</sub> reactivity is lower than oxygen reactivity. Measurements of surface area  $S$  showed that char for conditions 1 and 2 were similar, suggesting that the difference in reactivity is caused by a change in the density of active sites,  $\rho$ . Figure 4b shows results for Pittsburgh Seam coal. The three curves are for: 4) 150 msec with a maximum temperature of 700°C (in air); 5) 660 msec with a maximum temperature of 1100°C (in air) and 6) same as 5 but reactivity in CO<sub>2</sub>. For equivalent cases (1 and 4), the reactivity for the Pittsburgh Seam coal is lower than for the Zap lignite prepared under equivalent conditions. Surface area measurements show the Pittsburgh Seam coal (which melts during pyrolysis) to have about 1/4 the surface area of the Zap lignite. This difference in surface area is not sufficient to account for the differences in reactivity, however. The extra reactivity appears to result from the lignite's mineral content, but could also be due to a difference in active site densities. Figure 4c compares curve 7 for the Zap lignite with curve 8 for the demineralized coal and curve 9 for a Montana Rosebud pyrolyzed under similar conditions and having a similar surface area. Curves 8 and 9 are similar, but lower in reactivity than the raw lignite. Figure 4 illustrates the variation in reactivity with surface areas, with active site density,  $\rho$  and with mineral content.

Figure 5 summarizes the results for a number of samples. The critical temperature  $T_{CR}$  is plotted as a function of the hydrogen content which is used as a measure of the extent of pyrolysis. For each char type, there is a trend for increasing  $T_{CR}$  with decreasing hydrogen. Most of the change occurs below 2 1/2% hydrogen, after the evolution of aliphatic hydrogen is complete. That is, the  $T_{CR}$  varies primarily with the concentration of aromatic hydrogen. It should be noted that there is also ring oxygen in the char which is removed at about the same rate as the hydrogen and which may be related to the reactivity changes. This variation is due to a variation in  $\rho$  possibly correlated with the ring condensation accompanying the elimination of aromatic hydrogen.

The vertical displacement of the curves is due to the variations in char surface area and catalytic activity of the minerals. The most reactive chars are for the Zap lignite. The chars have surface areas in the neighborhood of  $200 \text{ m}^2/\text{g}$ . As pyrolysis proceeds the critical temperature  $T_{\text{CR}}$  first decreases and then increases with temperature as hydrogen is lost. There does not appear to be any drastic effects due to heating rate, as chars for a wide range of conditions all fell along the same curve. The low values of  $T_{\text{CR}}$  are believed to be due to the char's mineral content (high Na and Ca). When the coal was demineralized (symbol  $\nabla$ ),  $T_{\text{CR}}$  increased substantially. A Montana Rosebud char with a similar surface area shows a somewhat higher  $T_{\text{CR}}$  than the raw Zap.

The highest  $T_{\text{CR}}$  values are for the Pittsburgh and Kentucky coals. These swell upon pyrolysis. Initial surface area measurements of the Pittsburgh coal show approximately  $50 \text{ m}^2/\text{g}$ , suggesting that the lower surface areas are responsible for the lower reactivity. Note that the reactivity of slowly heated Pittsburgh Seam coal is higher than that of a rapidly heated char.

#### CONCLUSION

A new reactivity test has been developed which allows relative rates of reactivity to be determined for chars of widely varying reactivity. The method was applied to study the dependence of reactivity on coal properties and pyrolysis conditions. Reactivities are seen to decrease with decreasing aromatic hydrogen concentration. Reactivities were insensitive to heating rate for a lignite but were quite sensitive to heating rate for a bituminous coal. Mineral catalytic effects were also observed.

#### ACKNOWLEDGEMENT

The authors are grateful for the support of the United States Army under contract DACA88-85-C-0020 in the development of the constant heating rate reactivity test and the support of the Morgantown Energy Technology Center of the United States Department of Energy under contract DE-AC21-85MC22050, for support of the study of char reactivity.

TABLE I

#### SAMPLE PROPERTIES

	WT% DAF			
	Zap, North Dakota Lignite	Montana Rosebud Subbituminous	Pittsburgh Seam Bituminous	Kentucky #9 Bituminous
Carbon	66.5	72.1	82.1	81.7
Hydrogen	4.8	4.9	5.6	5.6
Nitrogen	1.1	1.2	1.7	1.9
Sulfur	1.1	1.2	2.4	
Oxygen (Diff.)	26.5	20.3	8.2	
Ash (Dry Wt%)	7.1	10.0	9.2	14.1

## REFERENCES

1. Essenhigh, R.H., "Chemistry of Coal Utilization", 2nd Supplementary Vol., M.A. Elliott, Editor, John Wiley & Sons, NY, pg. 1162.
2. Smith, I.W., 19th Symposium (Int) on Combustion, The Combustion Institute, Pittsburgh, PA, pp 1045-1065, (1982).
3. Wells, W.F., Kramer, S.K., Smoot, L.D., and Blackham, A.U., 19th Symposium (Int) on Combustion, The Combustion Institute, Pittsburgh, PA, pp 1539-1546, (1982).
4. Ashu, J.T., Nsakala, N.Y., Mahajan, O.P., and Walker, P.L., Jr., Fuel, 57, 251, (1978).
5. Essenhigh, R.H. and Farzar, H., 19th Symposium (Int) on Combustion, The Combustion Institute, Pittsburgh, PA, pp 1105-111, (1982).
6. Nsakala, N.Y., Patel, R.L., and Lao, T.C., "Combustion and Gasification Characteristics of Chars from Four Commercially Significant Coals of Different Rank", Final Report, Electric Power Research Institute, Report No. 1654-6, (1982).
7. Solomon, P.R., Hamblen, D.G., Carangelo, R.M., and Krause, J.L., 19th Symposium (Int) on Combustion, The Combustion Institute, Pittsburgh, PA, pp 1139-1149, (1982).
8. Solomon, P.R. and David G. Hamblen, D.G., in Chemistry of Coal Conversion, R.H. Schlosberg, Editor, Plenum Press, NY, Chapter 5, pg. 121, (1985).
9. Solomon, P.R., Serio, M.A., Carangelo, R.M., and Markham, J.R., Fuel, 65, 182, (1986).
10. Solomon, P.R., Hamblen, D.G., and Carangelo, R.M., in Analytical Pyrolysis, K.J. Voorhees, (Editor), Butterworths, London, Chapter 5, pg. 121 (1984).
11. Mahajan, O.P., Yarzab, R., and Walker, P.L., Jr., Fuel, 57, 643, (1978).
12. Jenkins, R.G., Nandi, S.P., and Walker, P.L., Jr., Fuel, 52, 288, (1973).
13. Larendeau, N.M., Prog. Eng. Combust. Sci, 4, pp. 221-270, (1978).
14. Radovic, L.R. and Walker, P.L., Jr., Fuel, 62, 849, (1983).
15. Solomon, P.R., Serio, M.A., Hamblen, D.G., Best, P.E., Squire, K.R., Carangelo, R.M., Markham, J.R., and Heninger, S.G., "Coal Gasification Reactions with On-line In-situ FT-IR Analysis" DOE/METC Final Report Contract No. DE-AC21-81FE05122, (1986).

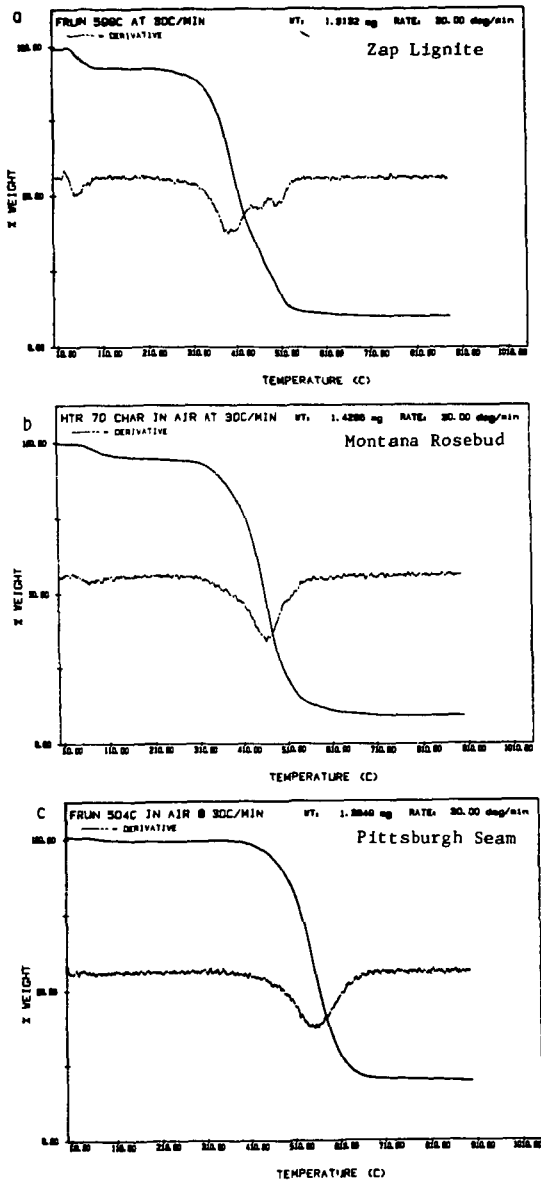


Figure 1. Non-isothermal TGA Reactivity Tests at 40 cc/min Air Flow. a) Zap Lignite, b) Montana Rosebud, and c) Pittsburgh Seam.

- ▲ Rosebud Subbituminous
- Pittsburgh Bituminous
- Zap Lignite
- × Zap Demineralized

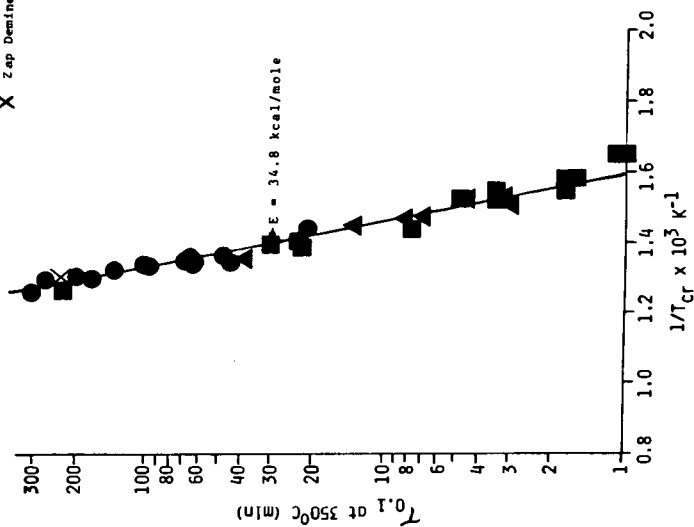


Figure 3.  $\tau_{0.1}$  (time for 10% burnoff) vs  $1/T_{cr}$ .  $T_{cr}$  is the Temperature at which the Weight Loss Rate Equals 0.11 wt. Fraction/min.

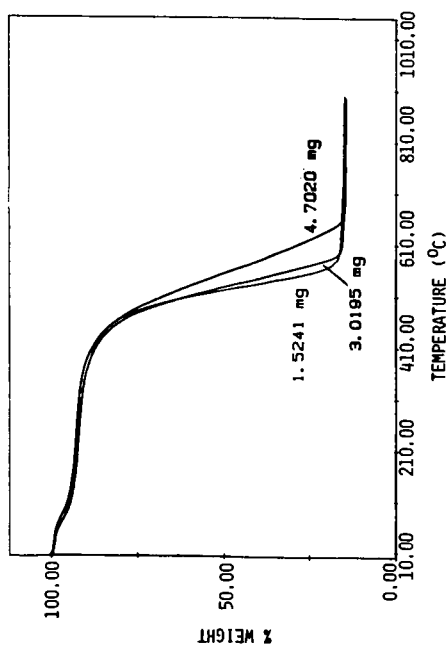


Figure 2. Comparison of Weight Loss Curves for Zap Lignite at 3 Sample Weights.

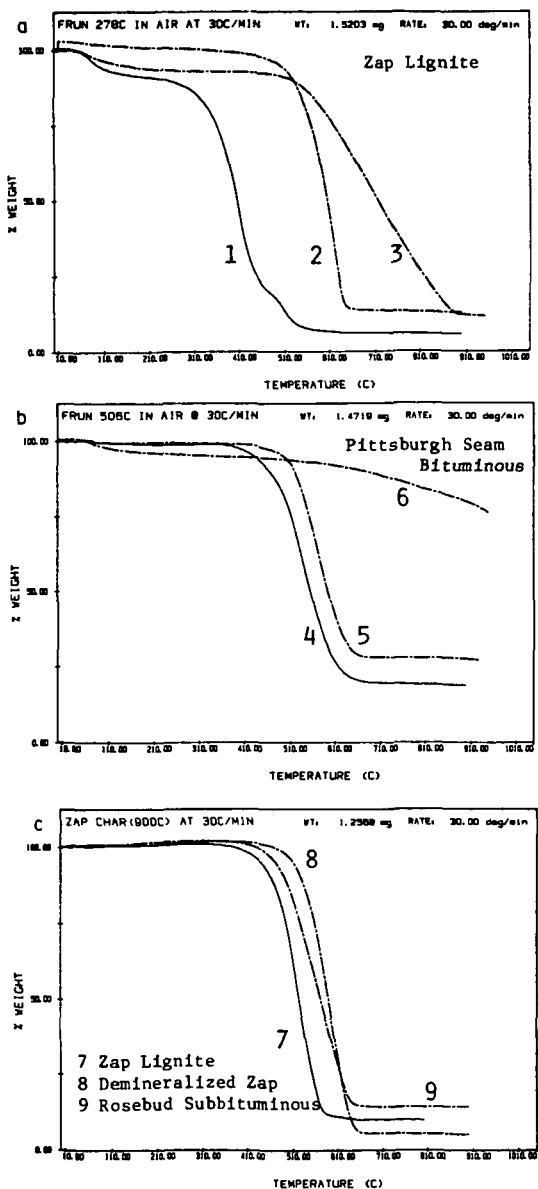


Figure 4. Comparison of Char Reactivity Curves Prepared for Three Coals Under a Variety of Conditions. Curves 3 and 6 are for Reactivity in  $CO_2$ . All the Rest are for Reactivity in Air.

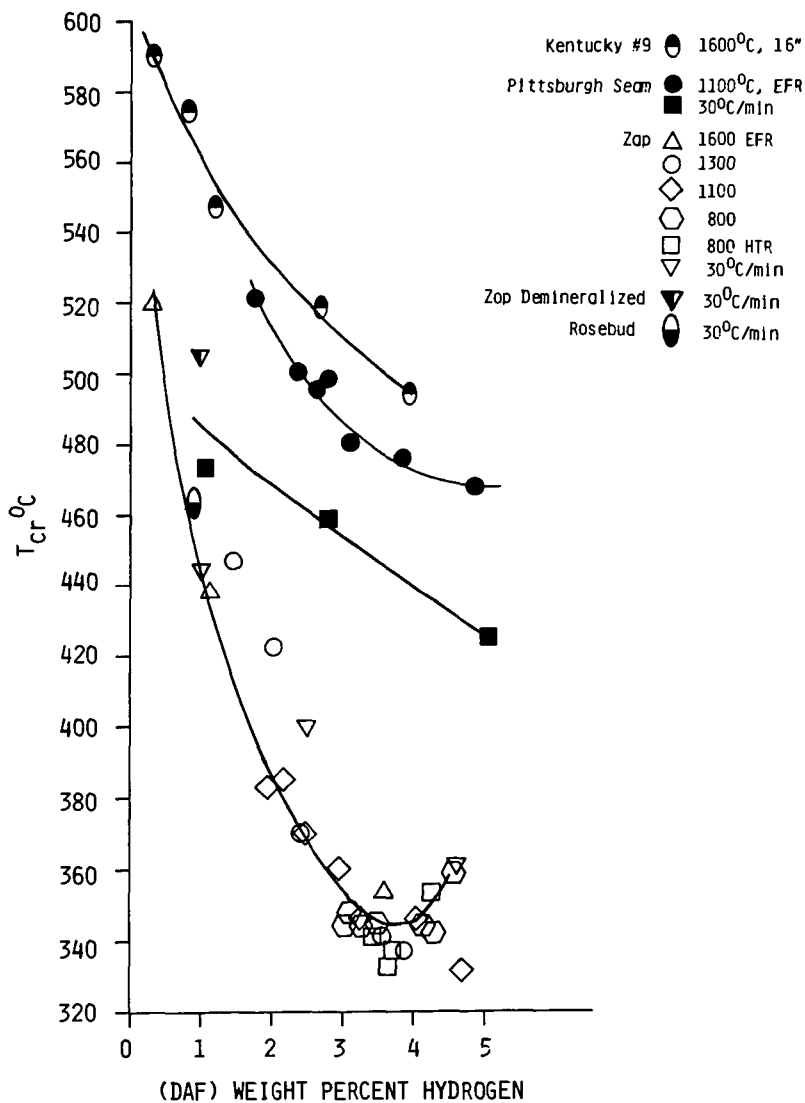


Figure 5. Variations in Reactivity with the Hydrogen Concentration in the Char (the extent of pyrolysis) and with Coal Type.

## COAL PYROLYSIS IN A HIGH PRESSURE ENTRAINED FLOW REACTOR

Michael A. Serio, Peter R. Solomon and Steven G. Heninger

Advanced Fuel Research, Inc. 87 Church Street, East Hartford, CT 06108

### INTRODUCTION

Many of the proposed coal gasification processes operate at elevated pressure. Since these processes also operate at elevated temperature, pyrolysis processes are important. However, there is relatively little data on pyrolysis yields at elevated pressure, particularly for continuous flow systems or on how pressure affects the reactivity of the char to subsequent gasification.

Most of the existing studies were done in batch, captive sample systems (1-3). For example, the work of Suuberg et al. (2) showed a significant effect of pressure on a bituminous coal and a modest effect for a lignite coal. The most important effect of pressure was a reduction in tar and increase in char yield at high pressure. However, one difficulty with interpreting the results from batch, captive sample systems is the pressure and residence time of the volatiles are not varied independently. As pressure is increased, the residence time of volatiles increases inside the particle as well as near the hot zone of the reactor.

In batch, semi-flow carbonization experiments, the effects of external pressure and external residence time can be varied independently. A review of the literature on semi-flow experiments by Dryden and Sparham (4) indicated that increases in inert gas pressure at constant volatile residence time did not have a significant effect on product yields. However, it should be noted that these experiments were done with very long volatile residence times (20 to 100 s). Recent work by Schobert et al. (5) examined the effect of pressure on tar yield in a semi-flow system (at constant residence times of about 1 s) and a pressure dependence of the tar yield was observed.

Entrained flow reactors are well suited to studies of pressure effects on pyrolysis and closely resemble real coal gasification systems. However, one must consider the effect of pressure on heat transfer as well. For example, Sundaram et al. (6) examined the effect of the pressure of various inert gases (He, CO, N<sub>2</sub>, Ar) on carbon conversion and found that yields went through a maximum before declining. It is likely that, at the short residence times of their experiments (0.6 to 1.9 s at 900°C), the enhanced heat transfer due to gas pressure was more beneficial than the detrimental effects on mass transfer.

This paper will present pyrolysis data for product yields for four coals from an entrained flow reactor operated at pressures up to 300 psig. In addition, the effect of pressure on char reactivity will be discussed.

### EXPERIMENTAL

A schematic of the high pressure reactor (HPR) system is given in Fig. 1. The furnace consists of a high pressure shell (capable of containing pressures up to 600 psig), a thick layer of insulation and a high temperature region heated by Kanthal Super 33 electrical heating elements. The high temperature section (capable of temperatures up to 1650°C) contains an alumina bed heat exchanger and a test section. The ambient gas enters the furnace through the heat exchanger to bring it up to furnace temperature and then turns downward into the test section. Coal is injected at a fixed point at the top of the test section using a water cooled injector. It mixes with the ambient gas and, after a fixed distance, enters a water-cooled collector. The reactor design is similar to a previously described atmosphere pressure entrained flow reactor (EFR) (7). The major differences are the smaller diameter test section in the HPR (1.27 cm vs 5.08 cm) and the absence of an optical port.

After the collector, the reaction products enter a cyclone to separate char, followed by a Balston filter to remove tar and soot. An electrostatic precipitator was tested for use after the cyclone but did not work as well as the filter. The gas stream is reduced in pressure and collected in a holding tank. The sample tank is a steel tank with glass-lined walls which is used to collect the total gaseous effluent from the reactor system during a typical run. It is initially evacuated and, during a run, the pressure gradually increases as it fills. After an experiment, a sample is taken from the tank and analyzed in an FT-IR cell and a GC. This allows the concentration of each species to be determined and the total yield of each product is calculated from a knowledge of the tank volume and pressure. The FT-IR can quantitatively determine many gas species observed in coal pyrolysis including CO, CO<sub>2</sub>, H<sub>2</sub>O, CH<sub>4</sub>, C<sub>2</sub>H<sub>2</sub>, C<sub>2</sub>H<sub>4</sub>, C<sub>2</sub>H<sub>6</sub>, C<sub>3</sub>H<sub>6</sub>, HCN, NH<sub>3</sub>, COS, CS<sub>2</sub>, SO<sub>2</sub>, and heavy paraffins and olefins. Additional characterization is performed by gas chromatograph to determine hydrogen, H<sub>2</sub>S, O<sub>2</sub>, N<sub>2</sub>, C<sub>3</sub>H<sub>8</sub>, C<sub>4</sub>'s, and C<sub>5</sub>'s. The overall material balance is generally better than 90 to 95%.

Routine monitoring of three temperatures (top of heating elements, bottom of heating elements, and top of preheated bed) is done with permanently mounted thermocouples. Platinum alloy thermocouples are used to meet the high temperature requirements and to allow the use of oxidizing atmospheres. Power is supplied to the heating elements by using welding power supplies with continuously variable voltage adjustment. The voltage is adjusted to maintain the reference temperatures (above) constant during a run. These reference temperatures are calibrated against the furnace wall and gas temperatures by a set of profiling experiments. The furnace wall temperature and the injector-collector separation are inputs into the particle-temperature model which allows description of the coal particle time-temperature history.

The coal feeder consists of a tube which passes up through a bed of coal, with feeder gas supplied above the bed. To feed coal, the gas is turned on and the feed tube is slowly lowered from a position where the entrance is above the bed. When the entrance of the tube reaches the bed level, the coal is entrained in the gas entering the feed tube. The rate of feed is controlled by the rate at which the tube is lowered. The total weight of coal fed during a run is determined by weighing the feeder system before and after the run.

At the end of a run, the water-cooled collector is removed and any tar or char which sticks to the collector is rinsed out with solvent and weighed. Most of the char is collected in the cyclone. Fine solids (e.g., soot and coal fines) and condensed tar vapor which pass through the cyclone are collected in a filter. The filter and other parts of the collection system are extracted with solvent (methylene chloride), which is subsequently evaporated to determine the tar yield.

## RESULTS AND DISCUSSION

The high pressure reactor (HPR) described above was used to determine the effects of pressure on pyrolysis behavior for four coals. The reactor was designed to provide similar temperatures and residence times as are employed in our atmospheric pressure reactor (EFR). To keep the gas requirements reasonable, a 1.27 cm I.D. tube was employed for the test section. It was found that swelling coals tended to plug the test section, so the coals tested were limited to subbituminous coals or lignites. The four coals tested were Montana Rosebud subbituminous, Gillette subbituminous, Jacob's Ranch subbituminous, and Zap (North Dakota) lignite. The coal analyses are presented in Table I. The pyrolysis yields for experiments at 800°C, 0.47 s residence time and 300 psig are given in Figs. 2-5 for these coals, respectively.

The most extensive amount of data was taken with the Montana Rosebud subbituminous due to a complementary program at AFR and Morgantown Energy Technology Center (METC) using this coal. The effects of pressure on product yields are observed to be modest in all cases. In general, with increasing pressure (at constant residence time and

temperature) there is a slight reduction in tar, olefin, and ethylene yields and increase in benzene, ethane and CH<sub>4</sub> yields. The trend for paraffin yield varies with the coal, as does the benzene yield trend. The subbituminous coals show a minimum benzene yield at intermediate pressures.

Data was obtained for the Zap, Jacob's Ranch, and Gillette coals at 685°C for the same residence time and range of pressures (not shown). The trends for tar, olefins, C<sub>2</sub>H<sub>4</sub>, and C<sub>2</sub>H<sub>6</sub> were similar, but the CH<sub>4</sub> and benzene yields declined with pressure. The complex variations of volatile yields with temperature and pressure would be expected since both in the internal secondary chemistry of the coal and the external gas phase chemistry there are temperature and pressure-dependent sources and sinks for the various species. For example, Suuberg et al. (2) have shown that methane yields increase with increasing external gas pressure in batch, capture sample experiments. This was attributed to evolution of CH<sub>4</sub> during secondary repolymerization of tar to form char. Arendt and van Heek (8) observed similar results for CH<sub>4</sub> yields in both batch and semi-flow reactors. Higher yields of methane under increased external gas pressure have also been attributed to the auto-hydrogenation phenomenon, where hydrogen evolved from the coal back reacts to form CH<sub>4</sub> (9). A recent paper has suggested that this reaction is more affected by residence time than external gas pressure for high and low rank coals (10).

There is also experimental evidence which suggests a decline in CH<sub>4</sub> yield would occur with increasing pressure. Methane decomposition is catalyzed in the presence of coal char (11,12). This has been attributed both to surface area and catalysis effects. At high pressure, the enhanced residence time of CH<sub>4</sub> in the pores would increase decomposition. In addition, the gas phase decomposition of CH<sub>4</sub> is believed to involve the following pressure dependent initiation reaction:



where M is any other molecule (13). This reaction would also be favored at high pressures. Consequently, numerous processes can operate on even such simple and relatively unreactive molecules as CH<sub>4</sub>, making a priori prediction of pressure trends for volatile yields over a wide range of temperature difficult.

In entrained flow systems, one must also contend with the effects of gas pressure on heat transfer. In our system, increasing the pressure also affects the shape of the temperature profile and, consequently, the length of the isothermal zone. In order to achieve the same nominal residence time it was necessary to reduce the gas flow rate at higher pressures. For this reason, an assessment of pressure effects for data from the reactor requires consideration of the effect of pressure on the particle time-temperature history due to: 1) changes in the experimental conditions, 2) changes in the physical properties of the entraining gas with pressure. To do this, an entrained flow reactor model was developed which is a modification of one developed recently for our atmospheric pressure reactor (EPR) (14,15). The latter model was validated by comparison to actual temperature measurements. For the HPR, direct validation is not possible because of the lack of an optical port in the reactor. Instead the model was validated by fitting CH<sub>4</sub> yields from low pressure HPR data (26 psig) where it was assumed that the validated kinetics from the EPR would still hold.

After the modified particle temperature model was developed and validated, the results of the HPR experiments were simulated. These simulations are shown as solid lines in Figs. 2-5. These trends, which account only for the effects of pressure on particle time-temperature history (and not on the pyrolysis chemistry) indicate that there are real pressure effects superimposed on a slight variation in the time-temperature history. The trends of the model predictions should be compared to the data trends in Figs. 2-5 to discern a pressure effect rather than the absolute values. This is because the pyrolysis model does not match all of the atmospheric pressure data (e.g., C<sub>2</sub>H<sub>4</sub> yields) due to an incomplete description of gas phase cracking.

**High Pressure Experiments in a Heated Tube Reactor** - A set of experiments was done at 800°C with Montana Rosebud coal in an electrically heated tube reactor at 1 atm and 5 atm pressure. The results for char, tar, and gas yields are shown in Fig. 6 for the two sets of experiments, which were done at the same volumetric flow rate. The total particle residence time at 200 cm distance is about 200 ms.

Initially, product yields are reduced when compared to the one atmosphere case. This is a result of the fact that the higher gas density causes a greater heat load on the tube and hence increases the distance required to heat the gas plus coal mixture to the equilibrium temperature. It is interesting that the maximum tar yield is lower in the 60 psig case. However, it is possible that an experiment in between 50 and 100 cm would reveal a higher tar yield. The asymptotic yield of about 10% is similar for both sets of experiments. It also agrees with the 26 psig data from the HPR. The advantage of the HTR relative to the HPR is that the good time resolution allows the maximum tar yields to be better defined.

**Comparison of Tar Yield Data from Three Reactors** - In Table II, tar yield data are listed for all three entrained flow reactors used at AFR. In each case, the final particle temperature was about 800°C. The residence times were lower for the HTR experiments but, due to the higher heating rate, the time at final temperature was nearly the same in each case ( $\sim 0.2$  s) according to our calculations. The lower pressure ( $< 5$  atm) results agree well between reactors. It is also apparent from the lower temperature HPR data in Table II, and the shorter residence time HTR data in Fig. 6, that some tar cracking occurred even under these relatively mild conditions. The reductions in tar yield due to cracking of about 35% agree well with previous data on Pittsburgh Seam bituminous coal tars cracked separately (16). The approximately 25% reduction in tar yield over a pressure range of 3 to 13 atm is in good agreement with the generalized plot developed by Suuberg (17).

**Char Reactivity Measurements** - Some reactivity measurements of the chars produced from the HPR experiments were made using a newly developed non-isothermal technique (18). The chars are heated at a constant rate (30°K/min) in a TGA in air. A reactivity index is defined based on a critical temperature to achieve a measurable weight loss rate, which is inversely related to reactivity. These data are given for the HPR chars in Table III. There does appear to be a slight decrease in char reactivity with increasing pressure. However, a portion of this could be attributed to the slightly increased severity of the higher pressure experiments. Additional data will be required on the kinetics of thermal deactivation in order to be more conclusive.

#### CONCLUSIONS

1. Pyrolysis experiments in a high pressure entrained flow reactor with three subbituminous and one lignite coal revealed an effect of pressure on product yields, even after allowing for changes in heat transfer. The tar and light hydrocarbon yields were most affected.
2. The relative reduction in tar yield as the pressure was increased from 3 to 13 atm was about 25%, in agreement with literature data.
3. The maximum tar yield was not observed in the 817°C, 0.5 s experiments, even at low pressure, due to tar cracking.
4. There was a small but consistent reduction of char reactivity with increased pressure. Some of this effect may be due to the slightly increased severity of the high pressure experiments.

#### ACKNOWLEDGEMENT

The authors gratefully acknowledge financial support of this work by the United States Department of Energy, Morgantown Energy Technology Center, under Contract No's. DE-AC21-81FE05122, DE-AC21-84MC21004, and DE-AC21-85MC22050.

#### REFERENCES

1. Anthony, D.B., Howard, J.B., Hottel, H.C., and Meissner, H.P., 15th Symposium (Int) on Combustion, The Combustion Institute, Pittsburgh, PA, p. 1303, (1975).
2. Suuberg, E.M., Peters, W.A., and Howard, J.B., "A Comparison of the Rapid Pyrolysis of a Lignite and a Bituminous Coal", in Thermal Hydrocarbon Chemistry, A.G., Oblad, H.H. Davis, and R.T. Eddinger, (Eds.), Adv. in Chem. Series, No. 183, pp 239-257, Am. Chem. Soc., Washington, DC (1979).
3. Niksa, S., Russel, W.B., and Saville, D.A., 19th Symposium (Int) on Combustion, The Combustion Institute, Pittsburgh, PA, p. 1151, (1982).
4. Dryden, I.G.C. and Sparham, G.A., B.C.U.R.A. Monthly Bulletin, 27, 1, (1963).
5. Schobert, H.H., Johnson, B.S., and Fegley, M.M., ACS Fuel Chem. Preprints, 23, #3, 136, (1978).
6. Sundaram, M.S., Steinberg, M., and Fallon, P.T., ACS Div. of Fuel Chem. Preprints, 28, #5, 106, (1983).
7. Solomon, P.R., Hamblen, D.G., Carangelo, R.M., and Krause J.L., 19th Symposium (Int) on Combustion, The Combustion Institute, Pittsburgh, PA, 1139, (1982).
8. Arendt, P. and van Heek, K.H., Fuel, 60, 779, (1980).
9. Rennhack, R., Brennstoff-Chemie, 45, 300, (1964).
10. Makino, M. and Toda, Y., Fuel, 58, 573, (1979).
11. Kamishita, M., Mahajan, O.P., and Walker, P.L., Jr., Fuel, 56, 444, (1977).
12. Stephens, D.R. and Clements, W., (Ed.) LLNL Underground Coal Gasification Project Quarterly Report, April to June 1983, Lawrence Livermore National Lab.
13. Back, M.H. and Back, R.A., Chapter 12 in Pyrolysis: Theory and Industrial Practice, Albright, L.F. Crynes, B.L., and Corcoran, W.H., (Eds.), Academic Press, NY, (1983).
14. Serio, M.A., Solomon, P.R., Hamblen, D.G., Markham, J.R., and Carangelo, R.M., "Coal Pyrolysis Kinetics and Heat Transfer in Three Reactors", paper submitted to 21st Symposium (Int) on Combustion, (Jan. 1986).
15. Solomon, P.R., Serio, M.A., Hamblen, D.G., Best, P.E., Squire, K.R., Carangelo, R.M., Markham, J.R., and Heninger, S.G., a) Final Report for METC Contract No. DE-AC21-81FE05122, (1985). b) First Quarterly Report for METC Contract No. DE-AC21-85MC22050, (1986).
16. Serio, M.A., Peters, W.A., Sawada, K., and Howard, J.B., "Secondary Reactions of Nascent Coal Pyrolysis Tars", paper in Proceedings, International Conference on Coal Science, Pittsburgh, PA, Aug. 15-19, 1983, pp 533-536.
17. Suuberg, E.M., Chapter 4, in Chemistry of Coal Conversion, R.H. Schlosberg, (Ed.), Plenum Press, New York, (1985).
18. Solomon, P.R., Serio, M.A., and Heninger, S.G., "Variations in Char Reactivity with Coal Type and Pyrolysis Conditions" ACS Div. of Fuel Chem., Anaheim Meeting, (1986).

**TABLE I**  
**SAMPLE PROPERTIES**

	<b>WT% DAF</b>			
	<b>Zap, North Dakota Lignite</b>	<b>Gillette Subbituminous</b>	<b>Montana Rosebud Subbituminous</b>	<b>Jacob's Ranch Subbituminous</b>
Carbon	66.5	72.0	72.1	74.3
Hydrogen	4.8	4.7	4.9	5.2
Nitrogen	1.1	1.2	1.2	1.1
Sulfur (Organic)	1.1	0.5	1.2	0.6
Oxygen (Diff.)	26.5	21.6	20.3	18.8
Ash (Dry Wt%)	7.1	5.0	10.0	7.8

**TABLE II**  
**OBSERVED TAR YIELDS (DAF) FROM VARIOUS REACTORS**  
**AT 800°C, 0.1-0.5 S RESIDENCE TIME**

Coal:			Zap Lignite	Gillette	Montana Rosebud	Jacob's Ranch
Reactor	Pressure (atm)	Time (s)				
HTR	1.0	0.2	10.3		10.0	
HTR	5.0	0.2			10.0	
EFR	1.0	0.4	10.0*			
HPR	2.6	0.5	6.0 (8.0)	9.4 (13.6)	9.2	7.6 (11.0)
HPR	13.0	0.5	4.5 (7.5)	7.8 (11.5)	6.0	6.5 ( 9.5)

NOTES: Values in parentheses are for 658°C experiments at the same residence time and pressure.

\* Tar plus missing.

HTR = Heated Tube Reactor  
EFR = Entrained Flow Reactor  
HPR = High Pressure Reactor

TABLE III

CRITICAL TEMPERATURE FOR OXIDATION OF CHARS FORMED AT VARIOUS PRESSURES

Coal:	Zap Lignite	Gillette	Montana Rosebud	Jacob's Ranch
Pressure (atm)				
2.6	365	368	403	370
7.8	366	378	415	370
13.1	378	381	419	376
21.4	---	---	429	---

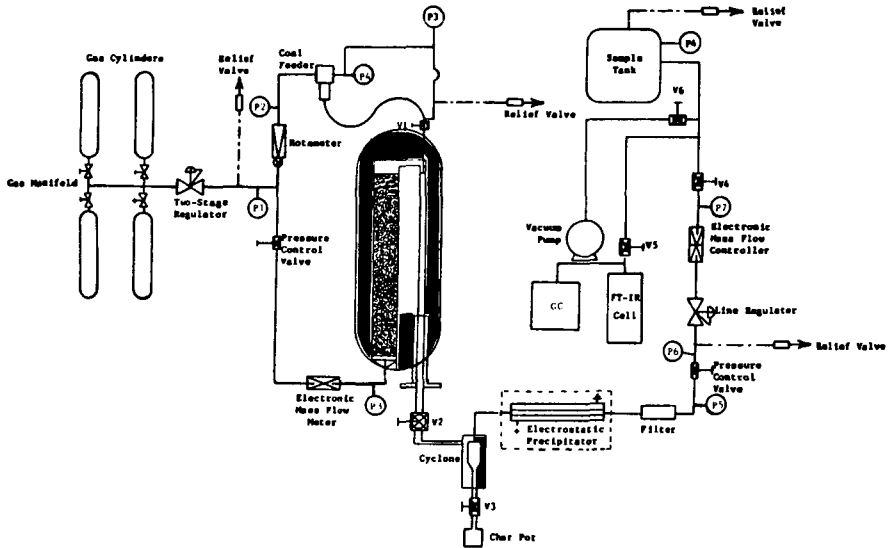


Figure 1. Schematic of High Pressure Entrained Flow Reactor System.

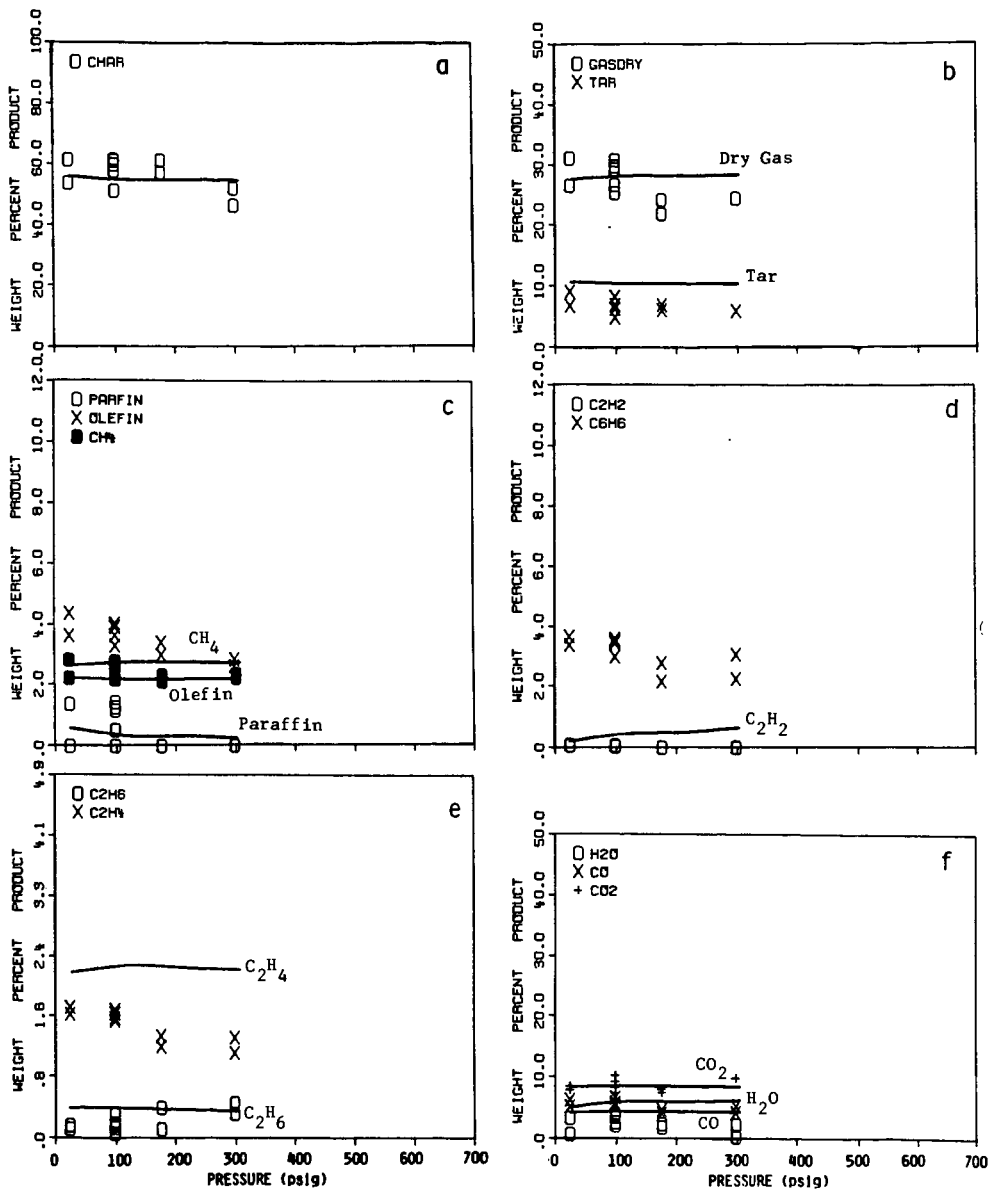


Figure 2. Pyrolysis Product Distribution for Montana Rosebud Subbituminous Coal as a Function of Pressure. Temperature = 817°C, Residence Time = 0.47 sec.

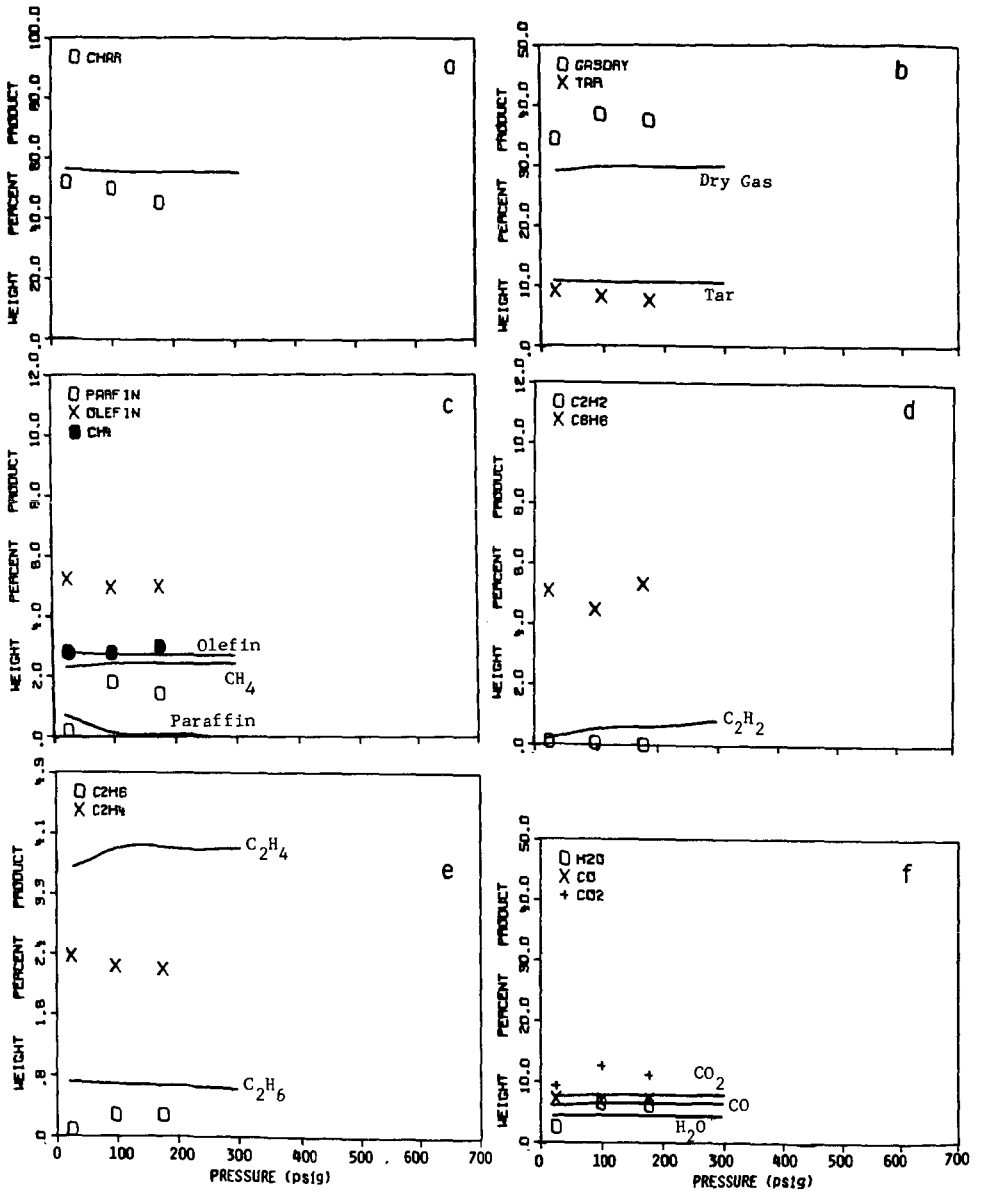


Figure 3. Pyrolysis Product Distribution for Gillette Subbituminous Coal as a Function of Pressure. Temperature = 817°C, Residence Time = 0.47 sec.

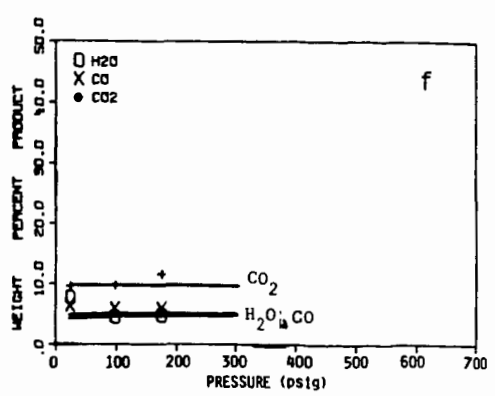
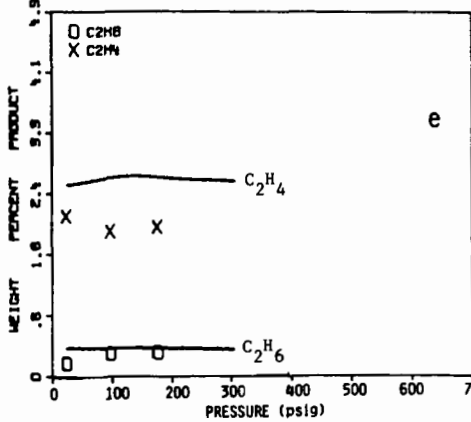
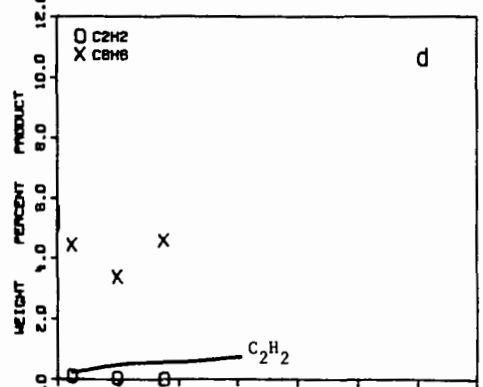
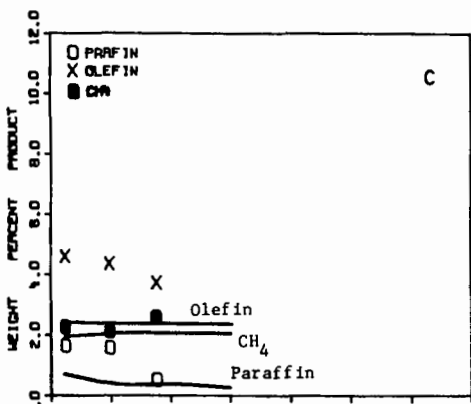
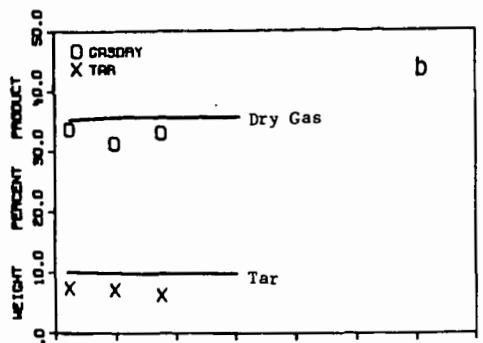
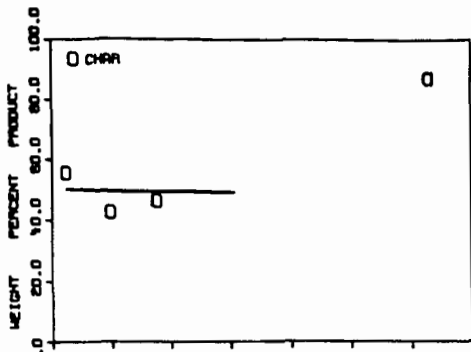


Figure 4. Pyrolysis Product Distribution for Jacob's Ranch Subbituminous Coal as a Function of Pressure. Temperature = 817°C, Residence Time = 0.47 sec.

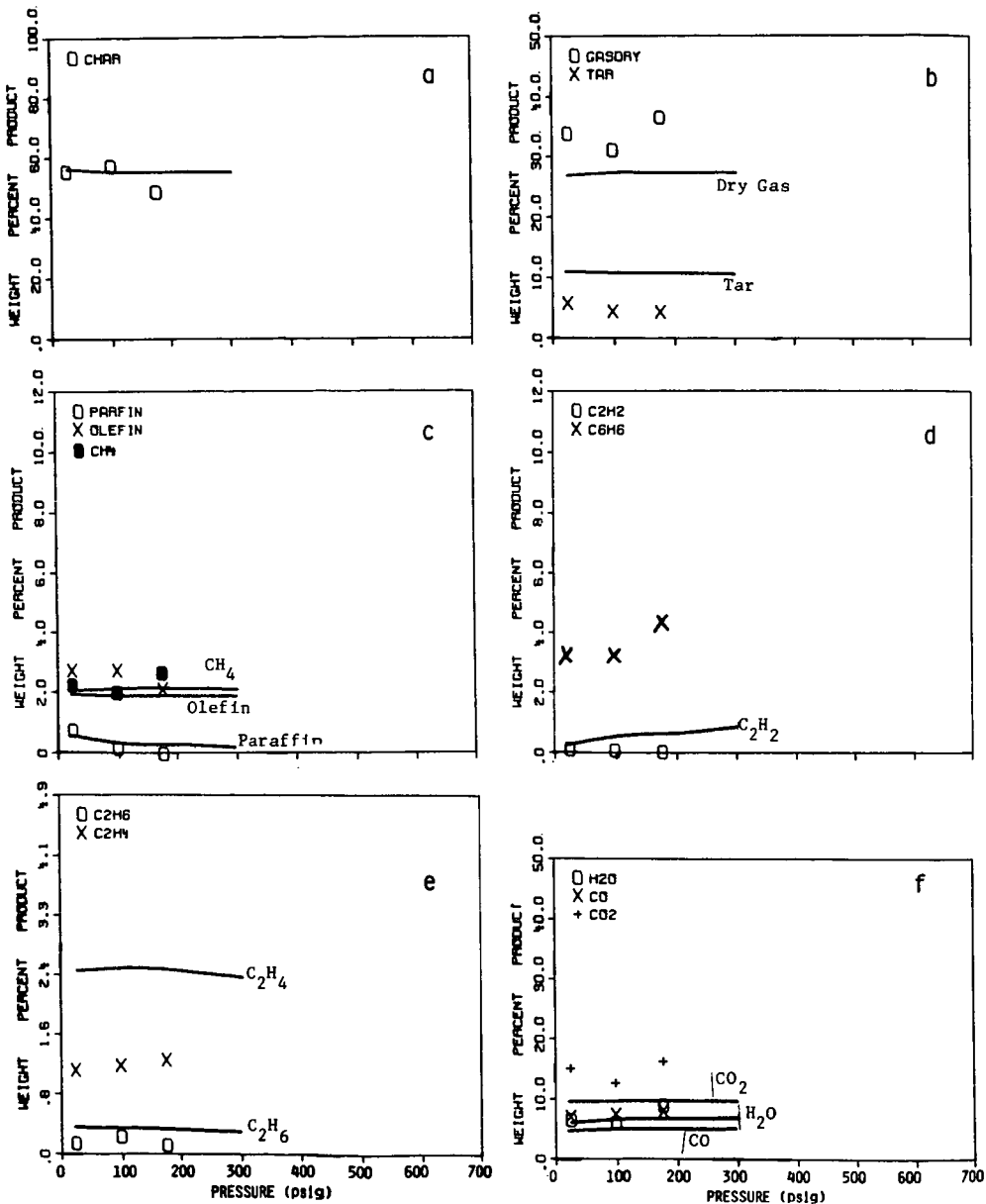


Figure 5. Pyrolysis Product Distribution for Zap, North Dakota Lignite as a Function of Pressure. Temperature = 817°C, Residence Time = 0.47 sec.

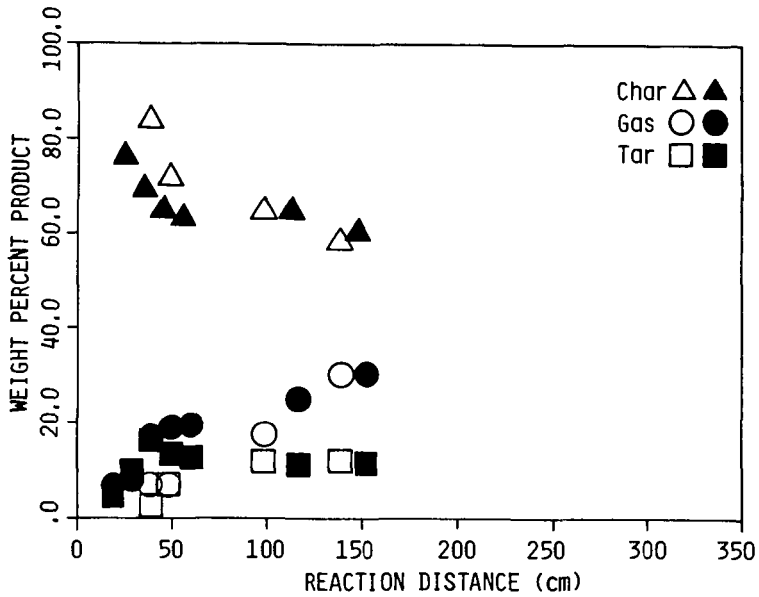


Figure 6. Comparison of Pyrolysis Data from One Atmosphere Pressure (solid symbols) and 5 atm pressure (open symbols) Experiments in the Heated Tube Reactor with Montana Rosebud Coal (200 x 270 mesh). The Equilibrium Tube Temperature was 800°C.

## RESPONSE SURFACE MODEL PREDICTIONS FOR THE FLASH PYROLYSIS OF MONTANA ROSEBUD COAL

Larry A. Bissett

Morgantown Energy Technology Center  
P.O. Box 880  
Morgantown, WV 26507-0880

### Abstract

Experiments covering a broad range of reaction conditions are being conducted to determine and model the effects of coal gasification environment on product yields. The research uses a 3-inch I.D., down-flow entrained reactor that turbulently mixes preheated gases with coal to achieve high particle heating rates. As part of the test program, a pyrolysis series reacting Montana Rosebud coal in a nitrogen-argon atmosphere was completed. A 3-variable, composite factorial experimental design was used in which reaction conditions ranged from 1,500° to 2,500°F temperature, 100 to 900 psig pressure, and 2.19 to 10.00 seconds gas residence time. Quadratic response surface models were used to analyze the product yield and composition data as a function of the reaction conditions. Trends predicted by some of the statistically significant regression models are presented and discussed.

### Introduction

For advancement to continue towards tailored, economic, and environmentally sound coal conversion technologies, further understanding of reaction mechanisms and product formations in relation to processing conditions and the physical and chemical structure of coal is needed. Devolatilization and associated phenomena are especially important in entrained gasification and pulverized coal combustion due to the small particle sizes, high temperatures, and short residence times involved. Although numerous studies have been conducted, recent reviews have concluded that there is little experimental verification at high-temperature, high-pressure conditions that exist in some current and advanced processes (1,2). Therefore, this project was initiated to determine the effects of gasification environment on product yields over a broad range of mild to severe conditions. A broad-range study was chosen to aid in the detection of reaction mechanism changes and to help integrate results from other related investigations.

### Experimental

A down-flow entrained reactor designed to be able to preheat reactant gases to 3,000°F along the horizontal axis and maintain the reaction mixture at 2,500°F along the vertical axis at pressures up to 1,000 psig is used for the research. Details of the reactor and experimental system have been previously presented (3,4). The reactor is uniquely characterized by a mixing configuration that turbulently combines argon-conveyed coal with highly preheated reactant gases and subsequently transitions the flow to laminar-like before it enters a 3-inch I.D., 4-foot long alumina reaction tube. The turbulent, nearly adiabatic mixing between reactant gases and coal results in high particle heating rates approaching 10<sup>5</sup>°F per second. In addition to being essential for properly studying the phenomena of interest, this enables reaction temperatures to be reached near the exit of the nozzle and provides the potential for achieving axial isothermal temperature profiles in the reaction tube.

A comprehensive test program with Montana Rosebud subbituminous coal is being conducted. The program is organized into three major test classes to study inert, steam, and carbon dioxide environments, and an additional class to investigate char gasification reactions. The classes are further subdivided into test series to

investigate other variables. The Class 3A pyrolysis tests reported here were conducted in an inert environment of 75 mole percent nitrogen and 25 mole percent argon and consisted of a composite factorially designed series to investigate the effects of reaction temperature, pressure, and gas residence time. The composite factorial experimental design enabled a wide range of conditions to be studied with 15 different tests and permitted the use of response surface and statistical techniques for data analyses. To help ensure that each test point carried about the same weight, uniform variable spacing was used for testing and analyzing. The variable levels and respective codes are given in Table 1. To facilitate the ability of the quadratic response surface models to adequately represent the true response surfaces, the temperature levels were equally spaced reciprocally as absolute temperature, and the pressure and gas residence time levels were equally spaced logarithmically as absolute pressure and seconds, respectively.

TABLE 1. Composite Factorial Variable Levels

Variable	Levels				
METC Test Code	1	2	3	4	5
Factorial Code	-2	-1	0	1	2
Temperature, °F	1,500	1,681	1,898	2,165	2,500
Pressure, psig	100	178	309	530	900
Gas Residence Time, sec	2.19	3.20	4.68	6.84	10.00

Experimentally, the gas environment, gas-coal ratio (400 scf/lb), and total material fed to the reactor during steady-state conditions were held essentially constant throughout the test series. A 200 x 270 mesh fraction of Montana Rosebud coal with an average particle diameter of 57 microns was used. Expressed as weight percent, the average ultimate analysis of the coal was 64.1 carbon, 4.4 hydrogen, 17.9 oxygen, 1.1 nitrogen, 1.0 sulfur, 10.4 ash, and 1.0 moisture; and the average volatile matter content was 40.6.

#### Results and Discussion

The overall material balance accountability of coal to product gases, liquids, and chars was greater than 98 weight percent. Quadratic response surface models which considered linear, quadratic, and interaction effects were used to analyze 50 variables. The Statistical Analysis System (SAS) computer program was used to perform the least squares regressions (5). Thirty-six variables had potentially adequate regression model fits at the 0.05 significance level or higher. Some regression model predictions of product yields and compositions from this test series have been previously reported (6). Only the regression models for elemental retentions in char will be discussed here.

Table 2 lists the experimental elemental char retentions, defined as the weight percentage of each major coal element that remained in the char, for this test series. The test numbers are derived from the METC test codes for the variable levels given in Table 1. The "3A" identifies the test class and is followed by three numbers which sequentially identify the temperature, pressure, and gas residence time levels. A fourth number is used when a test condition is repeated and represents the repetition number. Thus, Table 2 also illustrates the 15 different variable combinations involved with the composite factorial design and shows

that the center point condition (i.e., 3A333) was repeated 4 times to determine experimental variation. Test No. 3A333-1 failed and therefore does not appear in the table.

Nitrogen was the only elemental retention that could not be adequately represented by a quadratic response model at the 0.06 significance, or alpha, level or higher. Of the four that could be adequately represented, all had statistically significant predicted temperature effects to at least the 0.07 alpha level, only hydrogen and sulfur retentions had significant predicted pressure effects to at least the 0.04 alpha level, and all but oxygen retention had significant predicted gas residence time effects to at least the 0.08 alpha level. The significance levels provided the criteria for selecting which regression models and what variable ranges were used for predictive purposes. In general, full experimental ranges were used when significance values were 0.05 or higher, and only small variations around the center point of the experimental design were used when significance values were between 0.05 and 0.10.

Figure 1 shows how the predicted carbon, hydrogen, oxygen, and sulfur retentions in char vary with reaction temperature at the experimental center point pressure and gas residence time conditions. Oxygen is the least retained (i.e., most converted) element, and is predicted to be essentially absent in the char at temperatures above 2,000°F. Hydrogen retention decreases steadily with temperature and begins to approach zero at the highest temperature. This behavior most likely reflects thermally induced dehydrogenation and condensation of the larger aromatic structures in the char. Carbon and sulfur retentions both initially decrease, but then increase at higher temperatures. This behavior mostly accounts for a similar trend in char yield, which was also shown to pass through a minimum (6). The tendency for carbon retention to increase at higher temperatures is probably due to the increased cracking of volatile species, either in the hotter, outer regions of the particles as they devolatilize or in the extraparticle environment. The possibility of decreased yields at higher temperatures due to secondary reactions was recognized prior to this experimental confirmation (7). The tendency for sulfur retention to increase may be due to the high-temperature reaction of hydrogen sulfide with char to form thiophenic structures, as has been reported (8), or capture of the sulfur by ash components.

Figure 2 indicates an interaction between temperature and pressure effects on hydrogen retention. The nature of the predicted pressure effect changes with reaction temperature and decreases in magnitude as temperature increases. The pressure effect is relatively unimportant at higher temperatures. At lower temperatures, however, hydrogen retention increases faster with pressure than hydrogen yield decreases which, if there is no pressure effect on carbon retention as indicated by a poor significance level, implies that the overall hydrogen-carbon ratio of the nonchar products decreases. Thus, in very general and relative terms, pressure may tend to shift the aromatic hydrocarbon spectrum to heavier components at lower temperatures, but has little or no effect at higher temperatures due to extremely low organic yields. This behavior may be due to equilibrium considerations or reflect pressure effects on the sequence of secondary cracking reactions.

Figure 3 shows that near the experimental center point temperature and at the center point gas residence time, sulfur retention is predicted to maximize in roughly the 200 to 300 psig pressure range. At lower pressures, sulfur retention decreases slightly with temperature and, conversely, increases slightly with temperature at the higher pressures. The occurrence of maxima and the inverted temperature dependencies suggest the presence of multiple phenomena. Candidate explanations could include some of the possible effects of pressure on the following: (1) reaction rates of sulfur species with char and ash, (2) initial distribution of devolatilized sulfur species, (3) sequence and rates of secondary reactions, (4) coal and char physical changes during devolatilization that affect reactant accessibility,

and (5) various sulfur absorption equilibriums. Planned analyses of the chars to obtain the proportion of organic and inorganic sulfur forms may clarify these trends.

Figure 4 shows how the predicted hydrogen and carbon retentions vary with gas residence time near the experimental center point temperature and at the center point pressure. Hydrogen retention decreases just slightly with residence time and has a comparatively much greater sensitivity to temperature. The decrease is probably due to an annealing-like phenomena which results in the slow dehydrogenation and condensation of aromatic structures in the char. The predicted trends show that the dehydrogenation rate increases with temperature. Carbon retention is predicted to increase with time at the lower temperatures, but decrease with time at the highest temperature. Furthermore, carbon retention increases with temperature at gas residence times less than approximately 3.5 seconds, but decreases with temperature at longer residence times. The explanation for this behavior is not clear, but may possibly involve the relative kinetics of some of the cracking and gasification reactions and the initial cracking sequence. Initially, more intraparticle cracking of volatile species may be occurring during devolatilization as temperature increases, and, hence, carbon retention increases with temperature at the shortest residence times. The volatile species that escaped intraparticle cracking at the lower temperatures may then, with time, continue cracking in the extraparticle environment and lead to a gradual increase in carbon retention. Because significant cracking may have already occurred at the highest temperature, there would be little material left for long-term extraparticle cracking and, hence, no tendency for carbon retention to increase. However, gasification reactions of the char with carbon dioxide and water formed during pyrolysis would have the opportunity to proceed and may account for the gradual conversion of carbon at the highest temperature. At the lower temperatures, the gasification reactions may not be fast enough to counter deposition resulting from cracking reactions, and thus, carbon retention continues to increase. To validate these explanations, more data are needed for yields at residence times under 2 seconds and for cracking rates of various light hydrocarbons in the presence of char at the experimental conditions.

Figure 5 shows that sulfur retention in char is very sensitive to gas residence time and relatively insensitive to temperature. The trends indicate that a low-sulfur char is initially produced, but increases in sulfur content as time proceeds. This implies that a large percentage of the sulfur in the coal is initially released to the extraparticle environment and that various mechanisms then return some of the sulfur to the char. Various organic sulfur compounds crack into hydrogen sulfide and carbon disulfide, and these as well as the hydrogen sulfide initially formed from pyrite probably back react with the char and ash components. Depending on the initial forms of the devolatilized sulfur and relative reaction rates, these trends could predominantly reflect the kinetics of either hydrogen sulfide absorption reactions or organic sulfur compound cracking reactions. The suggested asymptote at approximately 75 percent sulfur retention possibly reflects approach to equilibrium or an absorption limit of the ash. Further analyses of sulfur forms in the chars may indicate the dominant effects.

### Conclusions

A composite factorial experimental design and response surface methods were successfully applied to study the flash pyrolysis of Montana Rosebud coal over wide ranges of temperature, pressure, and gas residence time. Statistically significant regression models were used to predict product yield and composition trends. The regression model predictions reported here for elemental retentions in char lead to the following conclusions: (1) char yields increased at the higher temperatures investigated due to carbon deposition from the cracking of volatiles and sulfur absorption by char and ash components, (2) carbon, hydrogen, and oxygen retentions

were most sensitive to temperature and sulfur retention was most sensitive to residence time, (3) pressure may tend to shift the aromatic hydrocarbon spectrum to heavier components at the lower temperatures investigated, (4) sulfur retention was likely affected by multiple phenomena, (5) char annealing effects and continued cracking of light hydrocarbons were present in the residence time range studied, and (6) a low-sulfur char was initially produced, but increased in sulfur content with time to an apparent asymptotic value due to back reactions of sulfur species with the char and ash.

#### References

1. Howard, J. B., W. A. Peters, and M. A. Serio. 1981. EPRI Report No. AP-1803.
2. Talwalkar, A. T. 1983. DOE/MC/19316-1408 (DE83006592).
3. Bissett, L. A. 1983. DOE/METC/84-8 (DE84000217):116-128.
4. Bissett, L. A. 1984. DOE/METC/85-2 (DE85001955):65-72.
5. Statistical Analysis System Institute. 1982. SAS User's Guide: Statistics.
6. Bissett, L. A. 1985. DOE/METC-85/6024 (DE85008618):80-89.
7. Howard, J. B. 1981. Chapter 12. Chemistry of Coal Utilization, Second Supple. Vol., Ed. M. A. Elliott, New York: John Wiley and Sons, Inc.
8. Calkins, W. H. 1985. ACS Div. of Fuel Chem. Preprints. 30(4):450-465.

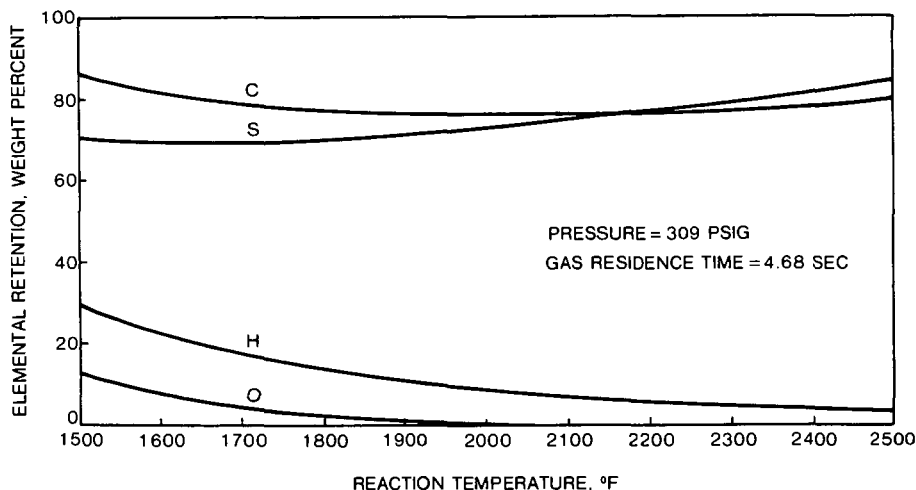


Figure 1. Regression Model Prediction for Elemental Retention in Char vs. Reaction Temperature, Class 3A Nitrogen-Montana Rosebud Coal Tests, METC Advanced Gasification Facility Entrained Reactor

TABLE 2. Elemental Char Retention, Weight Percent, Class 3A  
 Nitrogen -- Montana Rosebud Coal Tests, METC  
 Advanced Gasification Facility Entrained Reactor

Test No.	Temperature, F°	Pressure, psig	Gas Residence Time, sec.	Carbon	Hydrogen	Oxygen	Nitrogen	Sulfur
3A133	1,500	309	4.68	85.9	31.7	11.0	89.6	67.9
3A222	1,681	178	3.20	75.1	16.3	7.3	69.3	66.2
3A224	1,681	178	6.84	82.9	15.8	13.3	36.2	70.9
3A242	1,681	530	3.20	78.1	19.6	11.1	69.8	47.1
3A244	1,681	530	6.84	85.6	19.7	5.8	76.6	70.1
3A313	1,898	100	4.68	78.1	6.7	1.5	80.4	62.3
3A331	1,898	309	2.19	77.0	12.7	5.5	73.5	41.1
3A333	1,898	309	4.68	77.5	11.0	0.1	89.5	67.6
3A333-2	1,898	309	4.68	76.6	10.0	2.4	58.9	71.4
3A333-3	1,898	309	4.68	76.3	11.5	0.2	70.5	76.5
3A333-4	1,898	309	4.68	75.5	11.9	0.5	68.2	70.6
3A335	1,898	309	10.00	76.4	8.0	1.6	76.9	74.5
3A353	1,898	900	4.68	76.3	12.5	11.2	67.6	51.1
3A422	2,165	178	3.20	76.2	8.0	1.1	80.2	59.0
3A424	2,165	178	6.84	71.3	2.6	0	41.4	66.4
3A442-1	2,165	530	3.20	78.0	5.2	0.7	62.4	68.6
3A444	2,165	530	6.84	78.0	6.5	3.9	56.4	71.4
3A533	2,500	309	4.68	80.5	3.0	0	49.4	89.0

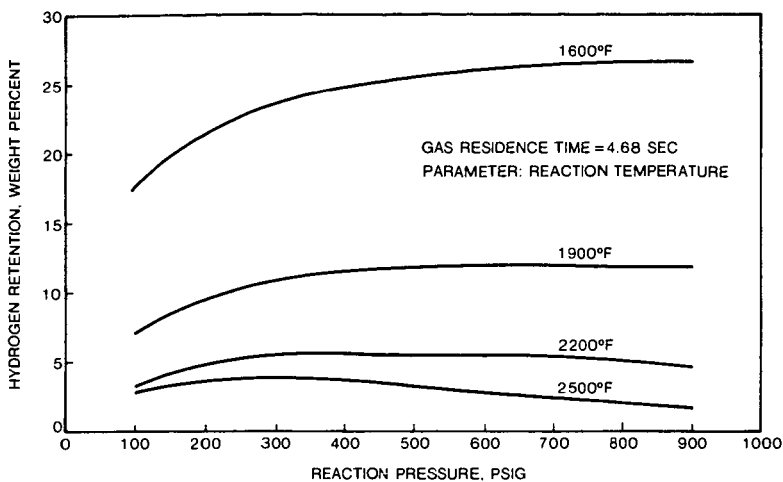


Figure 2. Regression Model Prediction for Hydrogen Retention in Char vs. Reaction Pressure, Class 3A Nitrogen-Montana Rosebud Coal Tests, METC Advanced Gasification Facility Entrained Reactor

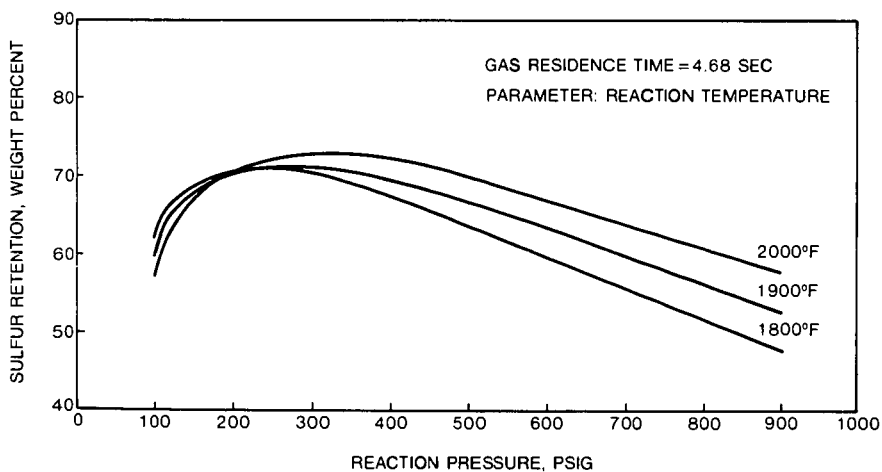


Figure 3. Regression Model Prediction for Sulfur Retention in Char vs. Reaction Pressure, Class 3A Nitrogen-Montana Rosebud Coal Tests, METC Advanced Gasification Facility Entrained Reactor

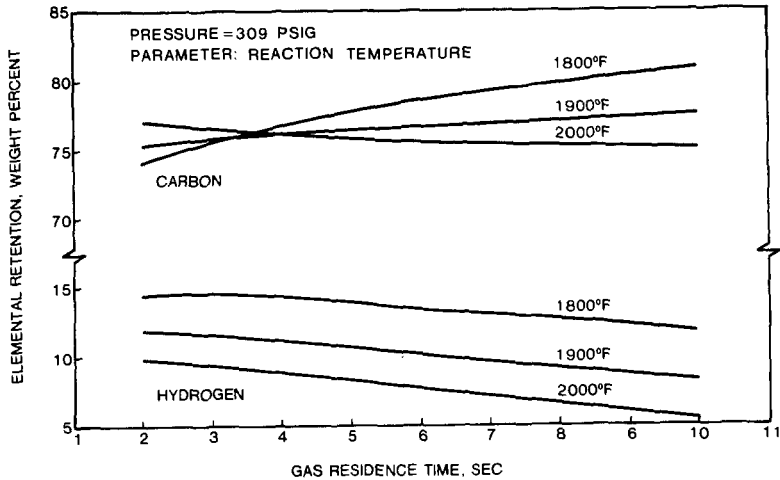


Figure 4. Regression Model Prediction for Carbon and Hydrogen Retention in Char vs. Gas Residence Time, Class 3A Nitrogen-Montana Rosebud Coal Tests, METC Advanced Gasification Facility Entrained Reactor

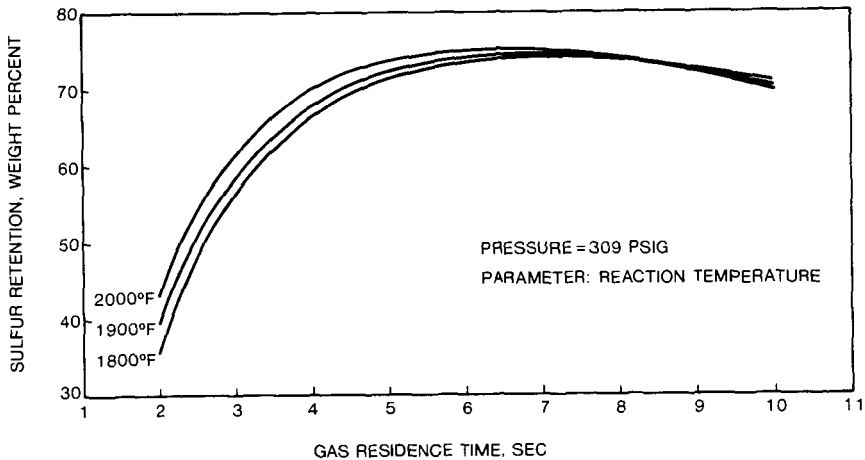


Figure 5. Regression Model Prediction for Sulfur Retention in Char vs. Gas Residence Time, Class 3A Nitrogen-Montana Rosebud Coal Tests, METC Advanced Gasification Facility Entrained Reactor

Flash Pyrolysis of New Mexico Sub-Bituminous Coal  
in Helium-Methane Gas Mixtures

Muthu S. Sundaram, Peter T. Fallon and Meyer Steinberg  
Process Sciences Division  
Brookhaven National Laboratory  
Upton, New York 11973

ABSTRACT

A New Mexico sub-bituminous coal was flash pyrolyzed in gas mixtures of helium and methane at 1000°C and 50 psi in an 1-in. I.D. entrained down-flow tubular reactor. The mixture contained 0 to 40% helium in methane. Under tested experimental conditions, pyrolysis in gas mixtures resulted in higher yields of ethylene and BTX than in pure methane. For example, under a coal flow rate of 1.0 lb/hr and methane flow rate of 4.0 lb/hr, pyrolysis in pure methane produced 7.7% C<sub>2</sub>H<sub>4</sub> and 9.0% BTX on the basis of carbon contained in coal; under similar coal and methane flow rates, as high as 14.8% C<sub>2</sub>H<sub>4</sub> and 15.3% BTX were obtained on pyrolysis in 25% He + 75% CH<sub>4</sub> gas mixture. The data show that the coal flow rate and methane flow rate both independently affect the yields of C<sub>2</sub>H<sub>4</sub> and BTX. At constant methane flow rate, increase in coal flow rate decreases the yields of C<sub>2</sub>H<sub>4</sub> and BTX; at constant coal flow rate, increase in methane flow rate increases the yields of C<sub>2</sub>H<sub>4</sub> and BTX.

Keywords: coal; natural gas; pyrolysis; gasification.

INTRODUCTION

The aim of the flash pyrolysis of coal is the production of smaller molecules from it in a shortest possible particle residence time. Therefore, the objective of studying the process chemistry of coal pyrolysis is to investigate the experimental parameters that permit this aim to be achieved and to establish the optimum conditions that produce a favorable product slate. The basic process parameters that influence the product yields during flash pyrolysis of coal are: (1) reaction temperature, (2) gas pressure and (3) residence times of coal particles and ensuing tar vapors. In addition to these major process parameters, product yields can be influenced by other factors such as the nature of the pyrolysis gas and its partial pressure and the gas-to-coal ratio.

Previous work on flash pyrolysis of coal at Brookhaven National Laboratory was performed with inert pyrolysis gases, He, N<sub>2</sub> and Ar, and reactive gas, H<sub>2</sub>.<sup>(1)</sup> Because of its process potential, our recent work has concentrated on the flash pyrolysis of coal with reactive methane gas.

Methane, in the form of natural gas, has become a readily available, low-cost raw material. Utilization and conversion of coal in conjunction with natural gas to produce higher valued fuel and feedstocks, becomes an attractive process proposition.

In general, pyrolysis experiments have been carried out in pure gases, either inert or reactive. In a few instances, mixtures of inert gases e.g. N<sub>2</sub>-Ar<sup>(2)</sup> or reactive gases e.g. H<sub>2</sub>-H<sub>2</sub>O were used as pyrolysis atmospheres.<sup>(3)</sup> The potential and usefulness of mixtures of inert and reactive gases towards the selectivity of pyrolysis products, heretofore, has not been investigated.

In order to determine if a relative increase in the heat transfer coefficient of the pyrolyzing gas could be used to increase the yields of ethylene and BTX from coal, a detailed examination of the pyrolysis of a New Mexico sub-bituminous coal was conducted in gas mixtures of helium and methane. The effects of gas mixture composition, coal feed rate and gas feed rate on the yields of ethylene and BTX are reported in this paper.

#### EXPERIMENTAL

The flash pyrolysis experiments were carried out in a 1-in. diameter-by-8-ft-long downflow entrained tubular reactor, details of which have been reported.<sup>(4)</sup> The gas mixture consisted of 0-40% helium by volume and the balance methane. Preheated methane or helium-methane gas mixture was fed into the reactor to desired total pressure. The partial pressure of methane was maintained constant at 50 psi in the experiments reported here. A New Mexico sub-bituminous coal, with analysis shown in Table 1, was used in the study. The coal, 150 $\mu$ m or less in size, premixed with 10% by weight of Cab-O-Sil (a fumed silica powder) to prevent agglomeration, was dried in a vacuum oven overnight. The high temperature gas feed is mixed with coal at the top of the reactor causing the pyrolysis reactions to take place. Routine gas analyses were performed with an on-line gas chromatograph. The product yields were determined on the basis of conversion of carbon contained in the coal feed.

Table 1  
Analysis of New Mexico Sub-bituminous coal (wt%)

Moisture (As Received)	7.8		
<u>Proximate Analysis:</u>		<u>Ultimate Analysis:</u>	(daf)
Dry Ash	22.8	Carbon	- 72.4
Dry V.M.	34.9	Hydrogen	- 5.6
Dry V.M.	34.9	Nitrogen	- 1.4
Dry P.C.	42.4	Oxygen (by diff)	- 20.6

## RESULTS AND DISCUSSION

Ethylene is an important raw material for the polymer market. Less attention has been focused in the past on the production of ethylene using coal as the raw material. We have shown earlier that there are definite advantages in the use of methane as an atmosphere in the flash pyrolysis of coal. At temperatures higher than 800°C, 2-5 times greater yields of ethylene are obtainable in methane atmosphere when compared to flash pyrolysis in an inert helium atmosphere.<sup>(5)</sup> The enhancement in the ethylene yield was determined to be due to an interaction between coal and methane at the pyrolysis conditions.<sup>(6)</sup> Though greater selectivity towards ethylene and BTX production can be achieved by pyrolysis of coal in a methane atmosphere, its relatively low thermal conductivity can limit the total volatiles yield obtainable from coal. Hydrogen is highly reactive and it also has the highest thermal conductivity of all gases; however, it is unsuitable if the aim is to maximize ethylene and BTX yields as they become hydrocracked in the presence of hydrogen. This, then, leads to the possibility of pyrolyzing coal in a mixture of helium with high thermal conductivity and methane with high reactivity.

One of the important process parameters that influenced the ethylene and BTX yields was found to be the methane-to-coal feed ratio. When the gas flow rate was held constant, the yields of C<sub>2</sub>H<sub>4</sub> and BTX tend to increase with lower mass loadings of coal. The results of flash pyrolysis of New Mexico sub-bituminous coal in pure methane at 1000°C and a constant methane flow rate of 3.8 lb/hr are shown in Figure 1. The curves for both C<sub>2</sub>H<sub>4</sub> and BTX follow the same pattern. The top curves show the total yield of C<sub>2</sub>H<sub>4</sub>, C<sub>2</sub>H<sub>6</sub> and BTX. At the lowest coal flow rate, the ethane yield was 1.0% and no ethane was produced at higher coal flow rates. The decrease in the yields of BTX, C<sub>2</sub>H<sub>4</sub> and C<sub>2</sub>H<sub>6</sub> at higher coal flow rates can be explained on the basis of accelerated decomposition of the above products on the surface of the hot char particles, the area of which also increases with higher mass loadings of coal. Furthermore, higher mass loadings of coal can also affect the heat transfer between the pyrolyzing gas and the coal particles which, in turn, can reduce the yield of the volatiles from coal. Thus, it becomes necessary to optimize the flow rates of coal and methane in order to maximize the desired product yields.

Table 2 shows the yields of the products obtained when the coal was pyrolyzed in gas mixtures of helium and methane. Three different compositions of gas mixtures were used which contained 6 to 40% He in methane. As shown in Table 2, the partial pressure of methane was constant at 50 psi in all experiments. The coal flow rate ranged from 0.8 to 1.3 lb/hr and the methane flow rate from 2.1 to 4.6 lb/hr. The flow rates shown here were obtained by averaging the flow rates throughout the run which lasted for about an hour. Though instantaneous flow rate of coal is not known, it is not expected to vary because successive gas analyses using on-line GC were consistent for a steady state reaction conditions. The instantaneous flow rate of the pyrolyzing gas which was recorded throughout the run, did not reveal any significant differences.

Table 2  
Flash Pyrolysis of New Mexico Sub-bituminous Coal at 1000°C  
in Helium-Methane Gas Mixtures  
(Partial Pressure of Methane: 50 psi)

Run No.	684	871	868	779	795	766	848	812	849	854	817	837	860	844	841	827
Helium (Vol. %)	0	6	6	6	6	6	12	12	12	12	25	25	25	25	40	40
Methane (Vol. %)	100	94	94	94	94	94	88	88	88	88	75	75	75	75	60	60
Total Pressure, psi	50	53	53	53	53	53	57	57	57	57	67	67	67	67	83	83
Coal Feed Rate (lb/hr)	1.00	1.22	1.22	0.75	0.81	0.87	1.00	1.18	1.22	1.28	0.97	0.93	0.95	1.01	1.09	1.24
Methane Feed Rate (lb/hr)	4.05	4.13	2.85	4.55	4.92	4.33	3.18	4.60	3.25	1.96	3.98	3.44	2.1	2.69	3.19	3.31
Coal Res. Time (sec)	1.5	1.4	1.9	1.3	1.2	1.3	1.7	1.2	1.7	2.2	1.2	1.3	2.3	1.9	1.6	1.2
Methane/Coal Ratio	4.1	3.4	2.3	6.1	6.1	5.0	3.2	3.9	2.7	1.5	4.1	3.7	2.2	2.7	2.9	2.7
Product Yields, (wt% Coal Carbon Basis)																
C <sub>2</sub> H <sub>4</sub>	7.7	7.9	4.7	14.1	10.5	6.7	7.6	8.6	6.1	3.3	14.8	10.7	6.1	6.1	7.3	9.3
C <sub>2</sub> H <sub>6</sub>	0.1	1.5	0.7	1.9	2.2	1.7	1.3	1.6	1.0	0.8	3.0	1.8	1.4	1.4	1.2	1.0
BTX	9.0	10.7	8.8	18.2	14.4	N.D.	11.1	10.2	10.2	7.5	15.3	13.7	10.3	10.5	11.3	10.6
C0	8.0	9.6	6.4	5.3	6.6	5.6	6.3	5.8	5.6	6.8	7.6	7.4	6.2	6.6	6.7	4.6
C0 <sub>2</sub>	1.7	1.6	1.0	1.8	1.9	1.5	1.5	1.8	1.3	1.6	2.3	1.5	1.5	1.4	1.4	1.3
Total																

N.D. - Not Determined.

Figure 2 shows the yields of ethylene and BTX as a function of volume percent helium in the pyrolyzing helium-methane gas mixture at methane-to-coal ratio of 3.9 to 4.1 and coal particle residence time of 1.2-1.5 sec. Both curves show that, under the conditions investigated, the yields of  $C_2H_4$  and BTX increase with the amount of helium in the gas mixture. It also appears that the yields of  $C_2H_4$  and BTX will be going through a maximum, since the yields with pure helium are much lower than with the mixtures of  $CH_4$  and He. The data in Table 2 indicate that the effect of the helium concentration in the gas mixture on  $C_2H_4$  and BTX yields is more pronounced at high methane-to-coal ratios than at low methane-to-coal ratios.

Figure 3 shows the effect of the methane flow rate on the yield of ethylene at a constant coal flow rate of 1.0-1.2 lb/hr. The curves for the three different gas mixtures used in our experiments, which contained 6, 12 and 25% helium by volume, all follow similar trends. For all gas mixtures,  $C_2H_4$  yield increased with the flow rate of methane. It is seen from Figure 3 that for a given methane flow rate, the yield of  $C_2H_4$  increased with the helium content of the gas mixture. If the increased ethylene yield came from the pyrolysis of methane alone, i.e., if the ethylene yields were additive, an effect opposite to this would have been noticed. A similar trend is noted in Table 3 with respect to BTX yield. Thus, there is greater selectivity in the production of ethylene and BTX in the presence of He/ $CH_4$  than in the presence of either pure He or pure  $CH_4$ . This indicates an attractive process application for the production of ethylene and BTX from coal via Flash Methanolysis.

#### ACKNOWLEDGEMENT

We gratefully acknowledge the support provided by the Advanced Research and Technology Development Program of the U.S. Department of Energy, Morgantown Energy Technology Center, Morgantown, W. Virginia.

#### REFERENCES

1. Steinberg, M., Fallon, P. T., and Sundaram, M. S., "Flash Pyrolysis of Coal with Reactive and Non-Reactive Gases." Report to DOE, No. DOE/CH/00016-1402 (DE 833011264). Available from NTIS, Springfield, Va., 22161.
2. Sundaram, M. S., Steinberg, M., and Fallon, P. T., "Flash Pyrolysis of Coal in Non-Reactive Gases." BNL 35947, ACS Div. Fuel Chem., Prepr. 30(1), 231 (1985).

REFERENCES (cont.)

3. Falk, A. Y. and Schuman, M. D., "Advancement of Flash Hydrogasification." Proc. 5th Ann. Gasification Projects Contractors' Meeting, p. 338, June 1985.
4. Sundaram, M. S., Steinberg, M., and Fallon, P. T., "Flash Hydropyrolysis of Coal for Conversion to Liquid and Gaseous Fuels: Summary Report," DOE/METC/82-48 (1982).
5. Sundaram, M. S., Steinberg, M., and Fallon, P. T., "Enhanced Ethylene Production Via Flash Methanolysis of Coal," ACS Div. Fuel Chem., Prepr. 29(2), 124 (1984).
6. Sundaram, M. S. and Steinberg, M., "Flash Methanolysis of Coal: A Mechanistic Study." Submitted to Fuel, BNL 37302 (July 1985).

Figure 1

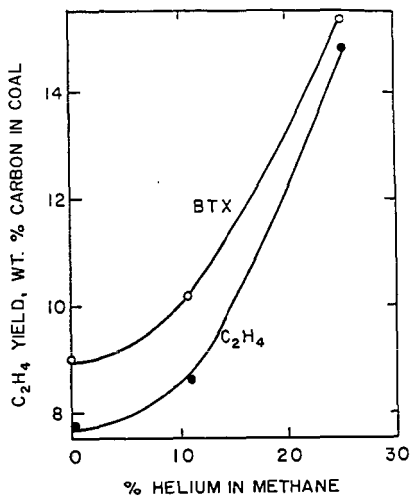
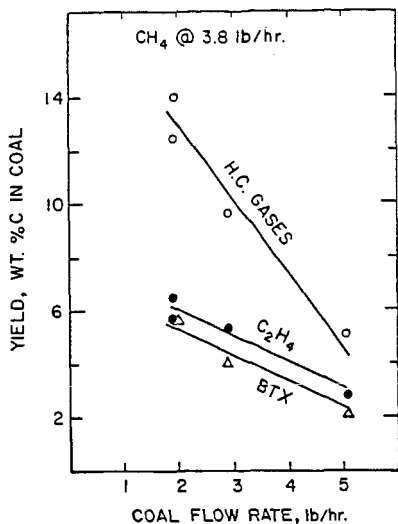


Figure 2

Figure 1. Effect of Coal Flow Rate on C<sub>2</sub>H<sub>4</sub> and BTX yield

Figure 2. Effect of Helium Concentration in Methane on C<sub>2</sub>H<sub>4</sub> yield

Figure 3. Effect of Gas Composition and Methane Flow Rate on C<sub>2</sub>H<sub>4</sub> yield

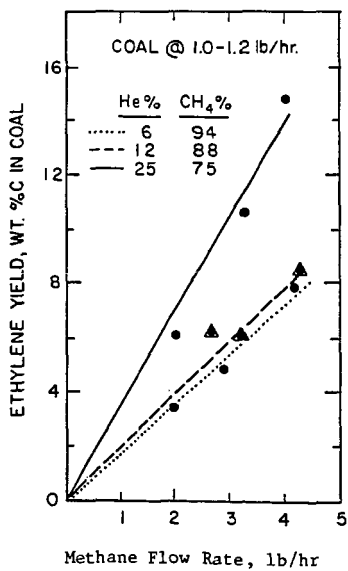


Figure 3

PREDICTING DEVOLATILIZATION AT TYPICAL COAL COMBUSTION  
CONDITIONS WITH THE DISTRIBUTED-ENERGY CHAIN MODEL

By

Stephen Niksa  
Mechanical Engineering Department  
Stanford University  
Stanford, CA 94305

and

Alan R. Kerstein and Thomas H. Fletcher  
Combustion Research Facility  
Sandia National Laboratories  
Livermore, CA 94550

INTRODUCTION

Hypothetical ultimate yields for rapid coal devolatilization arose from the historical notions that a well-defined amount of volatile precursors are present in coal, and that their rate of release is directly proportional to a decaying reactant concentration. However, as reviewed elsewhere(1,2), wet chemical and spectroscopic analyses of coal structure from the past decade suggest a far less direct relationship between the reactive species in coal and the pyrolysis products. According to the aromatic/hydroaromatic model, bituminous coals are composed of aromatic "nuclei" interconnected by various bridges and substituted with smaller functional groups on their periphery. Although there is no well-defined repeating unit, bituminous coal is an extensively crosslinked macromolecular network which swells on solvation and exhibits viscoelasticity(3).

The aromatic/hydroaromatic model suggests three broad classes of chemical reactions: dissociation of bridges, recombination of nuclei, and elimination of peripheral groups. When peripheral groups present initially are converted to light gas, there is a direct correspondence between their initial concentrations and ultimate gas yields. But in contrast, when a bridge breaks, tars do not form at a rate governed by stoichiometric proportions, and furthermore, there is no predetermined concentration of tar precursors, per se, present initially in the coal. In depolymerizations, stoichiometric proportionalities are replaced by probabilities assigned from molecular conformation; i.e., the spatial arrangement of the atoms in a molecule(4). The probabilities relate the fragment size distribution to the concentration of unbroken bridges in the network, independent of the chemical reaction rates. During devolatilization, nuclei disconnect and recombine concurrently, and many fragments never become small enough to vaporize. Tar and char yields are determined by competitive kinetics which depend on complex conformational probabilities as well as chemical reaction rates. Each nucleus can become either tar or char, depending on the transient conditions for the competition. The fate of nuclei is not predetermined, as implied in formulations which include hypothetical ultimate yields for tar and char. Moreover, the disintegrating macromolecular skeleton of coal and the reintegration of intermediates into char are not taken into account in the historical notions mentioned above, nor in any of the available devolatilization rate models.

We formulated the Distributed-Energy Chain Model (DISCHAIN) to account for the conformational aspects of coal depolymerization and char formation in a phenomenological way. The derivation of the model and the qualitative mechanisms for product formation have been described(5). Rate parameters have been specified by correlating transient weight loss from a bituminous coal over a broad range of thermal histories for heating rates to  $10^3$  K/s and temperatures to 1300K(6). In the present study, predictions from DISCHAIN are compared with volatiles yields from very similar bituminous coals for heating rates between  $10^3$  and  $10^5$  K/s and temperatures between

800 and 2100K. No further adjustments of any of the parameters in the model have been made. Nevertheless, predicted yields and reaction times differ significantly among the comparisons, reflecting the influence of the different transient histories in the cases considered.

#### PRODUCT FORMATION FOR VARIOUS HEATING RATES

Chain statistics introduce several novel qualitative features into the formation mechanism for devolatilization products. In DISCHAIN, the monomer formation rate is not directly proportional to either the bridge dissociation or the char formation rate. Limiting cases establish that (1) the conversion of bound aromatic units into monomers accelerates with progressive bridge dissociations, regardless of the chemical reaction rate for bridge dissociation, and (2) the number of char links needed to eliminate all monomers is less than the original number of monomers. Most important, the formation of stable char links is concurrent with the disintegration of bridges during slow heating. This inhibits the subsequent formation of monomers, thereby accounting for reduced yields for lower heating rates.

The mechanistic basis for yield enhancement at faster heating rates in DISCHAIN is not solely the disparity of the activation energies for tar and char formation. Rather, the heating rate dependence is the joint result of the competition between the processes of char and tar formation in conjunction with suppression of monomer generation due to char formation. The activation energy disparity determines the selectivity to tar and char from the common intermediate; i.e., monomer. Independently, chain statistics determine the conversion of the bound aromatic units into the intermediate. Obviously, bound aromatic units which never become monomers are excluded from the competition between char and tar formation.

To further illustrate the role of monomer selectivity, predicted tar yields at four heating rates are shown in Figure 1. In these simulations, the thermal histories are linear temperature ramps at the indicated heating rates to 1900K. The onset of devolatilization moves to higher temperatures for greater heating rates, due to kinetic restraints(7). The devolatilization rate increases in rough proportion to increases in the heating rate. Reaction time constants range from 3 s at  $10^2$ K/s to 5 ms at  $10^5$ K/s. Each transient yield reaches an asymptote while the temperature ramp is being traversed, even at  $10^5$ K/s.

Faster heating tends to preclude char formation, which increases the monomer selectivity, and higher temperatures shifts the selectivity to tar formation. Consequently, ultimate tar yields increase by 70 % over this range of heating rates. Since the mass of aromatic units distributed between char and tar is fixed, char yields are decreasing throughout this range of conditions. Gas yields, which are not shown, are fixed at 8%, although at  $10^5$ K/s, peripheral groups are transported away with tar before they can be eliminated as gases. Product distributions consisting of tars but no light gases have actually been observed during laser pyrolysis at very high heating rates(8).

#### COMPARISONS WITH TRANSIENT CONVERSION MEASUREMENTS

Predictions from DISCHAIN are compared with three sets of data for single-particle, transient devolatilization of high volatile bituminous coals for a broad range of thermal histories. In Bautista's wire grid study of vacuum pyrolysis, thermal histories consist of uniform heating at  $10^3$ K/s to temperatures between 750 and 1200K, followed by sufficiently-long reaction times to observe ultimate yields at each temperature(9). In Kobayashi's entrained-flow study of pyrolysis at atmospheric pressure, the operating conditions encompass heating rates between  $10^4$  and  $10^5$ K/s and temperatures between 1000 and 2100K(1). Time-temperature histories are based on calculations which account for mixing between the dilute coal jet and the preheated coaxial gas stream. In Midkiff et al.'s study of an excessively fuel-rich stabilized coal flame, the nominal heating rate is  $10^5$ K/s and the ultimate temperature is 2000K(11).

The different pressures in these studies may seem objectionable in light of significant reductions in yield for pressures between vacuum and a few atmospheres. Many models invoke competing mass transport and redeposition of tar from the gas phase within and around the particles to rationalize this effect, but this basis is inconsistent with measured tar deposition rates and time scales for volatiles escape. Only a summary explanation is given here, as additional detail is given elsewhere(6).

Vaporization mechanisms determine which heavy compounds leave the condensed phase, depending on the molecular weight, temperature, and pressure. DISCHAIN presumes instantaneous vaporization and escape of all tars formed when monomers dissociate, which is a limiting form for low pressures if volatiles escape by viscous flow. Therefore, the model applies to vacuum pyrolysis regardless of temperature, and to pyrolysis at atmospheric pressure, provided that temperatures are high enough to compensate for the influence of pressure on tar vaporization. Regarding the assumed instantaneous vaporization of tar, the equilibrium vapor pressure of heavy compounds increases rapidly with increasing temperature, so that this assumption is well satisfied throughout the combustion temperatures in both of the selected studies at 1 atm. Based on an equilibrium vapor pressure law for coal liquids(12), the ratio of the vapor pressure and the internal pressure are identical at 1000K and an internal pressure of 1 atm, and at 1250K and an internal pressure of 10 atm.

Predicted product distributions for gas, tar, char, and unreacted coal are compared with measured yields of gas and total weight loss for vacuum pyrolysis in Figure 2. The simulations are based on uniform heating at  $10^3$ K/s to the stated reaction temperature, followed by an isothermal reaction period between 6 and 30 s, depending on reaction temperature. In all cases, ultimate yields were reached before the end of the experimental reaction time. Model predictions were converted to the daf-basis with a reported ash content of 9.2 %.

The relative yields of tar and gas are reliably predicted only beyond 900K, while predicted and measured weight loss differ by several percent at temperatures below 1000K. The predicted temperature dependence is more consistent for tar yields than for gas yields. Predicted yields for unreacted coal and char seem reasonable, but cannot be assessed quantitatively. Unreacted coal persists through 1000K as a result of the broad range of dissociation energies for bridges. The amount of char increases monotonically throughout this temperature range, but exhibits a maximum for higher temperatures and heating rates.

In succeeding comparisons, only weight loss is shown because gas phase chemistry alters the product distribution at high temperatures. The product distributions from DISCHAIN constitute flux conditions for detailed modeling of the rate phenomena in the vicinity of the particles, rather than conditions in the free stream.

The comparison for the atmospheric entrained flow study appears in Figure 3. The simulations are based on thermal histories calculated by Kobayashi which account for mixing effects near the injector(10). These thermal transients are significantly longer than for an individual particle injected into a quiescent gas at the reactor temperature, as expected. Also shown in Figure 3 are correlations from the competing two-step model(10). Kobayashi assigned rate parameters in order to fit these data; in contrast, rate parameters from DISCHAIN were not readjusted from the values assigned from data at much slower heating rates and lower temperatures.

Predicted weight loss is within the experimental error at both the extremes in temperature, but several percent too high at 1510K and 1260K (not shown). Predicted reaction time scales are as reliable as those from the correlation assigned from this data. Also, the predicted ultimate yield of 62 % at 2100K is substantially greater (15 % daf) than the greatest value in the data set used to assign the parameters in DISCHAIN (47 %  $10^3$ K/s and 1300K). Moreover, it is 22 % daf greater than the measured yield at  $10^2$ K/s and 1300K (12). Since the parameters have not been adjusted, these yield enhancements can be attributed to the influence of heating rate, as described in the previous section.

The final comparison involves a stabilized one-dimensional coal flame(11). Factors beyond devolatilization arise in coal flames, but most complications are absent under excessively fuel-rich conditions. The coal density was 470 mg/l, corresponding to fuel equivalences of 3.30 with respect to the whole coal and 1.34 with respect to the ASTM proximate volatile matter. All oxygen was consumed before one-third of the ultimate volatiles yield was observed, and heterogeneous oxidation was negligible.

Complete transient thermal histories, from the point of injection to the onset of devolatilization, have not yet been measured for any coal flame, including this one. Midkiff, et al. report transient weight loss, gas temperatures, and optically-determined particle temperatures on a time coordinate referenced to the first measurement point, rather than the point of injection. The first reported temperature, 1750K, exceeds the threshold for devolatilization at heating rates as fast as  $10^4$  K/s (DISCHAIN predicts that devolatilization begins at 1250K for a heating rate of  $2 \times 10^5$  K/s; c.f. comparison with Kobayashi's data at 1940K in Figure 3). Therefore, a simulated thermal history, instead of the measured particle temperatures, has been used to obtain the predictions discussed below.

Predicted weight loss is compared to the sum of the measured losses of volatile matter and fixed carbon in Figure 4. The thermal history in the simulations consists of uniform heatup at  $10^5$  K/s to 2000K, the ultimate temperature observed in the experiment. The time coordinate for the predictions and measurements is referenced to the onset of devolatilization. The reaction time scale is adequately described, but the predicted ultimate yield exceeds the measurements by 5 %. However, soot was observed but not separated from the collected char samples, so the measured yields are less than the true values. An upper bound for this influence far exceeds the discrepancy in this comparison, as Nenninger et al. observed soot yields of 22 % from the high temperature pyrolysis of a high volatile bituminous coal(13).

#### CONCLUSIONS

The accuracy of the predicted reaction time scales and yields from DISCHAIN is significant because hypothetical ultimate yields are absent, model parameters were not adjusted, and a wide range of thermal histories was spanned in the comparisons with data. Experimental errors necessarily increase as coal combustor conditions are approached. Nevertheless, this evaluation is more stringent than previous comparisons between devolatilization models and measurements, and provides the basis for the following conclusions:

1. Bridge dissociation concurrent with char formation diminishes the conversion of bound aromatic nuclei in coal into unattached tar precursors, which constitutes a mechanistic basis for enhanced yields for faster heating rates.
2. Predicted yields based on the same parameters ranged from 40 % at  $10^2$  K/s and 1300K to 62 % at  $10^5$  K/s and 2100K, in agreement with measured yields at the respective conditions within the experimental error.
3. Predicted reaction times and yields from DISCHAIN agree quantitatively with transient measurements from high volatile bituminous coals for heating rates between  $10^3$  and  $10^5$  K/s and reaction temperatures between 800 and 2100K.

#### REFERENCES

- 1 Gavalas, G.R., "Coal Pyrolysis," Elsevier, New York (1982).
- 2 Davidson, R.M., "Molecular Structure of Coal," IEA (Rep. No. ICTIS/TR 08), London, 1980.
- 3 Larsen, J.W., in "Coal Science," R.A. Meyers, Ed., Academic Press, NY (1982).

- 4 Tanford, C., "Physical Chemistry of Macromolecules," John Wiley and Sons, New York (1961).
- 5 Niksa, S. and Kerstein, A.R., Combust. Flame, to appear (1986).
- 6 Niksa, S., Combust. Flame, to appear (1986).
- 7 Niksa, S., Heyd, L.E., Russel, W.G., and Saville, D.A., Twentieth Symp. (Int.) on Comb., The Combustion Institute, Pittsburgh (1984), p. 1445.
- 8 Ballantyne, A., et al., Final Report prepared for the U. S. Dept. of Energy, Pittsburgh Energy Technology Center, Contract No. DE- AC22-84PC30291, October, 1983.
- 9 Bautista, J.R., "Time-Resolved Product Distributions of Softening Coals," Ph.D. Thesis, Department of Chemical Engineering, Princeton University, Princeton, NJ (1984).
- 10 Kobayashi, H., "Devolatilization of Pulverized Coal at High Temperatures," Ph.D. thesis, Department of Chemical Engineering, MIT, Cambridge, MA (1976).
- 11 Mickiff, K.C., Altenkirch, R.A., and Peck, R.E., Paper No. 1- 2A, CSS/WSS Joint Technical Mtg., Combustion Institute, San Antonio, TX (1985).
- 12 Unger, P.E. and Suuberg, E.M., Fuel 63:606 (1984).
- 13 Nenninger, R. D., Howard, J. B., and Sarofim, A. F., Proc. Int'l. Conf. on Coal Science, p. 521, IEA, Pittsburgh, PA (1983).

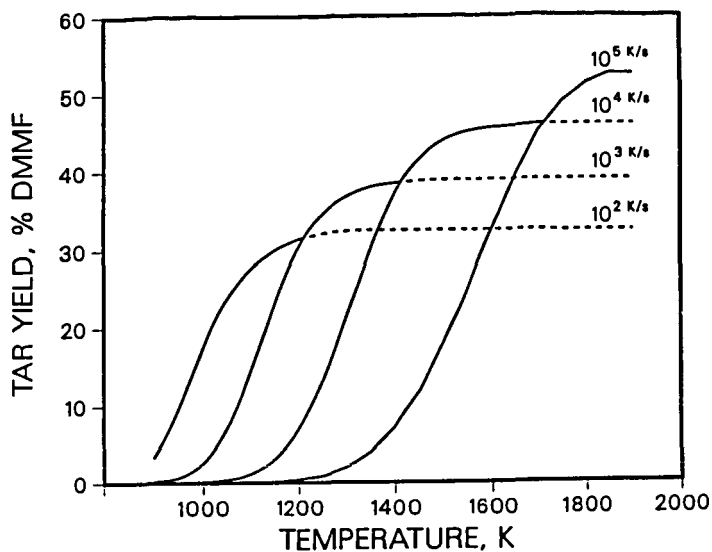


Figure 1. Predicted transient yields for tar during heatup at  $10^2$ ,  $10^3$ ,  $10^4$ , and  $10^5$  K/s along a linear temperature ramp to 1900K.

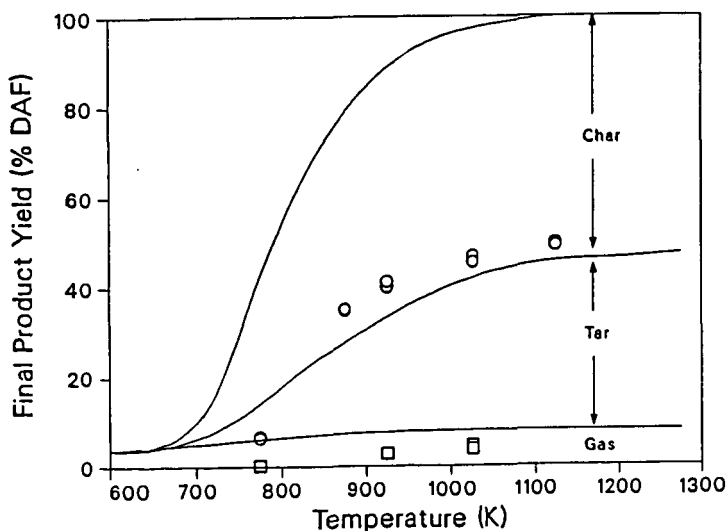


Figure 2. Comparisons between predicted and measured weight loss (O) and gas yields (□) from vacuum pyrolysis of Pittsburgh seam bituminous coal, from Bautista<sup>16</sup>.

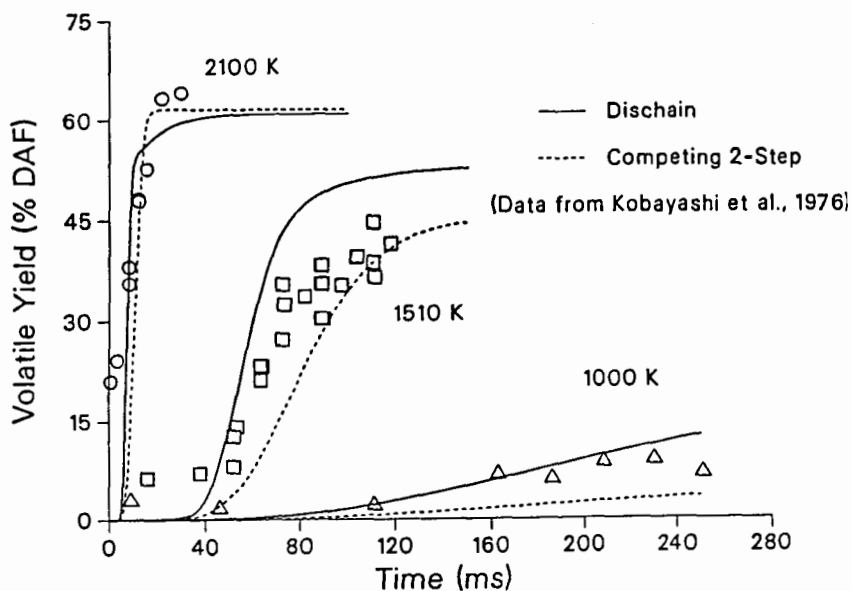


Figure 3. Weight loss observed in an atmospheric entrained flow reactor by Kobayashi<sup>17</sup> compared to predictions from DISCHAIN (solid curves) and from Kobayashi's<sup>6</sup> competing two-step model (dashed curves).

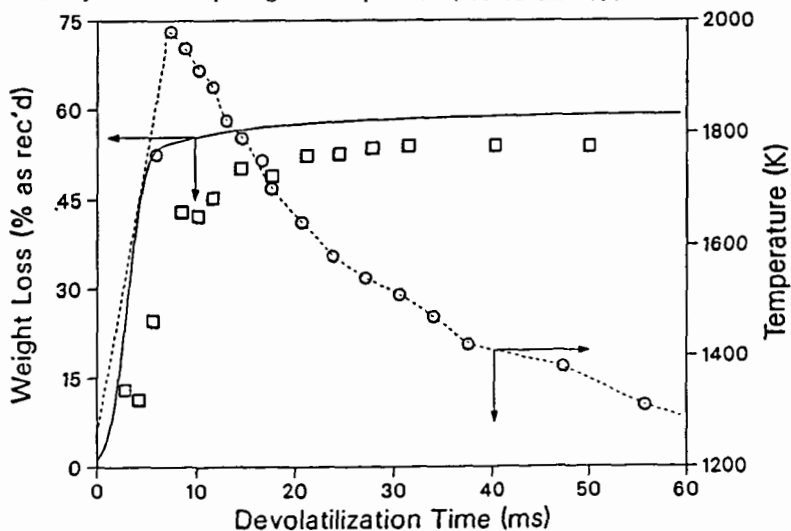


Figure 4. Predicted weight loss (solid line) for uniform heating at  $10^5$  K/s to 2000K compared to the sum of losses of volatile matter and fixed carbon (□) reported by Midkiff, et al.<sup>18</sup>. The simulated temperature profile (dashed line) includes optically-measured particle temperatures (○) during the cooling phase.

# ADVANCED COAL GASIFICATION AND DESULFURIZATION WITH CALCIUM BASED SORBENTS

J. Weldon, G. B. Haldipur, D. A. Lewandowski, K. J. Smith

KRW Energy Systems Inc.  
Madison, PA 15663

## 1.0 ABSTRACT

In-bed desulfurization using calcium based sorbents has been evaluated in the KRW pressurized fluidized bed gasifier as part of a joint program with KRW Energy Systems Inc. and the U. S. Department of Energy. For combined cycle power generation or synthesis gas applications such a system has large potential economic advantages over second generation gasifiers which use conventional cold gas cleanup.

In addition to achieving over 90% desulfurization, the process has also demonstrated significant gains in cold gas efficiency and fines consumption. Pilot plant performance data are presented for the KRW gasifier-desulfurizer process and the preliminary results of an in-bed waste characterization study are also presented. Though untreated in-bed wastes contain potentially hazardous calcium sulfide, laboratory-scale tests have shown that roasting processes can be adapted for converting the waste to a non-hazardous form.

## 2.0 INTRODUCTION

The production of low-Btu (120-160) Btu/scf gas from coal for use in combined cycle power generation is attractive to the utility industry because the feedstock is an abundant domestic natural resource and because it offers economic advantages over conventional coal fired steam plants.(1)

Conventional stack gas clean-up technologies are proving to be capital expensive and have the added disadvantage of poor thermal efficiency. In-bed clean-up with calcium sorbents offers an effective and economical method of removing the sulfur species from the product gas without pre-cooling. The particulate free hot gas can then be used directly in a gas turbine providing improved overall process efficiency.

The market incentive for an economical coal gasification combined cycle electric power generating plant will be substantial in the 1990's. According to the U. S. Department of Energy (1), 18% of the current U. S. generating capacity is greater than 25 years old. The KRW coal gasification combined cycle hot gas cleanup process is ideally suited to the needs of the electric power industry in the 1990's on the basis of environmental, cost and plant size considerations.

## 3.0 BACKGROUND

### 3.1 KRW Coal Gasifier

The KRW gasifier is a pressurized fluidized bed process which can convert a variety of solid carbonaceous feedstocks into low-Btu (100-160 Btu/scf) or medium-Btu (200-300 Btu/scf) gas. The essential features of the gasifier are shown in Figure 1. Run-of-mine coal or lignite in the size range of 1/4-inch x 0 is surface dried, pressurized in lockhoppers, and injected concentrically into a high energy oxidizing jet located in the combustion zone. The coal is rapidly devolatilized and caked, and the residual char is gasified by steam in the upper region of the fluidized bed. The jet induces a vigorous toroidal motion of solids between the lower heat producing combustion region and the upper heat consuming gasification region. The coal ash undergoes partial melting and sintering in the hotter combustion jet, and the resulting 'glue' action causes fine ash particles to agglomerate. These ash agglomerates are separated from the char in a fluidized bed

separator located in the bottom section of the gasifier, are cooled with recycle gas, and are extracted by means of a rotary feeder and depressurizing lockhoppers. Fines elutriated from the gasifier are captured in an external cyclone and recycled directly to the gasifier by means of a nonmechanical valve. Fines escaping the cyclone are captured in a full-flow sintered metal filter. This filter is capable of operation up to 1200°F and removing all fines one micron or greater in size. The gasifier may be operated either in the air-blown mode for low-Btu gas (100-160 Btu/scf) or in the oxygen-blown mode for medium-Btu fuel or synthesis gas (200-300 Btu/scf).

The process has been demonstrated for a wide range of feedstocks and conditions at the Waltz Hill 15-30 tons/day Process Development Unit (PDU) under funding by the DOE and its predecessor agencies. In addition to its ability to process a variety of feedstocks, the process has also demonstrated effective utilization of coal fines, high overall carbon conversion efficiency, and virtual elimination of tar and oil in the product gas.

### 3.2 In-Bed Desulfurization

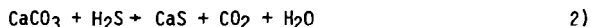
In-bed desulfurization has been identified as a potential hot gas cleanup concept for meeting environmental regulations on sulfur emissions from the KRW gasifier. Such a system would have economic advantages over cold gas clean-up in a coal gasification combined cycle power generation application. KRW has conducted four in-bed PDU tests in 1984 and 1985 to demonstrate the feasibility of this concept. In addition to achieving over 90% desulfurization to meet the New Source Performance Standards for sulfur emissions, the process cold gas efficiency improved by 20% over conventional PDU gasifier operation.

Hot gas clean-up via the in-bed concept involves the removal of sulfur bearing gases, H<sub>2</sub>S and COS, by reacting them with dolomite (CaCO<sub>3</sub>.MgCO<sub>3</sub>) or limestone (CaCO<sub>3</sub>) to form sulfided or spent sorbent (CaSMgO or CaS). Sorbent is fed into the gasifier freeboard to mix with the the bed char and remove H<sub>2</sub>S and COS from the product gas. The spent sorbent is eventually withdrawn through the gasifier annulus along with ash agglomerates.

The overall reaction occurring in the gasifier bed is:



for the dolomite/hydrogen sulfide reaction, or similarly:



for the limestone/hydrogen sulfide reaction. Calcium sulfide (CaS) is a reactive waste which can recombine with acidic water to release toxic H<sub>2</sub>S gas. Further treatment is necessary to convert the CaS to the environmentally acceptable sulfate:



The primary goal of oxidation is to reduce the activity of the sulfide with the environment and render the waste non-hazardous. The waste could then be disposed of in conventional solid waste landfills.

#### 4.0 DESULFURIZATION PERFORMANCE

The development program has comprised a series of PDU tests to first demonstrate gasifier operability and, thereafter, to optimize the desulfurization process. During tests TP-036-1 and TP-036-2, the gasifier was successfully operated with dolomite injection in a controlled and balanced manner. The subsequent tests, TP-036-3 and TP-036-4, demonstrated that high levels of desulfurization could be achieved with both dolomite and limestone sorbents. Table 1 summarizes the significant achievements of the in-bed desulfurization program.

TABLE 1. SUMMARY OF KRW IN-BED DESULFURIZATION RESULTS\*

Coal Type	Coal Sulfur Content (%)	Sorbent Type	H <sub>2</sub> S (ppm)	COS (ppm)	Ca/S Molar Feed Ratio	Steady State Desulfurization Achieved (%)
Pgh. #8	2.3	Glass Dolomite	550	263	1.67	86
Pgh. #8	4.5	Glass Dolomite	679	216	1.55	92
Pgh. #8	4.5	Greer Limestone	651	258	1.84	90
Wyoming	2.0	Glass Dolomite	484	167	2.0	91

\*preliminary

The equivalent desulfurization for limestone injection into conventional furnaces and atmospheric fluidized bed combustors (AFBC) require Ca/S molar feed ratios of 3 to 6 (2, 3) compared to the ratios of 1.5 to 2.0 demonstrated by the KRW process. The advantages of desulfurization in the reducing gasifier environment are attributed to the faster rate of hydrogen sulfide/calcium oxide reaction compared to the sulfur dioxide/calcium reaction and the absence of sintering. Sintering is indicated by low BET surface areas (4). Sorbent surface area measurements of the bed material were relatively high at 10-40 m<sup>2</sup>/g compared to typical calcine surface areas which range from 0.5 to 40. m<sup>2</sup>/g for calcined carbonates (5). The reducing environment apparently does not increase sintering.

PDU results indicate desulfurization is a function of the sulfur input rate and output rate. The sulfur species concentrations in the product gas were characteristically in the range of 500-650 ppm for H<sub>2</sub>S and 160-270 ppm for COS for large variations in feedstock sulfur content. Since the sulfur output rate is limited, the degree of desulfurization increases as the sulfur input rate (coal sulfur content) increases.

Desulfurization varies inversely with product gas steam concentration based on recent PDU tests. A negative correlation coefficient of 0.8 was found linking steam and hydrogen sulfide concentrations for the KRW Data Base. Equilibrium effects via the reaction



4)

are probably negligible because the value of the equilibrium constant is so large for gasifier temperatures in the range of 1600 to 1900°F (6). In fact, H<sub>2</sub>S concentrations were generally on the order of 200-400 ppm higher than equilibrium levels, so it seems improbable that equilibrium limits desulfurization. (If, however, gas phase diffusion of H<sub>2</sub>O from the reacting core is the limiting rate the equilibrium concentrations of H<sub>2</sub>S in the particle core may limit desulfurization). KRW investigations of the mechanism by which H<sub>2</sub>O limits desulfurization are currently underway.

Small incremental increases in desulfurization were also achieved with large increases in the calcium/sulfur feed ratio as shown in Table 2.

Table 2  
Incremental Increase in Desulfurization as a  
Function of Ca/S Ratio for Pgh. 4.5% Sulfur Coal

<u>Ca/S Feed Ratio</u>	<u>Observed % Desulfurization</u>	<u>Observed H<sub>2</sub>S ppm</u>	<u>Equilibrium H<sub>2</sub>S ppm</u>
1.84	91	651	180
3.41	94	424	242

These results differ significantly from fluidized bed combustor experience where desulfurization is directly proportional to and highly dependent on the Ca/S feed ratio.

## 5.0 WASTE CHARACTERIZATION

Because of the complexity of environmental regulations, an investigation of waste characterization testing and disposal laws' was conducted. Section 3001 of the RCRA directs the EPA to promulgate criteria for identifying and listing hazardous waste. In a large number of cases, it is possible to determine a wastes classification by its specific exclusion or identification as a hazardous waste. For other wastes, the EPA has prescribed tests to determine whether it possesses one of four hazardous characteristics - corrosivity, ignitability, reactivity, and extraction procedure (EP) toxicity. Since coal gasification wastes are not on any of the promulgated hazardous wastes lists by specific and nonspecific sources, it is the responsibility of the generator to determine if the released waste possesses any of the four hazardous characteristics.

Reactivity and EP toxicity are the most critical characteristic for in-bed waste disposal. Presently, the EPA has not yet promulgated a test procedure or a quantitative threshold for toxic gas generation reactivity. During the interim they have recommended a draft test method and interim reactivity thresholds

(7, 8). The quantitative threshold for the total available sulfide measured via the draft test method is 500 mg evolved H<sub>2</sub>S/Kg waste when subjected to an acid leach (ph = 2.0) for 30 minutes. Wastes releasing more than that level may be regulated as hazardous.

Unsulphated in-bed solid waste samples from the fines loss, separator pit sludge and gasifier discharge were analyzed for reactive sulfide levels and EP toxicity. Table 3 contains typical EP toxicity test results.

TABLE 3. TYPICAL RCRA EP TOXICITY TEST RESULTS OF KRW IN-BED DESULFURIZATION SOLIDS WASTES (mg/L)

Metal	Ag	As	Ba	Cd	Cr	Hg	Pb	Se
Maximum Allowable Concentration	5	5	100	1.0	5.0	0.2	5.0	1.0
Gasifier Discharge	0.03	0.048	<0.1	<0.005	0.03	<0.03	<0.002	<0.004
Fines Loss	0.01	0.068	0.4	<0.005	<0.01	<0.03	0.012	0.009
Separator Pit Sludge	0.01	0.002	0.6	<0.005	<0.01	<0.03	<0.002	<0.004

The level of EP toxic metals in samples taken during TP-036-3 and TP-036-4 were all significantly below the RCRA toxic levels.

Typical reactive sulfide levels for the in-bed process are shown in Table 4.

TABLE 4. REACTIVE SULFIDE TEST RESULTS FOR KRW IN-BED DESULFURIZATION SOLID WASTES FROM TP-036-3

Sample	Sulfide Wt %	Reactive Sulfide (mg/kg)
Untreated Gasifier Discharge	8.6	>1200
Fine Loss	1.3	<5
Separator Pit Sludge	0.9	<5

The fines loss samples from the process had extremely low reactive sulfide levels of less than 5 ppm. Separator pit sludge, which consists of wet fines carryover from the quench/cooling system, also had less than 5 ppm reactive sulfide. However, all untreated PDU withdrawal wastes generated during TP-036-3 sorbent injection may be potentially hazardous when subjected to the interim EPA reactivity test.

As part of an extensive study of the characteristics of in-bed wastes, the gasifier discharge material was sulfated in laboratory scale reactors under a variety of experimental conditions. Table 5 summarizes the reactor conditions, reactive sulfide levels, and sulfur analysis of several samples.

TABLE 5. EXPERIMENTAL CONDITIONS, SULFUR ANALYSIS AND REACTIVE SULFIDE LEVELS OF SULFATED GASIFIER DISCHARGE

Reactor Type	Furnace Temp. (°F)	Oxygen Concn. (Vol %)	Gas Flow Rate (liters/min)	Contact Time (hrs)	Reactive Sulfide (mg/kg)	Total Sulfur (Wt%)	Percent Sulfation (mole %)
Packed Bed	1500°F	21	5	1	5	5.00	80.7
Fluidized Bed	1500°F	5	>10	1	<5	NM	NM
Open Dish	1500°F	21	0	1	<5	7.48	63.4
Open Dish	1500°F	21	0	3	<5	8.02	74.0

NM - Not Measured

The configuration and experimental conditions tested were adequate for reducing the reactive sulfide levels of the withdrawal sample to less than 500 mg/kg. These results are encouraging for the in-bed program because sulfation is the simplest and most direct method of treating in-bed wastes. Further studies of reaction kinetics are necessary to determine the optimal conditions for sulfation of the in-bed wastes to meet RCRA requirements. Tests are underway at the PDU to evaluate the technical feasibility of a continuous waste treatment process.

## 6.0 GASIFIER PERFORMANCE

Gasifier performance was observed to improve during in-bed testing. The results of those set points in which gasifier performance was significantly enhanced due to sorbent injection are shown for tests TP-036-3 and TP-036-4 in Table 6.

TABLE 6. PILOT PLANT PERFORMANCE WITH IN-BED DESULFURIZATION

Coal	Sorbent	Air/Coal (lb/lb)	Gasifier Bed Temp. (°F)	Carbon Conversion Efficiency (%)	Cold Gas Efficiency (%)
Pittsburgh	--	4.28	1846	90	50
Pittsburgh	Dolomite	3.39	1950	90	73
Pittsburgh	Dolomite	3.37	1970	91	72
Pittsburgh	Limestone	3.27	1830	92	70
Wyoming	Dolomite	3.03	1820	91	65

Results from set points without sorbent injection are also shown for comparison. The benefits of sorbent injection are an increase in the cold gas efficiency and a decrease in the apparent fines elutriation rate.

Cold gas efficiencies increased dramatically during in-bed desulfurization from 50 to 70%. The increase in cold gas efficiency and corresponding drop in air/coal ratio may indicate improved gasification.

The catalytic effect of calcium on gasification rates has been documented by Walker (9), Freund (10), and Van Heek and Muhlen (11). Freund (9) found calcium catalyzed carbon reacted at a rate 100 times the rate of uncatalyzed carbon for the gasification of CO<sub>2</sub>. Catalytic effects are one of several potential contributing factors being investigated by KRW.

Fines loss rates and elutriation decreased dramatically with the bed weight of the gasifier/desulfurizer as shown in Figure 2. Increasing bed weight reflects the replacement of low density char (25 lb/ft<sup>3</sup>) by high density sorbent (80 lb/ft<sup>3</sup>) and the reduction of bed voidage. Reduced fines loss and elutriation rates are primarily the result of increased gasification rates and longer fines residence times. Improved gasification is attributed to the presence of the calcium based sorbents in the bed. Low bed voidage indicates low gas bypassing as bubbles. Fluidized bed filtering of fine material increases with decreased gas bypassing (12). The filter mechanism increases the fines residence time in the bed so that a larger portion is consumed before escaping the bed surface.

## 7.0 CONCLUSIONS

In-bed desulfurization integrated with hot particulate removal is potentially the most economical fossil energy process for converting all types of U.S. coals to electricity while complying with New Source Performance Standards (NSPS) for sulfur removal.

The in-bed program for direct injection of calcium-based sorbents into the KRW gasifier has demonstrated

- o desulfurization exceeding 90% for a 4.5% sulfur coal
- o cold gas efficiencies over 70%
- o feasible waste treatment by sulfation

Future development work at KRW includes pilot-scale sulfation of the gasifier discharge and demonstration of through put improvements. Laboratory scale investigations of desulfurization and the effect of calcium-based sorbents on char gasification will be conducted in parallel with the pilot plant testing to determine the controlling mechanisms for the relevant reactions.

KRW is also developing an external bed desulfurization system using zinc ferrite sorbent which is capable of removing sulfur compounds in a hot (1100°F) coal gas stream to a level of 10ppm. Installation and testing of the external bed desulfurization system is currently underway at the KRW Process Development Unit.

#### REFERENCES

1. Pitrillo, (Director, U. S. DOE's Morgantown Energy Technology Center) "A view of the Future. Technical Choices of the Utility Industry -- Power and Fuel Mix Alternatives". Keystone Energy Future Project, February 4, 1986.
2. Green, O. P. "The Utility Perspective on Dry SO<sub>2</sub> Control Technologies". First Joint Symposium on Dry SO<sub>2</sub> and simultaneous SO<sub>2</sub>/NO<sub>x</sub> Control Technologies. November 13-16, 1984, San Diego, CA.
3. Keairns, D. L., et. al. Chemically Active Fluid Bed for SO<sub>x</sub> Control: Vol I. Process Evaluation Studies. EPA-600/7-79-158a, December 1979.
4. Borgwardt, R. H. "EPA Experimental Studies of the Mechanisms of Sulfur Capture by Limestone". First Joint Symposium Dry SO<sub>2</sub> and Simultaneous SO<sub>2</sub>/NO<sub>x</sub> Control Technologies. November 13-16 1984, San Diego, CA.
5. Borgwardt, R. H. "Properties of Carbonate Rocks Related to SO<sub>2</sub> Reactivity". Environmental Science and Technology, Vol. 6, No. 4, April 1972.
6. Spencer, J. Sulfidation of Half-Calcined Dolomite in Hydrogen-Sulfide/Deuterium/Water/Nitrogen-2 -- Kinetics, Structure and Mechanisms. Carnegie-Mellon University. PH.D., 1985.
7. "Interim Methods for Toxic Gas Generation Reactivity". Office of Solid Waste and Emergency Response. U.S. EPA, Washington, D.C., July, 1985.
8. "Test Method to Determine Hydrogen Sulfide Released from Wastes". Office of Solid Waste and Emergency Response. U.S. EPA, Washington, D.C., July 1985.
9. Walker, P.L. et. al. "Catalysis of Gasification of Coal Derived Cokes and Chars". Fuel, Vol. 62, February, 1983. pg. 140.
10. Freund, H. "Gasification of Carbon by CO<sub>2</sub>: A Transient Kinetics Experiment". Fuel, Vol. 65, February 1986.
11. Van Heek, K. H. and H. J. Muhlen. "Coal Properties and Constitution". Fuel, Vol 64, October 1985, Pg. 1408.
12. Peters, M. H., Liang Shih Fan and T. L. Sweeney. "Simulation of Particulate Removal in Gas Solid Fluidized Beds." AIChE Journal, Vol. 28, No. 1, January 1982.

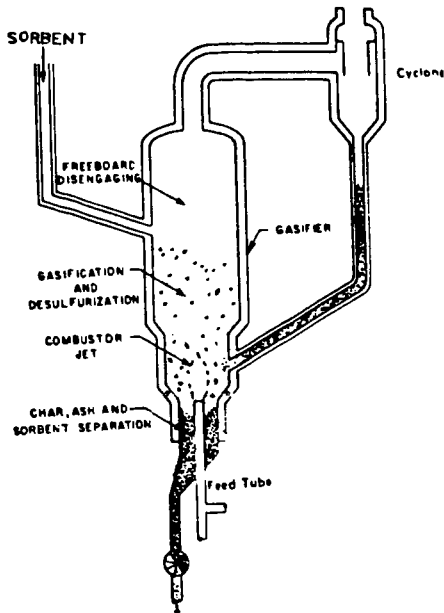


Figure 1. KRW Gasifier/Desulfurizer

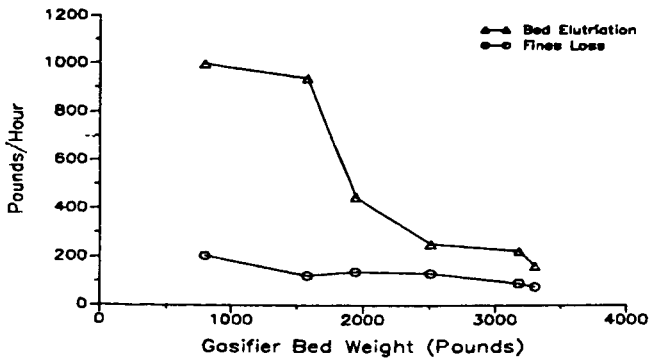


Figure 2. Variation of Fines Elutriation and Loss with Bed Weight in Gasifier/Desulfurizer

MOUNTAIN FUEL RESOURCES 30 TONS PER DAY ENTRAINED  
FLOW COAL GASIFICATION PROCESS DEVELOPMENT UNIT

Chiang-liu Chen and Ralph L. Coates

Questar Development Corporation  
141 East First South Street  
Salt Lake City, Utah 84147

INTRODUCTION

Pressurized gasification of coal in experimental entrained flow gasifiers was studied rather extensively during the period between 1953 and 1962 at the U.S. Bureau of Mines Morgantown Coal Research Center (1,2). A laboratory-scale gasifier with some similarity to the Bureau of Mines unit was operated by the Eyring Research Institute (MFI) between 1974 and 1978 (3,4). This work was followed by extensive process design studies carried out by Mountain Fuel Resources (5) which also led to the issuance of a U.S. patent (6). One of the important conclusions from this study was that feeding the dry coal to an entrained flow gasifier with recycle product gas was inherently more efficient than feeding the coal as a water slurry.

A 30 tons per day process development unit (PDU) was designed, constructed and operated between 1980 and 1984 to provide data for further scale-up of system components. Controlled continuous dry-feeding of pulverized coal into the gasifier at pressures between 100 and 260 psia (600 and 1700 kPa) was achieved. The unit was operated for more than 2000 hours on six different feedstocks. Most of the tests were conducted with Utah bituminous coal, achieving above 90 percent carbon conversion without char recycle.

DESCRIPTION OF PDU

Coal, 2" x 0" in size, was brought to the PDU site by trucks and piled on asphalt pads. The coal was reduced to less than 1/4" in size in a hammer mill, then pulverized to 70 percent minus 200 mesh in a roller mill. The pulverized coal was carried by hot gas into a cyclone where 90 to 95 percent of the coal was separated and dropped into a 20 ton storage bin. The remaining fine coal carried over from the cyclone was collected in a baghouse and also stored in the storage bin.

Coal was conveyed from the storage bin to a 3 ton lock hopper with nitrogen and, after being filled with coal, the lock hopper was pressurized with recycled product gas to the same pressure as the coal feed hopper below and the coal was discharged into the feed hopper. From the feed hopper the coal was fed into the coal feed line and carried to the gasifier by recycled product gas. Approximately 8 to 10 percent of the product gas was recycled to carry the pulverized coal. Twin augers located in the bottom of the coal feed tank were used to regulate the rate of coal flow into the feed line. Figure 1 presents a simplified process flow diagram of the PDU.

The gasification reactions were carried out at pressures up to 260 psia and at temperatures around 1565°C (2850°F) in a refractory-lined chamber approximately 2.3 cubic feet (0.065 cubic meters) in volume. Both heated oxygen and superheated steam were fed to the reactor. The reactor residence time was in the range of 0.5 to 1 second for most of the tests conducted. A radiant heat exchanger is located immediately below the gasifier in the same pressure vessel. The raw product gas leaves the vessel at a temperature about 670°C (1240°F). Approximately 50 to 60 percent of the ash in the form of slag droplets and char is collected at the base of the vessel. A water spray is used to cool the slag. Periodically, the slag and char are discharged into a slag lock hopper. Then the lock hopper is depressurized and the contents discharged into the slurry discharge tank where they are combined with fly ash, soot, and water discharged from the scrubber. This mixture is then pumped

to a hydroclone. The underflow from the hydroclone is discharged to the waste water pond and the overflow to the recycle water pond.

The hot product gas from the radiant heat exchanger vessel passes through a section of double-wall pipe heat exchanger and into a scrubber and packed tower. The gas is metered and sampled on-line for analysis downstream of the scrubber and then is flared.

#### GASIFIER

A schematic drawing of the pressure vessel containing the gasification chamber, the heat exchanger internals, and slag quench section is presented in Figure 2. This vessel is 48 inches in diameter and 20.5 feet in length. The diameter of the refractory-lined reaction chamber is 16 inches. The refractory is supported by a water-jacketed cylinder. Coal, oxygen and steam are injected into the gasifier at the top of the chamber. Coal is injected through a water-cooled 1-1/2 inch feed nozzle and oxygen and steam mixture is injected through an annular space around the coal feed injector. Figure 3 shows a schematic drawing of the injector nozzle and head assembly. The head is fabricated from beryllium copper alloy, which is cooled by passing water through a slot parallel to the surface facing the reactor.

The heat exchanger internals inside the pressure vessel consist of three separate sections. The first section, the radiant heat exchanger, is a cylindrical membrane wall manufactured from steam tubes with strips of metal welded between them. Saturated water from the steam drum enters the tubes from the bottom and flows up through the tubes producing steam. The tube wall is also equipped with four soot blowers. The second section is a coil that cools the lower portion of the pressure vessel and protects it from the hot product gas. A small amount of steam is generated in this coil through convective heat transfer. The third section is located in the bottom of the vessel and consists of the slag quench equipment. A spray ring is installed in the bottom of the exchanger. Cooling water from the recycle water pond is sprayed through nozzles on this ring to form a pool of water in the bottom of the vessel.

Corrosion tests were conducted by IIT Research Institute (7) by installing test coupons in the slag quench pool. Test results show that at the bottom of the radiant heat exchanger, where corrosion coupons were submerged in the slag quench pool most of the time and the temperature scarcely exceeded 220°F, materials like A515 carbon steel, aluminized carbon steel, 2 1/4Cr-1Mo, 1 1/4Cr-1Mo, 9Cr-1Mo, and 410 SS suffered from heavy corrosion. Types 304 SS and 316 SS exhibited acceptable overall corrosion, but they have a tendency to pit in this environment. The Incoloy 800 specimens showed excellent resistance to general corrosion and pitting.

#### TEST RESULTS WITH UTAH BITUMINOUS COAL

Extensive tests were conducted with Utah bituminous coal from Southern Utah Fuel Company's (SUFCO) Mine No. 1 located near Salina, Utah. Table 1 presents typical proximate and ultimate analyses of the pulverized coal. The coal received at the plant usually contained about 8 to 10 percent moisture.

The range of the principal operational parameters and test results from July through September 1984 are presented in Table 2. Figure 4 presents product gas rate, and gas composition versus coal feed rate. The gas production rate averaged 29.3 SCF/lb of coal. For the range of coal feed tested, carbon monoxide was found to increase and carbon dioxide to decrease slightly with coal feed rate, while hydrogen seemed to reach a maximum at about 1400 pounds per hour coal rate. The ranges of the dry volume percent of the major gas components are 51 to 60 percent for CO, 30 to 36 percent for H<sub>2</sub>, and 6 to 12 percent for CO<sub>2</sub>. The cold gas efficiency and fraction carbon gasified increase with oxygen/coal ratio and coal feed rate for the range of conditions tested. It is obvious that the fraction of carbon gasified will increase toward a value of 1 with increasing oxygen to coal ratio;

however, the cold gas efficiency is expected to reach a maximum value then start to fall as hydrogen and carbon monoxide react with oxygen and reduce the heating value of the product gas.

#### COMPUTER MODEL PREDICTIONS

Several sets of computations were made with a theoretical gasifier model to assess the effect of systematic variations in reactor conditions on performance of the gasifier and product gas composition. Model parameters were empirically determined from fitting the experimental data. Table 2 also presents a range of predicted performance by computer model. The variations examined were: (1) oxygen/coal feed ratio, (2) steam/coal feed ratio, (3) recycle gas/coal ratio, and (4) reactor heat loss. Results from these computations are presented in Figures 5 through 8. The cases were run using the model parameters as optimized for the July-September SUFCO coal data. The predicted product gas volume and product gas composition are plotted versus the oxygen coal feed ratio, with other variables as parameters.

It was found that the heating value of the product gas is at a maximum for an oxygen/coal ratio of between 0.8 and 0.9. Variations in the recycle gas to coal ratio were calculated to have only a weak influence on the product gas composition and volume. The steam/coal ratio, Figure 6, demonstrates a strong influence on the product gas composition with little effect in the product gas volume. The carbon monoxide concentration is highest for a lower steam/coal ratio. For lower oxygen feed rates, the temperature is a strong factor in the product gas volume. However, at an oxygen/coal ratio between 0.8 and 0.9, the cold gas efficiency is unaffected by the steam feed rate.

Variations in the reactor heat loss were calculated to significantly affect the product gas volume and composition, mainly through lowering the reactor temperature. Figure 7 shows significantly lower product gas volume and quality with a higher reactor heat loss. Figure 8 again presents the effect of reactor heat loss; however, here the oxygen/coal feed ratio was adjusted to yield the desired reactor temperature. For a constant reactor temperature, a higher reactor heat loss deteriorates the product gas quality only slightly.

The oxygen/coal feed ratio is the controlling parameter on reactor temperature and performance. The effect of variations in steam, recycle gas ratio and the reactor heat loss on the cold gas efficiency are relatively small compared with the effects of varying the oxygen/coal ratio.

Table 3 presents a direct comparison of PDU data with the design assumptions for a scale-up unit utilizing SUFCO Utah bituminous coal.

#### CONCLUSIONS

The dry-feed, entrained coal gasification PDU was operated successfully for a total of about 2200 hours. Controlled continuous dry-feeding of pulverized coal into the gasifier at pressures up to 260 psia was achieved. Reactor throughputs of up to 754 lbs/hr/ft<sup>2</sup> or 317 lbs/hr/ft<sup>3</sup>, gas yields of about 32 SCF/lb coal and gas heating values of 294 BTU/SCF were achieved. Carbon conversion efficiencies above 90 percent without char recycle were achieved with Utah bituminous, Wyoming sub-bituminous, and North Dakota lignite coals. Cold gas efficiencies as high as 80 percent were achieved with SUFCO coal. Sufficient reproducible data were obtained for scale-up design for applications utilizing Utah bituminous coal from SUFCO Mine No. 1.

#### ACKNOWLEDGEMENT

The authors gratefully acknowledge support of this work by the Department of Energy under Contract No. DE-AC21-81FE05121, Gary R. Friggens, Contractor Monitor.

#### REFERENCES

1. Holden, J.H., et al., "Operation of Pressure-Gasification Pilot Plant Utilizing Pulverized Coal and Oxygen: A Progress Report," Report of Investigations 5573, U.S. Dept. of the Interior, Bureau of Mines (1960).
2. Holden, J.H., Plants, K.D., et al., "Operating a Pressurized Gasification Pilot Plant Using Pulverized Coal and Oxygen: Effect of Heat Loss on Economy," Report of Investigations 5956, U.S. Dept. of the Interior, Bureau of Mines (1962).
3. Coates, R.L., "High Rate Coal Gasification," in Volume 3, "Coal Processing Technology," American Institute of Chemical Engineers, New York, N.Y., 1977, pp. 89-94.
4. McIntosh, M.J., and Coates, R.L., "Experimental and Process Design Study of a High Rate Entrained Coal Gasification Process," Final Report under Contract No. EX-76-C-01-1548, Eyring Research Institute, Provo, Utah, 1978.
5. Coates, R.L., and Mantyla, R.G., "Process Design Studies for High-Rate, Entrained-Flow Coal Gasification," Proceedings of the First International Gas Research Conference, June 1980, Chicago, Illinois, published by Government Institutes, Inc., Rockville, Md., October 1980, pp. 224-242.
6. U.S. Patent No. 4,272,255, "Apparatus for Gasification of Carbonaceous Solids."
7. Yurkewycz, R., "Corrosion and Degradation of the Test Materials in the Mountain Fuel Resources 30 Ton/Day Coal Gasification Process Development Unit," Report of Materials Evaluation conducted in 1983-1984 by IIT Research Institute for the Metal Properties Council, Inc., support by the U.S. Department of Energy, Morgantown Energy Technology Center, Report No. MPCI-22241-2, January 31, 1985.

TABLE 1

## SUFCO UTAH BITUMINOUS COAL ANALYSIS

PROXIMATE ANALYSIS, WT. %		ULTIMATE ANALYSIS, WT. %	
Moisture	2.55	Moisture	2.55
Ash	9.23	Carbon	69.60
Volatile	39.37	Hydrogen	4.84
Fixed Carbon	48.85	Nitrogen	1.15
	100.00	Chlorine	0.02
		Sulfur	0.42
Btu/lb	12180	Ash	9.23
		Oxygen (diff.)	12.19
			100.00

TABLE 2

 RANGE OF THE PRINCIPAL OPERATIONAL PARAMETERS  
 AND SUMMARY OF THE RESULTS AND CORRELATIONS  
 OF THE SUFCO COAL DATA, JULY - SEPTEMBER 1984

Range of Test Conditions		Actual	Predicted
Reactor pressure, psia	90.4 - 212	23 - 36	24.5 - 35.4
Coal feed rates, lbs/hr	633 - 1812	50.7 - 59.8	49.8 - 61.7
Oxygen/coal ratios	0.62 - 0.94	27.5 - 36.8	29.9 - 40.7
Recycle gas/coal ratios	0.11 - 0.22	5.4 - 15.0	6.0 - 12.8
	0 - 0.33	0.0 - 2.7	0.2 - 2.2
		266 - 307	282 - 313
		0.67 - 1.00	0.72 - 1.00
		0.53 - 0.85	0.60 - 0.85
Range of Calculated Balances			
Hydrogen Balance		0.626 - 1.176	
Mass Balance		0.980 - 1.039	

TABLE 3

 COMPARISON OF SCALE-UP UNIT DESIGN  
 ASSUMPTIONS WITH JULY-NOVEMBER 1984 PDU DATA

	Scale-Up Unit Design Assumptions	PDU Data Averages for SUFCO Coal Runs
Coal Rate, lbs/hr	11,686	1,055
Feed Ratios		
Oxygen/coal	0.80	0.849
Steam/coal	0.17	0.274
Recycle gas/coal	0.12	0.215
Reactor Pressure, psia	200	157
Reactor Throughput Rate Lbs/hr/ft <sup>3</sup>	1,000	754
	190	317
Reactor Heat Loss BTU/lb coal	100	325
Product Gas Yield (net, dry)		
MSCFR	371	33.4
SCF/lb coal	31.7	31.5
Product Gas Composition		
Hydrogen	31.6	33.6
Carbon monoxide	56.0	51.3
Carbon dioxide	9.0	12.1
Methane	1.2	0.9
Nitrogen, argon	2.0	2.1
Hydrogen sulfide	0.2	-
Total	100.0	100.0



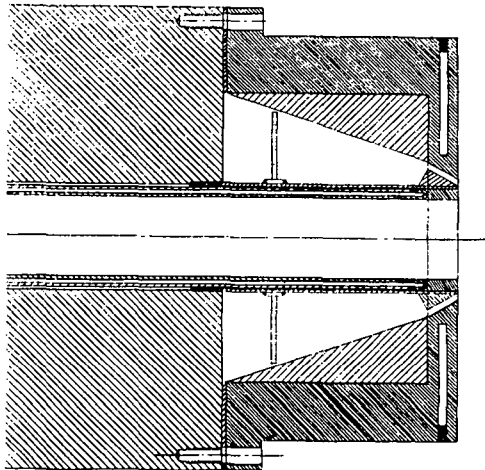


FIGURE 3. Schematic Drawing of Injector Nozzle and Head Assembly

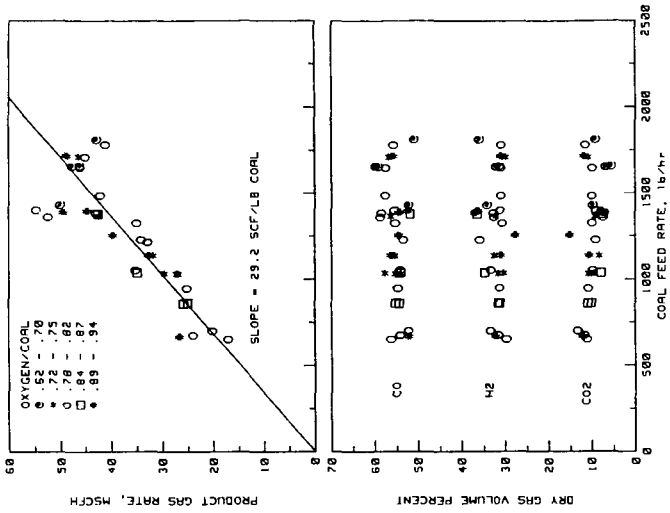


FIGURE 4. Gasifier Performance Data Gas Composition and Product Gas Rate Versus Coal Feed Rate

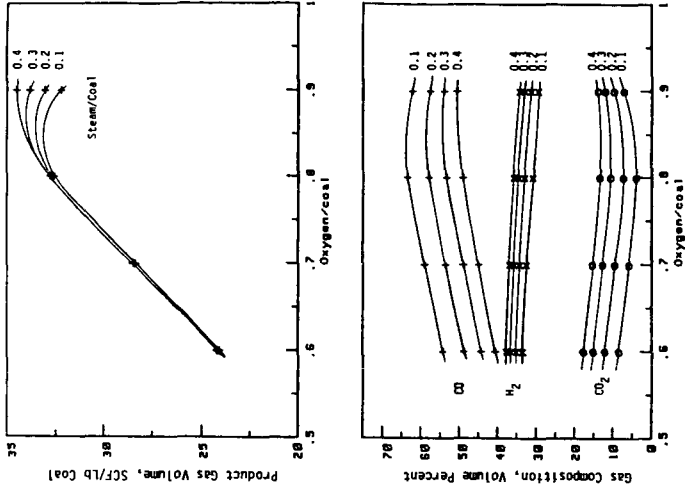


FIGURE 6. Predicted Performance of SUFCO Coal Using Best Fit Parameters from July - September 1984 Data Recycle/Coal = 0.12, Reactor Heat Loss = 200 BTU/Lb Coal

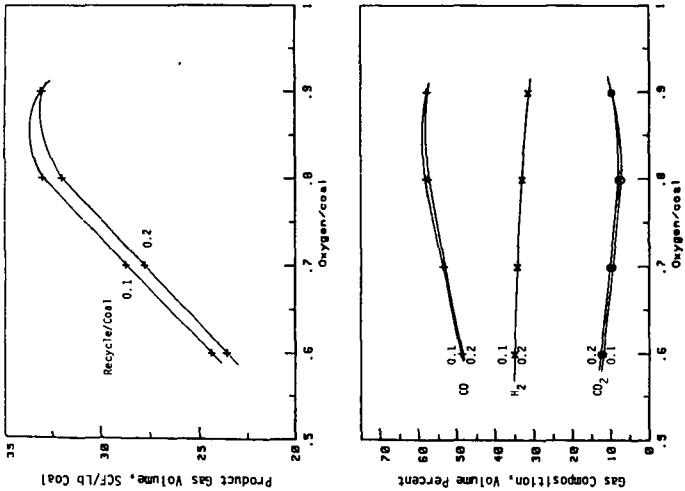


FIGURE 5. Predicted Performance of SUFCO Coal Using Best Fit Parameters from July - September 1984 Data Steam/Coal = 0.2, Reactor Heat Loss = 200 BTU/Lb Coal

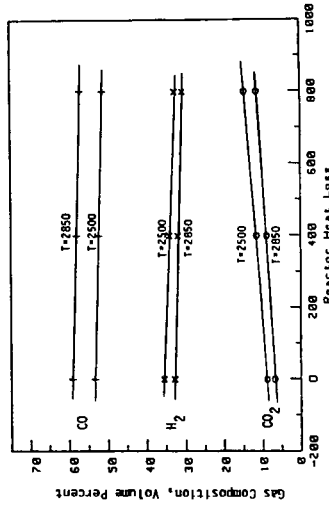
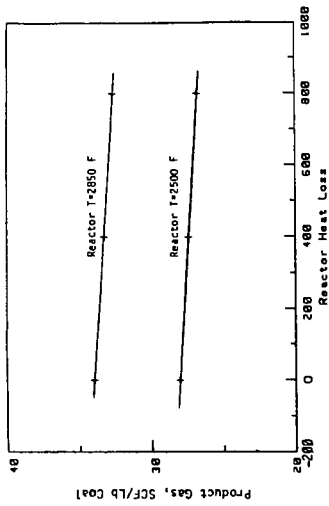


FIGURE 8. Predicted Effect of Heat Loss on Product Gas Steam/Coal = 0.2, Recycle Gas/Coal = 0.12

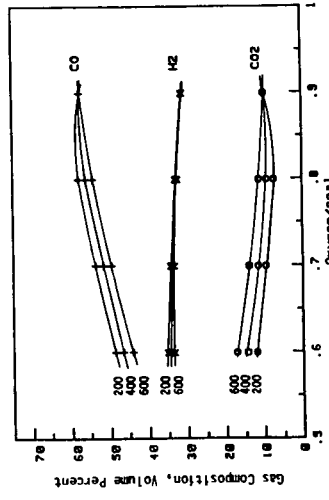
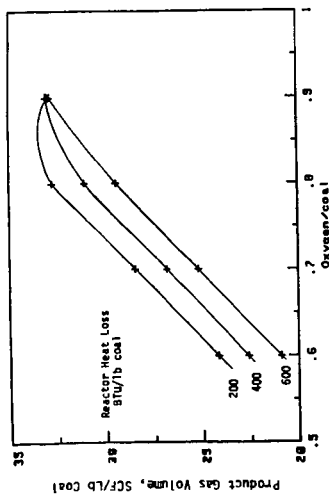


FIGURE 7. Predicted Performance of SUECO Coal Using Best Fit Parameters from July - September 1984 Data Steam/Coal = 0.2, Recycle Coal = 0.12